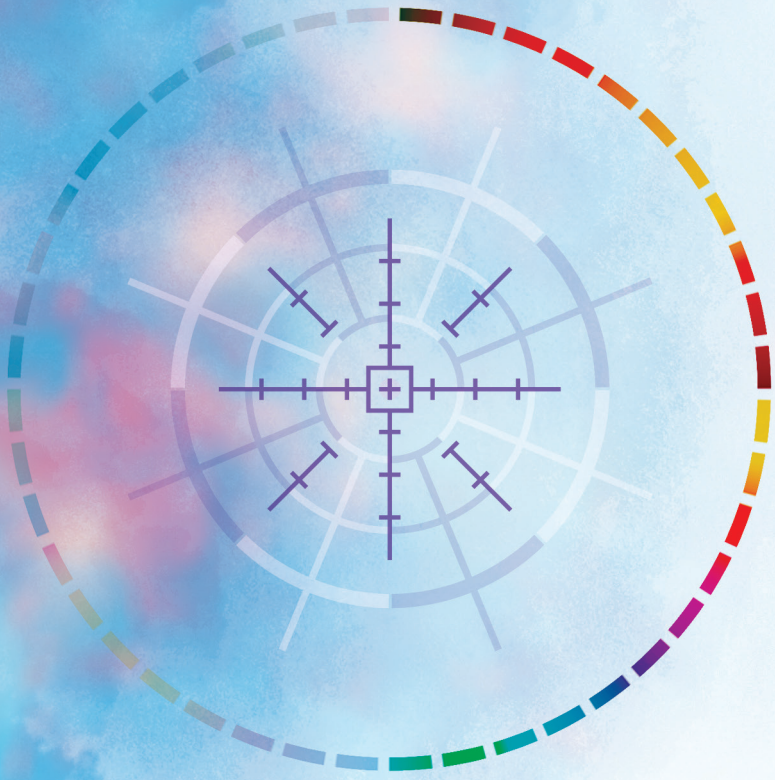

HIGH-PRECISION ADJUVANT RADIOTHERAPY FOR EARLY-STAGE BREAST CANCER PATIENTS TO REDUCE TOXICITY AND IMPROVE SURVIVAL

NIENKE HOEKSTRA

Design/lay-out
Promotie In Zicht | www.promotie-inzicht.nl

Print
Ipskamp Printing

High-precision Adjuvant Radiotherapy for Early-stage Breast Cancer Patients to Reduce Toxicity and Improve Survival

Hoge precisie adjuvante radiotherapie voor vroeg-stadium borstkanker patiënten om de toxiciteit te verminderen en de overleving te verbeteren

Proefschrift

ter verkrijging van de graad van doctor aan de
Erasmus Universiteit Rotterdam
op gezag van de
rector magnificus

Prof. dr. A.L. Bredenoord

en volgens besluit van het College voor Promoties.

De openbare verdediging zal plaatsvinden op

dinsdag 15 februari 2022 om 13.00 uur

door

Nienke Hoekstra
geboren te 's-Hertogenbosch

Erasmus University Rotterdam

Promotiecommissie

Promotoren
Prof. dr. M.S. Hoogeman
Prof. dr. J.P. Pignol

Overige leden
Prof. dr. R.A. Nout
Prof. dr. L.J. Boersma
Prof. dr. B.W. Raaymakers

Copromotor
Dr. S.J.M. Habraken

Contents

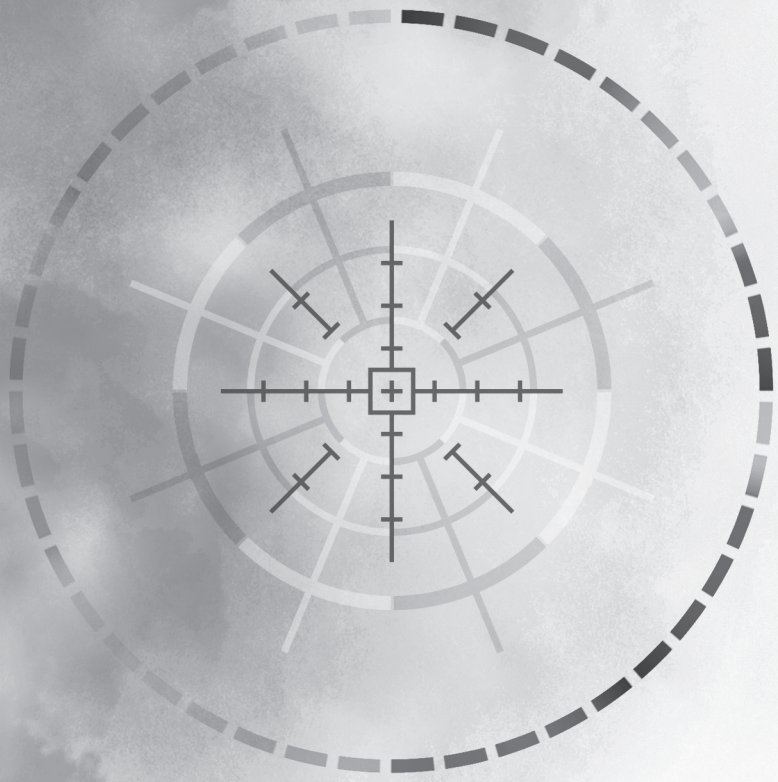

1

General introduction

General introduction

Breast cancer

Breast cancer is the most common type of cancer worldwide [1]. The incidence is estimated to be almost 60 per 100.000 person-years. In the Netherlands, more than 17.000 persons were diagnosed with in-situ or invasive breast cancer in 2019 [2]. The vast majority of patients are female and 50 years of age or older. About 1 in every 7 females will get breast cancer at some time during her lifetime.

In many countries, there is a population screening program for breast cancer, and most cases are diagnosed at an early stage. In the United States for example, 63% of all breast cancer patients is diagnosed at a local stage without any regional or distant dissemination [3].

The current standard for the treatment of early-stage breast cancer is breast conserving surgery followed by adjuvant radiotherapy and, in selected cases, systemic therapy. With this treatment, the prognosis of early-stage breast cancer patients is excellent. The 5-year disease-specific survival is 99% [2, 3]. It is practically impossible to improve this substantially. Thus, the focus of clinical research has shifted from decreasing recurrence rates to reducing treatment-induced toxicity and improving quality of life.

Standard radiotherapy treatment

Following major randomized clinical trials in the 90's establishing the value of adjuvant radiotherapy, the standard adjuvant treatment for early-stage breast cancer has been whole breast irradiation (WBI) to a dose of 50 Gy in 25 fractions of 2 Gy for many years [4]. More recently, trials have investigated moderate hypofractionation, including the START and the Ontario hypofractionation trials [5-8]. They showed that a treatment schedule of 15 to 16 fractions of 2.66 Gy in 3 weeks was equally effective as 25 fractions of 2 Gy in 5 weeks and resulted in similar or less breast toxicity. Because of these favorable results and the increased convenience for both patients and radiotherapy facilities, these schedules were adopted worldwide. Advances in knowledge about the radiobiology of breast cancer and healthy breast tissue from these trials led to the start of other trials investigating even shorter treatment schedules for WBI [9, 10].

In parallel to decreasing the number of fractions, the volume to be irradiated has also been reduced. The idea for partial breast irradiation (PBI) originated from the fact that most ipsilateral breast recurrences occurred close to the original tumor bed [11, 12]. For selected low-risk patients, it is sufficient to irradiate the tumor bed area with a small margin of 10 – 20 mm. Because of the volume reduction, the number of fractions could be also reduced, leading to accelerated partial breast irradiation (APBI). Several large randomized clinical trials have confirmed the efficacy and safety of external beam APBI [13-16]. The most

common treatment schedules for external beam APBI is 10 fractions of 3.85 Gy delivered in one week, and more recently 5 fractions of 5.2 to 6 Gy.

Long-term toxicities after external beam radiotherapy for breast cancer

The long-term toxicity of radiotherapy is related to the dose received by the surrounding healthy tissues. In the case of breast cancer treatment, it includes the heart, lungs, skin, and the healthy non-target breast tissue. Thus, the most concerning toxicities include cardiovascular diseases, radiation-induced cancers, telangiectasia, and breast fibrosis.

The incidence of cardiovascular disease is proportional to the mean dose to the heart [17]. Every Gy mean heart dose causes a relative increase in the incidence of major cardiovascular events of 7.4%. Recent technological advances such as more conformal treatment planning and deep inspiration breath hold reduced the mean heart dose [18-20]. The introduction of APBI is also predicted to lead to lower mean heart doses, thus reducing the cardiovascular toxicity [21, 22]. It is important to notice that the absolute increase depends on the baseline risk of the individual patient. Independent factors such as age, comorbidity and smoking are just as important as the mean heart dose.

The occurrence of breast fibrosis and telangiectasia are associated with worse cosmetic outcomes, which in turn impact the quality of life of breast cancer survivors. Severe fibrosis can also impact the mobility of the arm or cause chronic pain, leading to functional impairment. Several normal tissue complication probability (NTCP) models have been proposed to predict the risk of breast fibrosis [23-25]. In these models, the risk of fibrosis depends mainly on the high dose region within the breast. This means that it is more important to reduce the high-dose volume than the low-dose volume within the breast.

The comparative risks of breast fibrosis and adverse cosmesis of external beam APBI compared to WBI is not yet established. The two large multicenter randomized trials, RAPID and NSABP B-39/RTOG 0413, presented conflicting results while using the same treatment schedule of 10 fractions of 3.85 Gy twice daily [13, 14, 26]. In the RAPID trial, adverse cosmesis was more common in the patients treated with APBI than in the patients treated with WBI. This difference was statistically significant [14]. In the NSABP B-39/RTOG 1403 trial, there was no significant difference in toxicity at all. It is important to notice that the standard arm differed between those trials: the RAPID used the Ontario hypofractionation regimen, 42.5 Gy in 16 fractions, while the NSABP B39/RTOG 1403 used the old standard of 50 Gy in 25 fractions. This led some to hypothesize that the old standard might have been slightly more toxic than the hypofractionated regimen and that this would erase the difference. Additionally, a smaller randomized trial found an improvement in cosmesis after APBI using a once-daily fractionation schedule compared to WBI [27]. A proposed explanation is the interval between two subsequent fractions [28]. The interval

had to be at least 6 hours in RAPID and NSABP B-39 / RTG 0413, which might be too short for the healthy breast tissue to fully recover. Trials investigating APBI with 5 fractions once-daily over one week are ongoing [29, 30].

The risk of inducing secondary cancers by radiation has been acknowledged for a long time. The challenge of the research in this field is first the very long delay to develop a secondary cancer and second the scarcity of exposure data. In addition, most of the research done on the relation between the secondary cancer risk and the magnitude of radiation dose is based on the Japanese atomic bomb survivors and on diagnostic radiation exposures [31]. Both patient groups received relatively low dose exposures. As a result, there is still debate about the dose-response relationship at higher dose levels, such as used for radiotherapy treatment [32, 33]. There are several epidemiological studies published on secondary cancer induction after breast radiotherapy published [34-38]. These studies show that there is a significantly higher risk of cancer for breast cancer patients treated with radiotherapy. An important limitation of these studies is the limited length of follow-up. It is known that the incidence of secondary cancers starts at least 5 years after treatment and increases for 20 to 30 years [31]. The longer the median follow-up of a study, the higher the number of secondary cancers that can be detected and the higher the chance of finding significant differences. Very long-term follow-up is difficult to attain and often limited in detail. In most studies, there is no information on the dose received by various tissues so dose-response relationships cannot be calculated. A challenge is that radiation techniques used a long time ago are vastly different than the ones used today. Finally, patients are diagnosed at an earlier stage nowadays due to population screening. Thus, it is difficult to use the data of these epidemiological studies to predict the secondary cancer risk of a patient treated today.

Several quantitative models are published that can be used to predict and compare secondary cancer risks after radiotherapy [31, 39, 40]. It is important to take into account the uncertainties of these models as discussed above, i.e. the limited evidence for the effect of high doses and differences in investigated populations. These uncertainties mean that these models are less accurate at predicting a secondary cancer risk for an individual patient, but suitable for the relative comparison of different treatment techniques [33].

In this thesis, ways to reduce the risk of radiation-induced toxicity after adjuvant breast radiotherapy will be discussed focusing on the risk of secondary cancer induction. Secondary cancers can increase mortality, depending on the length of follow-up and the life expectancy of the breast cancer patients after treatment. Patients diagnosed today are diagnosed earlier in their life and at an earlier stage, due to the generalization of mammography screening. They are hence at higher risk of developing a secondary cancer. The reduction of cardiac toxicity has received a lot of attention in the recent literature.

In contrast, the induction of secondary cancer has received less attention, probably because cardiac toxicity occurs at shorter intervals after radiotherapy. This thesis aims to improve overall survival and quality of life of breast cancer patients by reducing the risks of secondary cancer and other treatment-induced toxicities.

Reducing dose to non-target tissues

Radiation dose in tissues outside of the treatment target must be minimized, as it has no benefit to the patient and can lead to toxicity. In the radiation oncology community, this is called "as low as reasonably achievable", or the ALARA principle. Reducing the dose to non-target tissue will reduce the risks of secondary cancer and other treatment-induced toxicities. There are several ways to achieve this.

The first option is to reduce the irradiated volume. The volume to be treated is called the clinical target volume (CTV) [41]. A safety margin is applied to this volume to compensate for uncertainties during treatment preparation and delivery. The expansion of the CTV with this margin results in the planning target volume (PTV). The smaller the margin, the smaller the PTV and the smaller the dose to surrounding healthy tissues will be. On the other hand, reducing the margin could lead to a higher risk of geographical miss and thus to a higher local recurrence risk. It is crucial to quantify the geometric uncertainties of treatment preparation and delivery to calculate the minimum margin needed to adequately treat the patient group. After quantification, the second step is to reduce the uncertainties and thus reduce the required PTV margin. Different aspects contribute to the total geometric uncertainty: the motion occurring between simulation and treatment fractions (interfraction motion), the motion occurring during treatment delivery (intrafraction motion), and the uncertainty in the delineation of the target.

The second option to reduce dose to non-target tissue is to optimize the dose distribution that can vary significantly between treatment techniques. There are large differences in non-target doses between brachytherapy, intra-operative irradiation and external beam (EB) APBI. Also, among the external beam techniques large differences exist [42, 43]. For example, the use of intensity modulation has a clear impact, just as whether it is a step-and-shoot or continuous arc delivery [43]. The use of breath hold can reduce the dose to heart and lungs [18]. The number of beams and the angles of the gantry, collimator and couch can dramatically influence the dose to a specific organ. Shifting the dose away from one organ will often lead to a higher dose in another organ. For partial breast radiotherapy, this trade-off is most pronounced for non-target breast tissue versus heart and lungs. Choices on this trade-off are made continuously in the clinical routine, but little is known about the long-term consequences. There is a lack of planning comparison studies that calculate normal tissue complication probabilities for the dose distributions of different treatment techniques.

Aims and outline of this thesis

This thesis aims to improve overall survival and quality of life of breast cancer patients by reducing the risks of secondary cancer and other treatment-induced toxicities. Methods are being investigated to reduce the risk of radiation-induced toxicity after adjuvant breast radiotherapy, focusing on the secondary cancer risk. These methods comprise of strategies improving treatment planning, geometric accuracy, and delineation.

The first part of this thesis focuses on assessing the magnitude of the risk of secondary cancers. **Chapter 2** describes a phantom study assessing the secondary cancer risks in various organs for different whole and partial breast irradiation techniques. In this chapter, we conclude that most secondary cancers arise in the lungs. Future efforts to reduce the overall secondary cancer risk of breast radiotherapy should be aimed at reducing the lung dose. In **Chapter 3** we describe the trade-off between reducing the secondary lung cancer risk and increasing the toxicity risk in other tissues using optimized treatment planning for external-beam APBI.

The second part of this thesis focuses on the geometric accuracy of EB-APBI delivery. Increasing the geometric accuracy will lead to smaller irradiated volumes, lower doses to non-target tissues, and lower toxicity risks. **Chapter 4** describes our results on the intrafraction motion during APBI treatment delivery. The motion due to breathing and due to the target drifting away during treatment are described separately. **Chapter 5** reports on the interfraction motion of fiducials relative to the tumor bed and incorporates this motion into a comprehensive PTV margin for geometric uncertainties in EB-APBI. In **chapter 6** we present a study on improving the delineation consistency of the tumor bed using a hydrogel marker.

At the end of this thesis in **chapter 7**, our conclusions are presented and discussed in a broader context. Our findings are summarized in **chapter 8** in English and in **Chapter 9** in Dutch**.**

References

[1] International Agency for Research on Cancer. 2021; https://gco.iarc.fr/today/home.

[2] Integraal Kankercentrum Nederland. Cijfers over kanker. 2020; http://www.cijfersoverkanker.nl/.

[3] Surveillance, Epidemiology, and End Results (SEER) Program (www.seer.cancer.gov) SEER*Stat Database: Incidence - SEER 18 Regs Research Data + Hurricane Katrina Impacted Louisiana Cases, Nov 2016 Sub (2000-2014) <Katrina/Rita Population Adjustment> - Linked To County Attributes - Total U.S., 1969-2015 Counties, National Cancer Institute, DCCPS, Surveillance Research Program, released April 2017, based on the November 2016 submission.

[4] Early Breast Cancer Trialists' Collaborative G, Darby S, McGale P, et al. Effect of radiotherapy after breast-conserving surgery on 10-year recurrence and 15-year breast cancer death: meta-analysis of individual patient data for 10,801 women in 17 randomised trials. Lancet. 2011;378:1707-16.

[5] Start Trialists' Group, Bentzen SM, Agrawal RK, et al. The UK Standardisation of Breast Radiotherapy (START) Trial B of radiotherapy hypofractionation for treatment of early breast cancer: a randomised trial. Lancet. 2008;371:1098-107.

[6] Start Trialists' Group, Bentzen SM, Agrawal RK, et al. The UK Standardisation of Breast Radiotherapy (START) Trial A of radiotherapy hypofractionation for treatment of early breast cancer: a randomised trial. Lancet Oncol. 2008;9:331-41.

[7] Whelan TJ, Pignol JP, Levine MN, et al. Long-term results of hypofractionated radiation therapy for breast cancer. N Engl J Med. 2010;362:513-20.

[8] Haviland JS, Owen JR, Dewar JA, et al. The UK Standardisation of Breast Radiotherapy (START) trials of radiotherapy hypofractionation for treatment of early breast cancer: 10-year follow-up results of two randomised controlled trials. Lancet Oncol. 2013;14:1086-94.

[9] Brunt AM, Haviland JS, Sydenham M, et al. Ten-Year Results of FAST: A Randomized Controlled Trial of 5-Fraction Whole-Breast Radiotherapy for Early Breast Cancer. J Clin Oncol. 2020;38:3261-72.

[10] Brunt AM, Haviland JS, Wheatley DA, et al. Hypofractionated breast radiotherapy for 1 week versus 3 weeks (FAST-Forward): 5-year efficacy and late normal tissue effects results from a multicentre, non-inferiority, randomised, phase 3 trial. Lancet. 2020;395:1613-26.

[11] Fisher ER, Anderson S, Redmond C, Fisher B. Ipsilateral breast tumor recurrence and survival following lumpectomy and irradiation: pathological findings from NSABP protocol B-06. Semin Surg Oncol. 1992;8:161-6.

[12] Vicini FA, Kestin LL, Goldstein NS. Defining the clinical target volume for patients with early-stage breast cancer treated with lumpectomy and accelerated partial breast irradiation: a pathologic analysis. Int J Radiat Oncol Biol Phys. 2004;60:722-30.

[13] Vicini FA, Cecchini RS, White JR, et al. Long-term primary results of accelerated partial breast irradiation after breast-conserving surgery for early-stage breast cancer: a randomised, phase 3, equivalence trial. Lancet. 2019;394:2155-64.

[14] Whelan TJ, Julian JA, Berrang TS, et al. External beam accelerated partial breast irradiation versus whole breast irradiation after breast conserving surgery in women with ductal carcinoma in situ and node-negative breast cancer (RAPID): a randomised controlled trial. Lancet. 2019;394:2165-72.

[15] Rodriguez N, Sanz X, Dengra J, et al. Five-year outcomes, cosmesis, and toxicity with 3-dimensional conformal external beam radiation therapy to deliver accelerated partial breast irradiation. Int J Radiat Oncol Biol Phys. 2013;87:1051-7.

[16] Livi L, Meattini I, Marrazzo L, et al. Accelerated partial breast irradiation using intensity-modulated radiotherapy versus whole breast irradiation: 5-year survival analysis of a phase 3 randomised controlled trial. Eur J Cancer. 2015;51:451-63.

[17] Darby SC, Ewertz M, McGale P, et al. Risk of ischemic heart disease in women after radiotherapy for breast cancer. N Engl J Med. 2013;368:987-98.

[18] Bartlett FR, Donovan EM, McNair HA, et al. The UK HeartSpare Study (Stage II): Multicentre Evaluation of a Voluntary Breath-hold Technique in Patients Receiving Breast Radiotherapy. Clinical Oncology. 2017;29:e51-e6.

[19] Lin A, Sharieff W, Juhasz J, Whelan T, Kim DH. The benefit of deep inspiration breath hold: evaluating cardiac radiation exposure in patients after mastectomy and after breast-conserving surgery. Breast Cancer. 2017; 24:86-91.

[20] Simonetto C, Eidemüller M, Gaasch A, et al. Does deep inspiration breath-hold prolong life? Individual risk estimates of ischaemic heart disease after breast cancer radiotherapy. Radiother Oncol. 2019;131:202-7.
[21] Oliver M, Chen J, Wong E, Van Dyk J, Perera F. A treatment planning study comparing whole breast radiation therapy against conformal, IMRT and tomotherapy for accelerated partial breast irradiation. Radiother Oncol. 2007;82:317-23.
[22] Merino Lara TR, Fleury E, Mashouf S, et al. Measurement of mean cardiac dose for various breast irradiation techniques and corresponding risk of major cardiovascular event. Front Oncol. 2014;4:284.
[23] Mukesh MB, Harris E, Collette S, et al. Normal tissue complication probability (NTCP) parameters for breast fibrosis: pooled results from two randomised trials. Radiother Oncol. 2013;108:293-8.
[24] Avanzo M, Stancanello J, Trovò M, et al. Complication probability model for subcutaneous fibrosis based on published data of partial and whole breast irradiation. Physica Medica. 2012;28:296-306.
[25] Hammer C, Maduro JH, Bantema-Joppe EJ, et al. Radiation-induced fibrosis in the boost area after three-dimensional conformal radiotherapy with a simultaneous integrated boost technique for early-stage breast cancer: A multivariable prediction model. Radiotherapy and Oncology. 2017;122:45-9.
[26] Olivotto IA, Whelan TJ, Parpia S, et al. Interim cosmetic and toxicity results from RAPID: a randomized trial of accelerated partial breast irradiation using three-dimensional conformal external beam radiation therapy. J Clin Oncol. 2013;31:4038-45.
[27] Meattini I, Marrazzo L, Saieva C, et al. Accelerated Partial-Breast Irradiation Compared With Whole-Breast Irradiation for Early Breast Cancer: Long-Term Results of the Randomized Phase III APBI-IMRT-Florence Trial. J Clin Oncol. 2020:JCO2000650.
[28] Bentzen SM, Yarnold JR. Reports of unexpected late side effects of accelerated partial breast irradiation--radiobiological considerations. Int J Radiat Oncol Biol Phys. 2010;77:969-73.
[29] Grendarova P, Roumeliotis M, Quirk S, et al. One-Year Cosmesis and Fibrosis From ACCEL: Accelerated Partial Breast Irradiation (APBI) Using 27 Gy in 5 Daily Fractions. Pract Radiat Oncol. 2019;9:e457-e64.
[30] Lozza L, Fariselli L, Sandri M, et al. Partial breast irradiation with CyberKnife after breast conserving surgery: a pilot study in early breast cancer. Radiat Oncol. 2018;13:49.
[31] National Research Council. Health risks from exposure to low levels of ionizing radiation: BEIR VII phase 2: National Academies Press; 2006.
[32] Schneider U, Zwahlen D, Ross D, Kaser-Hotz B. Estimation of radiation-induced cancer from three-dimensional dose distributions: Concept of organ equivalent dose. Int J Radiat Oncol Biol Phys. 2005;61:1510-5.
[33] Nguyen J, Moteabbed M, Paganetti H. Assessment of uncertainties in radiation-induced cancer risk predictions at clinically relevant doses. Medical Physics. 2015;42:81-9.
[34] Taylor C, Correa C, Duane FK, et al. Estimating the Risks of Breast Cancer Radiotherapy: Evidence From Modern Radiation Doses to the Lungs and Heart and From Previous Randomized Trials. J Clin Oncol. 2017;35:1641-9.
[35] Grantzau T, Overgaard J. Risk of second non-breast cancer among patients treated with and without postoperative radiotherapy for primary breast cancer: A systematic review and meta-analysis of population-based studies including 522,739 patients. Radiother Oncol. 2016;121:402-13.
[36] Bazire L, De Rycke Y, Asselain B, Fourquet A, Kirova YM. Risks of second malignancies after breast cancer treatment: Long-term results. Cancer/Radiothérapie. 2017;21:10-5.
[37] Burt LM, Ying J, Poppe MM, Suneja G, Gaffney DK. Risk of secondary malignancies after radiation therapy for breast cancer: Comprehensive results. Breast. 2017;35:122-9.
[38] Mellemkjaer L, Friis S, Olsen JH, et al. Risk of second cancer among women with breast cancer. Int J Cancer. 2006;118:2285-92.
[39] Schneider U, Sumila M, Robotka J. Site-specific dose-response relationships for cancer induction from the combined Japanese A-bomb and Hodgkin cohorts for doses relevant to radiotherapy. Theoretical Biology and Medical Modelling. 2011;8:27.
[40] Berrington de Gonzalez A, Iulian Apostoaei A, Veiga LH, et al. RadRAT: a radiation risk assessment tool for lifetime cancer risk projection. J Radiol Prot. 2012;32:205-22.
[41] International Commission on Radiation Units and Measurements. ICRU REPORT 62 Prescribing, Recording and Reporting Photon Beam Therapy (Supplement to ICRU Report 50) 1999.
[42] Qiu JJ, Chang Z, Horton JK, Wu QR, Yoo S, Yin FF. Dosimetric comparison of 3D conformal, IMRT, and V-MAT techniques for accelerated partial-breast irradiation (APBI). Med Dosim. 2014;39:152-8.

[43] Stelczer G, Major T, Meszaros N, Polgar C, Pesznyak C. External beam accelerated partial breast irradiation: dosimetric assessment of conformal and three different intensity modulated techniques. Radiol Oncol. 2019;53:123-30.

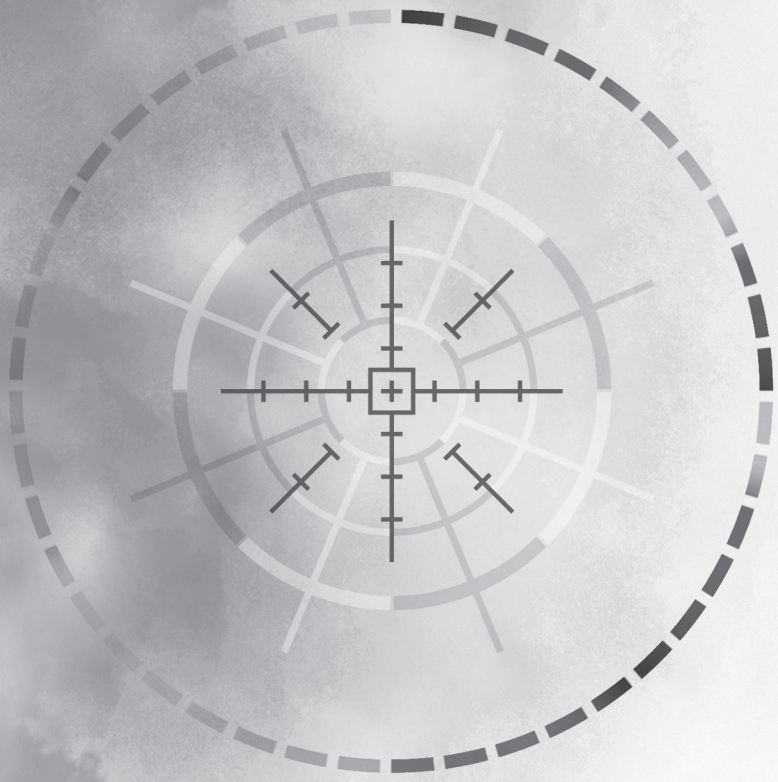

2

Assessment of secondary cancer risks

Published as

Long-term risks of secondary cancer for various whole and partial breast irradiation techniques

Nienke Hoekstra, MD[1]; Emmanuelle Fleury, MSc [1]; Tomas Rodrigo Merino Lara, MD[2]; Peter van der Baan, BSc [1]; Andy Bahnerth[1]; Mischa Hoogeman, PhD[1]; Jean-Philippe Pignol, MD, PhD[3]

1. Erasmus MC Cancer Centre, Department of Radiation Oncology, Groene Hilledijk 301, 3075 EA Rotterdam, The Netherlands
2. Pontificia Universidad Catolica de Chile, 340 Avenida Libertador Bernardo O'Higgins, Santiago, Chile
3. Dalhousie University, Department of Radiotherapy, 5820 University Avenue, Halifax NS B3H1V7, Canada

Radiotherapy and Oncology 128 (2018) 428–433, doi: 10.1016/j.radonc.2018.05.032

Abstract

Introduction – For early-stage breast cancer patients, non-breast cancer mortality including secondary cancers and cardiac events can overshadow the benefit of adjuvant radiotherapy. This study evaluates the excess risk of secondary cancer for new breast radiotherapy techniques including accelerated partial breast irradiation (APBI).

Methods - Secondary cancers Lifetime Attributable Risks (LAR) were calculated using a modified BEIR-VII formalism to account for the specific survival of breast cancer patients. Those survivals were extracted from the SEER database. Doses scattered to various organs were measured into a Rando phantom with custom-made breast phantoms. Treatments delivered typical doses of brachytherapy APBI (34 Gy in 10 fractions), external beam APBI (38.5 Gy in 10 fractions) using 3D-conformal, Cyberknife stereotactic (CK), or VMAT, as well as whole breast irradiation (WBI) delivering 42.5 Gy in 16 fractions.

Results - WBI resulted in the highest total LAR, with 4.3% excess risk of secondary cancer for a patient treated at age 50 years. Lung cancers accounted for 75% to 97% of secondary malignancies. For a typical early-stage patient irradiated at age 50, the risks of secondary lung cancer were 1.1% for multicatheter HDR, between 2.2% to 2.5% for 3D-CRT or CK, 3.5% for VMAT APBI, and 3.8% for WBI.

Conclusions – APBI reduces the risk of secondary cancer 2 to 4 fold compared to WBI. These techniques are well suited for long-living early-stage breast cancer patients. HDR brachytherapy and 3D-conformal APBI achieve mean lung doses between 1 and 1.5 Gy, which could serve as reference.

Introduction

Today breast cancer is frequently diagnosed at an early stage and has an excellent prognosis. SEER data show that 60% of the patients are diagnosed at a localized stage, without extension to the regional nodes, and the 5-year cancer specific survival for those patients is 98.9% [1]. Standard treatment includes limited surgery followed by whole breast irradiation (WBI). Long-term follow-up of large randomized trials comparing lumpectomy with or without adjuvant radiotherapy has shown that the benefit of radiotherapy is eclipsed by non-breast cancer mortality [2, 3]. The most common causes of non-breast cancer mortality include major cardiac events and secondary cancers [4-6]. To reduce cardiac toxicity, the radiation oncology community has massively adopted preventive measures like breath-hold [7, 8]. The issue of secondary cancer has not yet lead to changes regarding the breast irradiation technique.

Accelerated partial breast irradiation (APBI) has been recently proposed for selected patients with favorable characteristics, and results of the few randomized trials suggest non-inferiority in local control compared to WBI [9-12]. Introducing new irradiation techniques may result in differences in the amount of dose to the whole body and thus to differences in the risk of radiation-induced secondary cancer [6, 13]. Scarce comparisons of secondary cancer risks for different techniques have been published [14-16]. They focused either exclusively on whole breast radiotherapy techniques or evaluated the scatter dose theoretically using Monte Carlo simulation. Currently there is no thorough comparison between whole breast radiotherapy and APBI.

The aim of this study is to evaluate the risk of secondary cancer of whole breast radiotherapy and several APBI techniques, using a modified BEIR VII formalism accounting for the specific survival of a breast cancer population, and experimentally measure the scatter dose to various organs for these breast radiotherapy techniques.

Materials and Methods

Calculation of Lifetime Attributable Risks (LARs)

LARs were calculated using the BEIR VII formalism [17]. This model includes empirical and *in vitro* data to calculate secondary cancer risks for specific organs depending on sex, age at exposure and attained age. For the esophagus, we used the organ specific parameters from the study by Berrington de Gonzalez [18]. We selected age at exposure of 40 years and older, since this age corresponds to the lower threshold of the "cautionary group" of the ASTRO guidelines and the "intermediate-risk group" of the GEC-ESTRO guidelines [19-21]. We used the probability of survival for the general population from the U.S. Decennial Life

Tables for 1999 – 2001 [22]. We corrected the probability of survival for breast cancer patients using the probability of survival after localized breast cancer from the SEER database [23]. The SEER database provides survival data up to 40 years after diagnosis. For the period after this, we extrapolated the linear trend in the survival probability. We used the baseline cancer risks for the general population from the SEER database [24]. To put the risks into perspective, we calculated the lifetime Relative Risk (RR) of secondary cancer per organ.

Radiotherapy planning and phantom treatments

Measurements of the scatter dose for various breast radiotherapy techniques were performed using a Rando-Alderson phantom (Radiology Support Devices, Inc., Long Beach, CA, USA) with custom-made tissue equivalent breast phantoms adapted from Ruschin et al. [25]. Five surgical clips were inserted in the upper outer quadrant of the right breast at typical places found on patients treated in our institutions, and creating a virtual seroma of about 3 cm in diameter.

Planning CT-scans of the realistic breast phantom were made according to our institutional protocol. The whole breast clinical target volume (CTV) was delineated up to the chest wall and excluded the first 5 mm below the surface. The whole breast CTV expanded by a 5 mm margin and limited 5 mm under the surface corresponded to the planning target volume (PTV) for whole breast radiotherapy. The tumor bed was delineated using the surgical clips. It was expanded with a margin of 15 mm to create the CTV for the APBI treatments following the NSABP B-39/RTOG 0413 protocol [26]. The PTV margin was 10 mm for the external beam APBI techniques and zero mm for the HDR techniques [26].

Whole breast radiotherapy used an hypofractionated regimen of 42.5 Gy in 16 fractions mixing 6 and 10 MV tangent beams. Beam angles were optimized to limit the contralateral breast and lung dose. Dynamic wedges were used to improve the dose distribution and the treatment was delivered using an Elekta Synergy S linear accelerator.

The technique described by Baglan et al. was used to plan the 3D-conformal (3D-CRT) APBI treatment [27]. The prescribed dose was 38.5 Gy in 10 fractions. The plan fulfilled the dose constraints of the NSABP B-39/RTOG 0413 protocol [26]. VMAT APBI was delivered using a single 6 MV arc ranging from 190° to 20°. The plan was optimized for breast conformality, minimizing the heart and lung dose according to the NSABP B-39/RTOG 0413 constraints [26]. The prescribed dose was 38.5 Gy in 10 fractions. Cyberknife plans were created in Multiplan version 5.3.0 (Accuray Inc., Sunnyvale, USA) with an inverse plan optimization. Plans used either the Iris (CK-Iris) or the MLC (CK-MLC) collimators. Beams were not allowed to enter through the contralateral breast or heart. The prescribed dose, margins and dose constraints applied were identical to the other external beam APBI techniques.

For HDR multicatheter APBI, 8 catheters were inserted in the breast phantom in 2 planes using a free hand implantation technique. A post-implant CT-scan was acquired, and the images were transferred to the Oncentra brachytherapy dose planning system version 4.5.1 (Elekta). The prescribed dose was 34 Gy in 10 fractions. Dwell times were optimized to ensure that coverage and dose homogeneity were optimized following the constraints of the NSABP B-39 protocol [26]. To mimic a balloon for HDR balloon-based APBI, a single catheter was inserted in the breast phantom. On the planning CT-scan, a sphere of 3.5 cm diameter was delineated around the catheter to represent the balloon. A dose of 34 Gy in 10 fractions was delivered to a point 1 cm away from the balloon surface. The plan also satisfied the constraints from the NSABP B-39/RTOG 0413 protocol for balloon-based HDR [26]. Both HDR APBI techniques were delivered using a 192-Ir Flexitron Remote Afterloading system (Elekta).

Dose measurement

Dose was measured in the lungs, contralateral breast, thyroid, esophagus, colon, ovaries and the uterus. Those organs were chosen because of elevated risks of radiation-induced cancers reported in these organs [5, 28-30]. Doses were measured using 34 ThermoLuminescent dosimeters (TLDs) distributed uniformly over the organs and Gafchromic film for the lungs (Ashland Advanced Materials, Bridgewater, USA). The LiF 700 powder TLDs were read out using the Pitman 654 TLD-reader and annealed with the Pitman 622/B annealing facility using a standard of 400°C for 1.5 hours and 80°C for 16 hours, with subsequent natural cooling down to room temperature. TLDs were calibrated for doses of 1 cGy to 10 Gy. Gafchromic EBT3 films were used next to TLDs to measure the scatter dose in the lungs in the presence of steep dose gradients. The films were analyzed after 24 h storage in the dark at room temperature using the dose-density curve for each batch of films.

For each technique a single dose of 10 to 12 Gy was delivered to the PTV, to ensure that the TLDs and films received a dose within its accuracy range. Measured doses were rescaled to the total dose that would be delivered per technique. Mean organ doses were calculated weighing the dose from each TLD or film for the percentage of the organ it represented. Each measurement was repeated 3 times.

Results

The mean organ doses per technique are shown in Table 1. The lungs had the highest mean doses, ranging from 50 to 200 cGy depending on the breast radiotherapy technique. The mean doses to the other organs varied a lot, but they generally remained well below 70 cGy. The only exception was the esophagus which received more than 100 cGy with the 3D-CRT APBI. The mean doses to the ovaries and uterus were very low, ranging from

1 to 8 cGy. Comparing the various techniques, whole breast radiotherapy delivered the highest doses overall. Conversely, all APBI techniques resulted in lower doses to the lungs and contralateral breast. The two Cyberknife techniques showed a slightly higher dose to the abdominal organs compared to other APBI techniques, which is due to the non-coplanar technique.

Table 1 Mean dose per organ for various breast radiotherapy techniques.

	WBI	3D-APBI	VMAT	MulticathHDR	Balloon HDR	CK-Iris	CK-MLC
Thyroid	17.6	10.4	1.6	15.5	20.6	9.0	14.3
Breast	45.5	6.6	14.9	17.4	24.2	18.8	30.2
Lung	202.1	114.6	182.1	58.4	93.7	129.5	132.6
Esophagus	33.0	116.3	48.4	41.8	63.5	40.5	25.8
Colon	21.8	3.7	0.5	12.4	19.6	59.0	32.7
Ovary	3.3	1.3	0.6	2.5	3.5	7.7	8.1
Uterus	2.6	1.1	0.5	1.8	2.4	5.6	6.0

Mean organ doses in cGy. WBI: Whole Breast Irradiation, 3D-APBI: 3D conformal Accelerated Partial Breast Irradiation, VMAT: Volumetric Modulated Arc partial breast radiotherapy, Multicath HDR: Multicatheter High Dose Rate brachytherapy, Balloon HDR: Balloon-based High Dose Rate brachytherapy, CK-Iris: Cyberknife stereotactic partial breast irradiation with Iris collimator, CK-MLC: Cyberknife stereotactic partial breast irradiation with multileaf collimator.

Table 2 shows the LARs for the individual organs and the total LARs per technique for ages at exposure of 40, 50, 60 and 80 years using the BEIR VII formalism. The results are presented graphically in Figure 1 for age at exposure of 50 years, which corresponds to the ASTRO "suitable group" and the GEC-ESTRO "low-risk group" [19-21]. As the secondary cancer risks are proportional to the mean organ doses, the comparison of the various techniques in terms of LAR yields the same findings as the comparison of the various techniques in terms of dose since the technique with the highest organ doses results in the highest LARs. The LAR values are highly variable between the organs. The lungs carry the highest LAR, with a 3.8% lifetime risk of a secondary lung malignancy for whole breast radiotherapy at age 50 years. In our calculations, lung tumors accounted for 75 to 97% of all secondary cancers. Conversely the LARs for the uterus were lower than 1/1000th of the LARs of the lungs.

Table 2 Lifetime Attributable Risks for various breast radiotherapy techniques.

Age		WBI	3D-APBI	VMAT	MulticathHDR	Balloon HDR	CK-Iris	CK-MLC
40	Thyroid	43	25	4	38	50	22	35
	Breast	521	76	171	199	277	215	346
	Lung	3687	2091	3322	1065	1709	2362	2419
	Esophagus	20	71	30	26	39	25	16
	Colon	148	25	3	84	133	402	223
	Ovary	7	3	1	5	7	16	17
	Uterus	3	1	1	2	3	6	6
	Total	**4429**	**2292**	**3531**	**1419**	**2219**	**3048**	**3061**
50	Thyroid	13	8	1	12	16	7	11
	Breast	283	41	93	108	151	117	188
	Lung	3847	2181	3466	1112	1784	2465	2524
	Esophagus	20	71	29	25	39	25	16
	Colon	142	24	3	81	127	383	212
	Ovary	6	2	1	5	7	14	15
	Uterus	3	1	0	2	2	5	6
	Total	**4314**	**2328**	**3594**	**1344**	**2124**	**3016**	**2972**
60	Thyroid	4	2	0	3	4	2	3
	Breast	132	19	43	51	70	55	88
	Lung	3668	2080	3305	1060	1700	2350	2406
	Esophagus	17	62	26	22	34	21	14
	Colon	124	21	3	71	112	336	186
	Ovary	5	2	1	4	5	11	12
	Uterus	2	1	0	1	2	4	4
	Total	**3952**	**2186**	**3378**	**1211**	**1927**	**2779**	**2713**
80	Thyroid	0	0	0	0	0	0	0
	Breast	16	2	5	6	9	7	11
	Lung	1580	896	1424	457	733	1012	1037
	Esophagus	6	21	9	8	12	7	5
	Colon	47	8	1	27	43	128	71
	Ovary	1	1	0	1	1	3	3
	Uterus	0	0	0	0	0	1	1
	Total	**1652**	**928**	**1439**	**499**	**797**	**1159**	**1128**

Lifetime Attributable Risks for a woman exposed at age 40, 50, 60 and 80 years. Excess cases per 100,000 exposed persons. WBI Whole Breast Irradiation, 3D-APBI 3D conformal accelerated partial breast radiotherapy, VMAT Volumetric Modulated Arc partial breast radiotherapy, Multicath HDR Multicatheter High Dose rate brachytherapy, Balloon HDR Balloon-based High Dose Rate brachytherapy, CK-Iris Cyberknife with Iris collimator, CK-MLC Cyberknife with multileaf collimator.

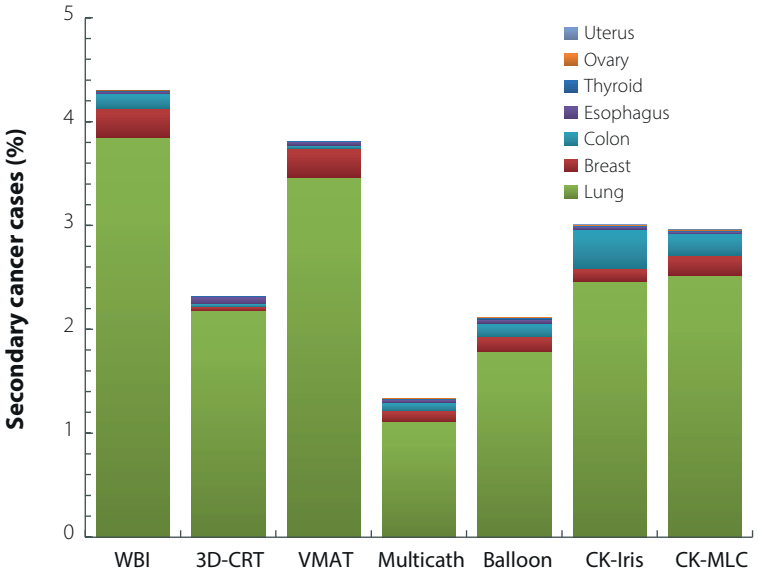

Figure 1 Lifetime attributable risk of secondary cancer per organ for the various breast radiotherapy techniques. Number of cases per 100,000 persons receiving adjuvant breast radiotherapy at age 50 years.

We calculated the RRs for women exposed at age 40, 50, 60 and 80 years as compared to non-irradiated breast cancer patients of the same age (Table 3). Selecting a threshold of 50% RR increase as being clinically significant, only the WBI and the VMAT technique are significantly increasing the risk of secondary lung cancer, which remains dominant in absolute numbers. Selecting a threshold of 10% as being clinically significant, there was an increased risk for lung cancer for all techniques at all ages. At this 10% threshold, there was also an increased risk for esophagus cancers, but the absolute numbers remain small. The risks for secondary malignancies of the thyroid, contralateral breast, ovaries and uterus were close to the baseline risks and may not be to detectable in population-based studies.

Table 3 Relative risks per organ for various breast radiotherapy techniques.

Age		WBI	3D-APBI	VMAT	Multicath HDR	Balloon HDR	CK-Iris	CK-MLC
40	Thyroid	1.046	1.027	1.004	1.040	1.054	1.023	1.037
	Breast	1.050	1.007	1.016	1.019	1.026	1.021	1.033
	Lung	**1.753**	1.427	**1.678**	1.217	1.349	1.482	1.494
	Esophagus	1.114	1.401	1.167	1.144	1.219	1.140	1.089
	Colon	1.040	1.007	1.001	1.023	1.036	1.108	1.060
	Ovary	1.007	1.003	1.001	1.005	1.007	1.015	1.016
	Uterus	1.001	1.001	1.000	1.001	1.001	1.003	1.003
50	Thyroid	1.018	1.011	1.002	1.016	1.021	1.009	1.015
	Breast	1.028	1.004	1.009	1.011	1.015	1.012	1.019
	Lung	**1.724**	1.410	**1.652**	1.209	1.336	1.464	1.475
	Esophagus	1.104	1.366	1.152	1.132	1.200	1.128	1.081
	Colon	1.036	1.006	1.001	1.020	1.032	1.097	1.054
	Ovary	1.006	1.002	1.001	1.004	1.006	1.014	1.014
	Uterus	1.001	1.000	1.000	1.001	1.001	1.003	1.003
60	Thyroid	1.007	1.004	1.001	1.006	1.008	1.004	1.006
	Breast	1.015	1.002	1.005	1.006	1.008	1.006	1.010
	Lung	**1.679**	1.385	**1.612**	1.196	1.315	1.435	1.446
	Esophagus	1.090	1.316	1.132	1.114	1.173	1.110	1.070
	Colon	1.032	1.005	1.001	1.018	1.029	1.086	1.048
	Ovary	1.005	1.002	1.001	1.004	1.005	1.012	1.013
	Uterus	1.001	1.000	1.000	1.001	1.001	1.002	1.002
80	Thyroid	1.000	1.000	1.000	1.000	1.001	1.000	1.000
	Breast	1.005	1.001	1.001	1.002	1.002	1.002	1.003
	Lung	**1.598**	1.339	**1.539**	1.173	1.277	1.383	1.392
	Esophagus	1.048	1.169	1.070	1.061	1.092	1.059	1.038
	Colon	1.017	1.003	1.000	1.010	1.015	1.046	1.025
	Ovary	1.003	1.001	1.001	1.002	1.003	1.007	1.007
	Uterus	1.001	1.000	1.000	1.000	1.001	1.001	1.001

Relative risks for a woman exposed at age 40, 50, 60 and 80 years, as compared to a non-irradiated localized breast cancer patient. Relative risks larger than 1.5 are shown in bold. WBI Whole Breast Irradiation, 3D-APBI 3D conformal accelerated partial breast radiotherapy, VMAT Volumetric Modulated Arc partial breast radiotherapy, Multicath HDR Multicatheter High Dose rate brachytherapy, Balloon HDR Balloon-based High Dose Rate brachytherapy, CK-Iris Cyberknife with Iris collimator, CK-MLC Cyberknife with multileaf collimator.

Discussion

Our study shows that all APBI techniques produce less scatter dose compared to whole breast radiotherapy, which translates into a lower secondary cancer risk. The use of APBI could eventually halve the lifetime secondary cancer risk. In our calculations, the lifetime risks are high, up to 4.3% for a woman treated at 50 years old. This strongly supports the generalization of partial breast irradiation as standard for early stage breast cancers or DCIS instead of whole breast radiotherapy.

Importantly our study also shows that the vast majority, between 75 and 97%, of the calculated secondary cancers involve the lungs. We calculated an absolute lifetime excess risk of lung cancer of 3.7% for patients treated with whole breast radiotherapy at age 60 years. The SEER database shows that the lifetime risk of lung cancer for a 60-year old female from the general population is 5.75% and the lifetime risk of dying from lung cancer is 4.66% [31]. This means that about 80% of lung cancer patients will die from their disease. Translated to our result, this means that whole breast radiotherapy could result in a 2.9% excess mortality due to secondary lung cancer.

One limitation of the present study is the use of a single phantom with average size breasts. Different patient geometries, for example larger breast volumes, may increase or decrease the mean lung dose for respectively brachytherapy or WBI [32]. However, those variations are relatively limited compared to the differences in techniques we tested. Also, the goal of this study was precisely to compare those techniques one with each other, which means we had to keep the patient's characteristics strictly identical between techniques, which is ideally performed using a phantom study.

Another limitation of the present study is the use of the BEIR-VII model for higher doses than intended in the report, where low doses were defined up to 0.1 Gy. Also, this model assumes a proportionality relationship that is not seen at doses above 3 or 4 Gy where a saturation effect has been demonstrated with a plateau between 10 and 20 Gy [33]. On the other hand, our predictions for lung cancer compare well with other studies. We calculated a lung cancer RR of 1.68 for patients receiving whole breast radiotherapy at age 60 years. This number is in good agreement with a meta-analysis of patients treated with whole breast radiotherapy between 1935 and 2007 at a median age of 56 years where the standardized incidence ratio for lung cancer after 15 years was 1.91 [5]. The mean lung doses were not reported in this meta-analysis, but they were likely higher compared to our phantom study as modern radiation machines have a reduced scatter dose compared to older ones. For example, we used a virtual wedge technique while patients treated between 1935 and 2007 in the Grantzau cohort had probably much more often treatment with physical wedges which generate a much higher scatter dose [32].

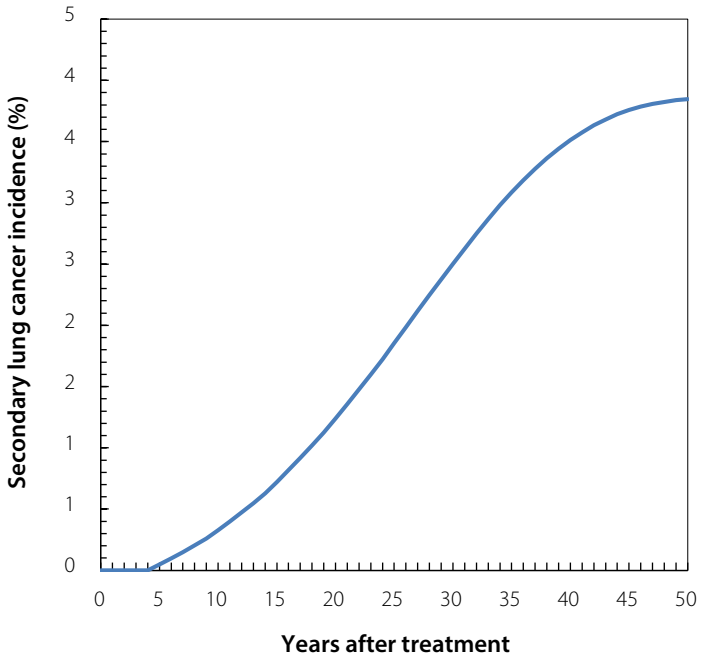

Figure 2 Time occurrence of secondary lung cancers for a person exposed at age 50.

Similarly, in the 2017 EBCTCG meta-analysis, which included 40,781 patients treated between 1972 and 1997 in randomized trials comparing the use of adjuvant radiotherapy or not, the RR of lung cancer at 10 years or more after irradiation was 2.1 [34]. This meta-analysis emphasized the large increased risk, about 10 times higher, for smokers versus non-smokers to develop secondary lung cancer applying the increased incidence probability to a population of non-smokers from the American Cancer Society Cancer Prevention Study II [35] and a population of smokers from the Million Women Study in the United Kingdom [36].

The calculated lifetime risk of secondary lung cancer mortality is high and is in the same order of magnitude as the survival benefit of radiotherapy. In the 2011 EBCTCG meta-analysis node negative patients had a 3.3% reduction of breast cancer related mortality at 15 years [37]. On the other hand Darby et al. calculated that a 50-year old woman would have a risk of death from ischemic heart disease of 0.5% before the age of 80 for a patient without pre-existing cardiac risk factors, and of 0.7% in case of one or more additional risk factors [4]. Such excess in cardiac mortality has encouraged the widespread implementation of preventive techniques, including deep inspiration breath-hold. Our

calculations showed an absolute increase in lung cancer mortality before age 80 of 2.4% for a 50-year old woman treated with WBI, which is about 4 times as high as the reported cardiac mortality. The excess of lung cancer mortality has not yet encouraged clinicians to actively adopt measures reducing the mean lung dose. It is noteworthy that cardiac events occur much earlier than secondary cancers. In the Darby study 44% of cardiac events occurred in the first 10 years after treatment [4]. The risk of secondary lung cancer is increased after a latency period of at least 5 years, and continued to increase up to 15 years [5]. In our calculations, 93% of all secondary lung cancers occurred after 10 years (Fig. 2). This latency may explain why earlier meta-analysis including trials with limited follow-up primarily stressed the cardiac morbidity and did not fully capture the risk of lung cancer mortality.

With this in mind, and in the context of the improved outcomes of early stage breast cancer, it is important to select radiotherapy techniques generating the lowest scatter dose possible. In this study the lowest mean lung dose was obtained using brachytherapy or 3D-conformal radiotherapy, both leading to doses between 1 and 1.5 Gy. Following the ALARA (As Low As Reasonably Achievable) principle [37], it is reasonable to recommend keeping the mean lung dose below this achievable level. For patients with more aggressive disease requiring loco-regional radiotherapy and who have a poorer prognosis, a higher value for the constraint on the mean lung dose may be acceptable, especially when regional nodes must be treated.

In conclusion, the present study finds an excess of lung cancer mortality due to irradiation that appears larger than the excess of cardiac mortality for early stage breast cancer patients having a very long survival. This risk can be greatly reduced using partial breast irradiation techniques minimizing the mean dose to the lung in addition to smoking prevention.

References

[1] National Cancer Institute Surveillance Epidemiology and End Results Program. Cancer Stat Facts: Female Breast Cancer. 2017; https://seer.cancer.gov/statfacts/html/breast.html.

[2] Clarke M, Collins R, Darby S, et al. Effects of radiotherapy and of differences in the extent of surgery for early breast cancer on local recurrence and 15-year survival: an overview of the randomised trials. Lancet. 2005; 366:2087-106.

[3] Cuzick J, Stewart H, Rutqvist L, et al. Cause-specific mortality in long-term survivors of breast cancer who participated in trials of radiotherapy. J Clin Oncol. 1994;12:447-53.

[4] Darby SC, Ewertz M, McGale P, et al. Risk of ischemic heart disease in women after radiotherapy for breast cancer. N Engl J Med. 2013;368:987-98.

[5] Grantzau T, Overgaard J. Risk of second non-breast cancer among patients treated with and without postoperative radiotherapy for primary breast cancer: A systematic review and meta-analysis of population-based studies including 522,739 patients. Radiother Oncol. 2016;121:402-13.

[6] Xu XG, Bednarz B, Paganetti H. A review of dosimetry studies on external-beam radiation treatment with respect to second cancer induction. Phys Med Biol. 2008;53:R193-241.

[7] Offersen B, Hojris I, Overgaard M. Radiation-induced heart morbidity after adjuvant radiotherapy of early breast cancer - Is it still an issue? Radiother Oncol. 2011;100:157-9.

[8] Vikstrom J, Hjelstuen MH, Mjaaland I, Dybvik KI. Cardiac and pulmonary dose reduction for tangentially irradiated breast cancer, utilizing deep inspiration breath-hold with audio-visual guidance, without compromising target coverage. Acta Oncol. 2011;50:42-50.

[9] Livi L, Meattini I, Marrazzo L, et al. Accelerated partial breast irradiation using intensity-modulated radiotherapy versus whole breast irradiation: 5-year survival analysis of a phase 3 randomised controlled trial. Eur J Cancer. 2015;51:451-63.

[10] Polgar C, Fodor J, Major T, Sulyok Z, Kasler M. Breast-conserving therapy with partial or whole breast irradiation: ten-year results of the Budapest randomized trial. Radiother Oncol. 2013;108:197-202.

[11] Rodriguez N, Sanz X, Dengra J, et al. Five-year outcomes, cosmesis, and toxicity with 3-dimensional conformal external beam radiation therapy to deliver accelerated partial breast irradiation. Int J Radiat Oncol Biol Phys. 2013;87:1051-7.

[12] Strnad V, Ott OJ, Hildebrandt G, et al. 5-year results of accelerated partial breast irradiation using sole interstitial multicatheter brachytherapy versus whole-breast irradiation with boost after breast-conserving surgery for low-risk invasive and in-situ carcinoma of the female breast: a randomised, phase 3, non-inferiority trial. Lancet. 2016;387:229-38.

[13] Hall EJ. Intensity-modulated radiation therapy, protons, and the risk of second cancers. Int J Radiat Oncol Biol Phys. 2006;65:1-7.

[14] Donovan EM, James H, Bonora M, Yarnold JR, Evans PM. Second cancer incidence risk estimates using BEIR VII models for standard and complex external beam radiotherapy for early breast cancer. Med Phys. 2012;39:5814-24.

[15] Han EY, Paudel N, Sung J, Yoon M, Chung WK, Kim DW. Estimation of the risk of secondary malignancy arising from whole-breast irradiation: comparison of five radiotherapy modalities, including TomoHDA. Oncotarget. 2016;7:22960-9.

[16] Pignol JP, Keller BM, Ravi A. Doses to internal organs for various breast radiation techniques--implications on the risk of secondary cancers and cardiomyopathy. Radiat Oncol. 2011;6:5.

[17] National Research Council. Health risks from exposure to low levels of ionizing radiation: BEIR VII phase 2: National Academies Press; 2006.

[18] Berrington de Gonzalez A, Iulian Apostoaei A, Veiga LH, et al. RadRAT: a radiation risk assessment tool for lifetime cancer risk projection. J Radiol Prot. 2012;32:205-22.

[19] Correa C, Harris EE, Leonardi MC, et al. Accelerated Partial Breast Irradiation: Executive summary for the update of an ASTRO Evidence-Based Consensus Statement. Pract Radiat Oncol. 2017;7:73-9.

[20] Smith BD, Arthur DW, Buchholz TA, et al. Accelerated partial breast irradiation consensus statement from the American Society for Radiation Oncology (ASTRO). Int J Radiat Oncol Biol Phys. 2009;74:987-1001.

[21] Polgar C, Van Limbergen E, Potter R, et al. Patient selection for accelerated partial-breast irradiation (APBI) after breast-conserving surgery: recommendations of the Groupe Europeen de Curietherapie-European Society for Therapeutic Radiology and Oncology (GEC-ESTRO) breast cancer working group based on clinical evidence (2009). Radiother Oncol. 2010;94:264-73.

[22] CDC. U.S. Decennial Life Tables for 1999-2001, United States Life Tables. 2008; ftp://ftp.cdc.gov/pub/Health_Statistics/NCHS/Publications/NVSR/57_01/Table02.xls.

[23] Surveillance, Epidemiology, and End Results (SEER) Program (www.seer.cancer.gov) SEER*Stat Database: Incidence - SEER 18 Regs Research Data + Hurricane Katrina Impacted Louisiana Cases, Nov 2015 Sub (1973-2013 varying) - Linked To County Attributes - Total U.S., 1969-2014 Counties, National Cancer Institute, DCCPS, Surveillance Research Program, released April 2016, based on the November 2015 submission.

[24] Surveillance, Epidemiology, and End Results (SEER) Program (www.seer.cancer.gov) SEER*Stat Database: Incidence - SEER 18 Regs Research Data + Hurricane Katrina Impacted Louisiana Cases, Nov 2016 Sub (2000-2014) <Katrina/Rita Population Adjustment> - Linked To County Attributes - Total U.S., 1969-2015 Counties, National Cancer Institute, DCCPS, Surveillance Research Program, released April 2017, based on the November 2016 submission.

[25] Ruschin M, Davidson SR, Phounsy W, et al. Technical Note: Multipurpose CT, ultrasound, and MRI breast phantom for use in radiotherapy and minimally invasive interventions. Med Phys. 2016;43:2508.

[26] National Surgical Adjuvant Breast and Bowel Project and Radiation Therapy Oncology Group. NSABP B-39/RTOG 0413: A randomized phase III study of conventional whole breast irradiation versus partial breast irradiation for women with stage 0, I, or II breast cancer. 2007; http://www.rtog.org/members/protocols/0413/0413.pdf.

[27] Baglan KL, Sharpe MB, Jaffray D, et al. Accelerated partial breast irradiation using 3D conformal radiation therapy (3D-CRT). Int J Radiat Oncol Biol Phys. 2003;55:302-11.

[28] Mellemkjaer L, Friis S, Olsen JH, et al. Risk of second cancer among women with breast cancer. Int J Cancer. 2006;118:2285-92.

[29] Raymond JS, Hogue CJ. Multiple primary tumours in women following breast cancer, 1973-2000. Br J Cancer. 2006;94:1745-50.

[30] Marcu LG, Santos A, Bezak E. Risk of second primary cancer after breast cancer treatment. Eur J Cancer Care (Engl). 2014;23:51-64.

[31] National Cancer Institute Surveillance Epidemiology and End Results Program. Table 15.20 Cancer of the Lung and Bronchus (Invasive). 2014; https://seer.cancer.gov/csr/1975_2014/browse_csr.php?sectionSEL=4&page-SEL=sect_04_table.17.html.

[32] Woo TC, Pignol JP, Rakovitch E, et al. Body radiation exposure in breast cancer radiotherapy: impact of breast IMRT and virtual wedge compensation techniques. Int J Radiat Oncol Biol Phys. 2006;65:52-8.

[33] Schneider U, Sumila M, Robotka J. Site-specific dose-response relationships for cancer induction from the combined Japanese A-bomb and Hodgkin cohorts for doses relevant to radiotherapy. Theor Biol Med Model. 2011;8:27.

[34] Taylor C, Correa C, Duane FK, et al. Estimating the Risks of Breast Cancer Radiotherapy: Evidence From Modern Radiation Doses to the Lungs and Heart and From Previous Randomized Trials. J Clin Oncol. 2017;35:1641-9.

[35] Thun MJ, Henley SJ, Burns D, et al: Lung cancer death rates in lifelong nonsmokers. J Natl Cancer Inst. 2006;98:691-9.

[36] Pirie K, Peto R, Reeves GK, et al: The 21st century hazards of smoking and benefits of stopping: A prospective study of one million women in the UK. Lancet 2013;381:133-41.

[37] Prasad KN, Cole WC, Haase GM. Radiation protection in humans: Extending the concept of as low as reasonably achievable (ALARA) from dose to biological damage. Br J Radiol 2004;77:97–99.

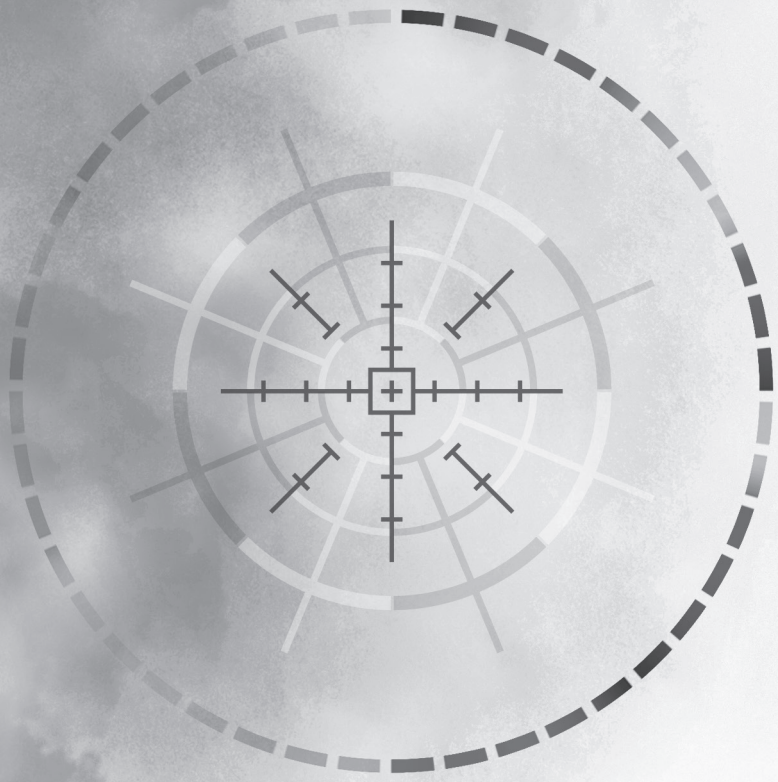

3

Reducing the risk of secondary lung cancer

Published as
Reducing the risk of secondary lung cancer in treatment planning of accelerated partial breast irradiation
Nienke Hoekstra, MD[1], Steven Habraken, PhD[1], Annemarie Swaak-Kragten, MD[1], Sebastiaan Breedveld, PhD[1], Jean-Philippe Pignol, MD, PhD[2], Mischa Hoogeman, PhD[1]

1. Erasmus MC Cancer Institute, Department of Radiation Oncology, PO Box 2040, 3000 CA Rotterdam, The Netherlands
2. Dalhousie University, Department of Radiotherapy, 5820 University Avenue, Halifax NS B3H1V7, Canada

Frontiers in Oncology, 10:1445, 2020
DOI: 10.3389/fonc.2020.01445

Abstract

Purpose Adjuvant accelerated partial breast irradiation (APBI) results in low local recurrence risks. However, the survival benefit of adjuvant radiotherapy APBI for low-risk breast cancer might partially be offset by the risk of radiation-induced lung cancer. Reducing the lung dose mitigates this risk, but this could result in higher doses to the ipsilateral breast. Different external beam APBI techniques are equally conformal and homogenous, but the intermediate to low dose distribution differs. Thus, the risk of toxicity is different. The purpose of this study is to quantify the trade-off between secondary lung cancer risk and breast dose in treatment planning and to compare an optimal coplanar and non-coplanar technique.

Methods A total of 440 APBI treatment plans were generated using automated treatment planning for a coplanar VMAT beam-setup and a non-coplanar robotic stereotactic radiotherapy beam-setup. This enabled an unbiased comparison of two times 11 Pareto-optimal plans for 20 patients, gradually shifting priority from maximum lung sparing to maximum ipsilateral breast sparing. The excess absolute risks of developing lung cancer and breast fibrosis were calculated using the Schneider model for lung cancer and the Avanzo model for breast fibrosis.

Results Prioritizing lung sparing reduced the mean lung dose from 2.2 Gy to as low as 0.3 Gy for the non-coplanar technique and from 1.9 Gy to 0.4 Gy for the coplanar technique, corresponding to a seven-fold and four-fold median reduction of secondary lung cancer risk respectively compared to prioritizing breast sparing. The increase in breast dose resulted in a negligible 0.4% increase in fibrosis risk. The use of non-coplanar beams resulted in lower secondary cancer and fibrosis risks ($p<0.001$). Lung sparing also reduced the mean heart dose for both techniques.

Conclusions The risk of secondary lung cancer of external beam APBI can be dramatically reduced by prioritizing lung sparing during treatment planning. The associated increase in breast dose did not lead to a relevant increase in fibrosis risk. The use of non-coplanar beams systematically resulted in the lowest risks of secondary lung cancer and fibrosis. Prioritizing lung sparing during treatment planning could increase the overall survival of early-stage breast cancer patients by reducing mortality due to secondary lung cancer and cardiovascular toxicity.

Introduction

The prognosis of early-stage breast cancer patients is excellent, with a cancer-specific survival of almost 99% at 5 years [1]. However, the mortality from radiation induced secondary cancers, especially lung cancers, may offset the survival benefit for certain subgroups [2, 3]. There are several models that quantitatively relate dose to the lungs to the risk of secondary lung cancer [4, 5]. Thus, reducing the amount of radiation to the lungs during treatment planning could reduce the long-term overall mortality of early stage breast cancer patients.

One option is the use of accelerated partial breast irradiation (APBI) instead of whole breast irradiation (WBI) for early stage breast cancer patients that are eligible according to international guidelines [6-11]. Long-term results of randomized trials indicate that local control and survival are non-inferior to whole breast radiotherapy [12-17]. Dose comparison studies have shown that the dose to the lungs is significantly lower with APBI compared to WBI but varies greatly depending on the APBI technique used [3, 18-23]. The conformality and homogeneity of the different contemporary APBI techniques were similar [21-23]. This means that the differences between the external beam APBI techniques are not in the high dose region but in the intermediate and low dose regions where radiation induced malignancies occur. The protocols used in these studies accepted a high lung dose constraint without recommendation to minimize the lung dose well below this constraint. It is unknown to what extent the lung dose can be reduced if highly prioritized during treatment planning and how this impacts the dose to other organs. In the case of APBI, reducing the dose to the lungs mainly results in a higher dose to the ipsilateral non-target breast tissue. For example, this might result in more breast toxicity including fibrosis.

The aim of this study was twofold: First, we explored the trade-off between reduction of the mean lung dose as a surrogate of secondary cancer risk and the ipsilateral breast dose distribution as a surrogate of the breast fibrosis risk. Second, we compared coplanar and non-coplanar external beam APBI treatment techniques, using two state-of-the-art techniques, VMAT APBI and stereotactic CyberKnife APBI (CK APBI).

Materials and Methods

Patients and CT-scans

Anonymized CT data of twenty female early-stage breast cancer patients treated at Erasmus MC were included. We randomly selected patients that were previously treated with WBI after breast conserving surgery at our institution. Ethical approval for this retrospective study was not required according to Dutch legislation and the Central

Committee on Research Involving Human Subjects. All patients were eligible for APBI according to the 2017 ASTRO selection guidelines [9] and institutional guidelines, meaning they were at least 50 years of age and had a Tis or T1 tumor of less than 2.5 cm. At Erasmus MC APBI is not used if the ratio of the PTV to the ipsilateral breast volume is more than 30%. A dose of 28.5 Gy in five daily fractions is prescribed.

All patients had a free breathing planning CT-scan in supine position with both arms raised. The tumor bed was delineated as the volume encompassing the seroma, the postoperative changes and the surgical clips. It was expanded with a uniform margin of 10 mm to create the CTV, excluding the thoracic wall and the skin. The skin was defined as the first 5 mm within the patient contour. Accounting for daily image guidance, a CTV to PTV expansion of 5 mm was used.

The delineated organs at risk (OARs) included the ipsilateral and contralateral lungs and breasts, the non-target breast tissue, defined as the ipsilateral breast minus PTV, and heart.

Treatment planning

We created coplanar VMAT and non-coplanar CyberKnife stereotactic APBI plans using Erasmus-iCycle [24]. For both techniques, the 28.5 Gy isodose line had to encompass at least 95% of the PTV volume. The maximum allowed dose over all voxels was 33 Gy. Planning constraints are summarized in Table 1.

Table 1 Planning constraints

Structure	Clinical constraints
PTV coverage	28.5 Gy in at least 95%
Ipsilateral breast	$V_{30\,Gy} < 20\%$, $V_{15\,Gy} < 40\%$
Contralateral breast	Maximum dose to 2 cc of 1 Gy
Ipsilateral lung	$V_{9\,Gy} < 15\%$
Contralateral lung	$V_{1.5\,Gy} < 15\%$
Heart	Right-sided lesions: $V_{1.5\,Gy} < 5\%$ Left-sided lesions: $V_{1.5\,Gy} < 40\%$

Erasmus-iCycle is an optimizer for multi-criterial beam-profile optimization and optional beam-angle selection applicable to coplanar and non-coplanar IMRT, VMAT and stereotactic RT. It uses a wish-list, including planning constraints and prioritized objectives. Details and validation of the algorithm have been described elsewhere [24, 25]. Plans created by Erasmus-iCycle are Pareto-optimal, which means that it is not possible to improve one objective without deteriorating another one. The primary endpoint of this study was the

dose distribution in the intermediate and low dose regions. As these regions are outside the actual target and include different densities such as lung, there may be a loss of electronic equilibrium. A Monte-Carlo based dose engine accurately accounts for these situations. We used the dose engine called GPUMCD [26].

The APBI wish-list for this study included constraints on the maximum dose to the PTV, heart and contralateral breast as well as constraints on conformality. The first objective was to ensure a PTV coverage of at least 95% of the volume with a minimum of 28.5 Gy. The second objective was to minimize the dose to the lungs and the ipsilateral breast. The clinical constraints are detailed in Table 1 and were derived from constraints used in clinical trials on external beam APBI, and more specifically stereotactic APBI using a five fraction regimen [27-29]. Left- and right-sided cases were optimized using separate wish-lists with different heart constraints.

Starting from a single personalized plan that equally weighted lung and ipsilateral breast tissue dose, we varied the priorities in ten incremental steps. This resulted in 11 plans per patient and per technique, ranging from maximally sparing the lung to maximally sparing the ipsilateral breast tissue. During this phase, the dose and coverage of the PTV and the doses to the other OARs were kept constrained to their already obtained values. The prioritization weights varied from a maximum reduction of dose to the breast tissue to a maximum reduction of the lung dose, in nine incremental steps in between. This resulted for each patient in 11 Pareto-optimal plans per technique, covering the full range of lung and breast dose sparing possible.

Coplanar VMAT was planned using 27 coplanar beams with 10° separation to create an arc of 260 degrees. For left-sided cases, the arc ranged from 280° to 180° and for right-sided cases from 80° to 180°. The non-coplanar CyberKnife technique used a multi-leaf collimator and a set of 41 nodes typically used clinically. For both techniques the energy was 6 MV. The planning optimization for the two techniques used the same wish-list, to ensure that trade-offs between PTV coverage, conformality and organ at risk sparing were identical between the coplanar and non-coplanar plans.

Analysis

For all plans, we collected an identical set of dose parameters including PTV coverage and mean doses to the lungs, the entire ipsilateral breast, the non-target ipsilateral breast tissue, and the heart.

We calculated the risk of ipsilateral breast fibrosis using the model of Avanzo et al. with complete repair, since the fractionation was once daily [30]. The parameters used were BEUD50 = 107.2 Gy, volume parameter n = 0.06, slope of dose response m = 0.22 and α/β ratio = 3 Gy.

We calculated the risk of secondary lung cancer for all scenarios using the model of Schneider et al. [5]. This model calculates the excess absolute risk (EAR) of secondary cancer for an organ at a specified age a and with a radiation exposure at age x. It takes into account the effects of dose fractionation, repair and repopulation and is based on the full dose distribution within an organ. The parameters used were $\beta = 8.0$, $\gamma e = 0.002$, $\gamma a = 4.23$, agea = 70 years, agex = 50 years, $R = 0.83$, $\alpha = 0.042$ Gy-1, and $\alpha/\beta = 3$ Gy.

We compared coplanar and non-coplanar plans with the Wilcoxon signed rank test. We compared the left-sided and right-sided cases with the non-parametric unrelated samples Mann-Whitney U test. A p-value of 0.05 or less was considered significant. All statistical analyses were done in SPSS Statistics version 25.

Results

Of the twenty early stage breast cancer patients included in this study, 11 cases were right-sided and 9 were left-sided and the median volume of the delineated tumor bed was 11.0 cc (range 1.6 to 51.7 cc). The median volume of the PTV was 92.2 cc (range 58.6 – 246.9 cc). The median ratio PTV/ipsilateral breast volume was 15.1% (range 7.2 – 22.3%).

Figure 1 shows an example of the dose distributions of coplanar and non-coplanar plans with different priorities. When giving more priority to lung sparing, the low dose isodose lines shift from a more opposing configuration to a more tangent one. The average DVHs over 20 patients is shown in Figure 2 for the coplanar and non-coplanar plans for maximum lung sparing and maximum breast sparing.

For 2 out of 20 patients, the coplanar treatment plans did not fulfil the clinical heart constraint. In one left-sided case, the heart was very close to the PTV. The $V_{1.5Gy}$ was 59% with a mean heart dose of 4.6 Gy. The other case was a very medial right-sided tumor. The $V_{1.5Gy}$ for this case was 22% and the mean heart dose 1.6 Gy. The PTV coverage and the other OAR constraints were not violated. Conversely, all non-coplanar plans fulfilled all the constraints.

The dose parameters, secondary lung cancer risks and fibrosis risks are summarized in Table 2. The median reduction in EAR for secondary lung cancer between the plans with maximum lung sparing and the plans with maximum breast sparing was five-fold, ranging from 1.1 to 14.8 folds. Comparing VMAT with CK ABPI, the median absolute difference was 11.6 cases per 10,000 patient years for the non-coplanar CK technique and 8.1 cases per 10,000 patient years for the coplanar VMAT technique. The reduction in mean lung dose when prioritizing lung sparing among all patients ranged from 0.21 Gy to 2.06 Gy for

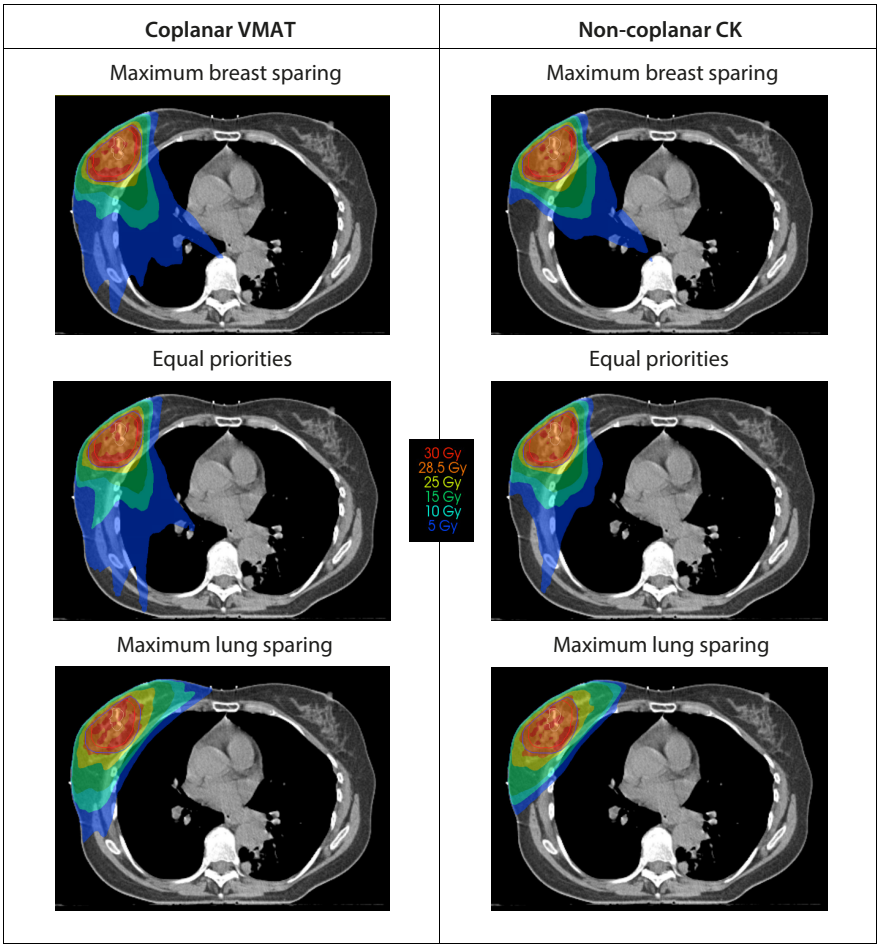

Figure 1 Dose distributions for an example case. The dose distributions on the left show coplanar VMAT plans, on the right non-coplanar CyberKnife (CK) plans. The upper dose distributions are plans with maximum priority to sparing of the breast tissue, and the lower dose distributions are plans with maximum sparing of the lungs. The middle dose distributions are plans with equal priorities to the sparing of lung and breast tissue.

the coplanar technique and from 0.69 Gy to 3.37 Gy for the non-coplanar technique. The median reduction of the dose to the ipsilateral breast in the breast sparing plans compared with the lung sparing plans was 3.5 Gy for the coplanar technique (range 0.41 – 4.73 Gy) and 5.1 Gy for the non-coplanar technique (range 2.21 – 6.55 Gy). This dose difference resulted in only a very small increase in fibrosis risk of 0.4% and 0.5% respectively.

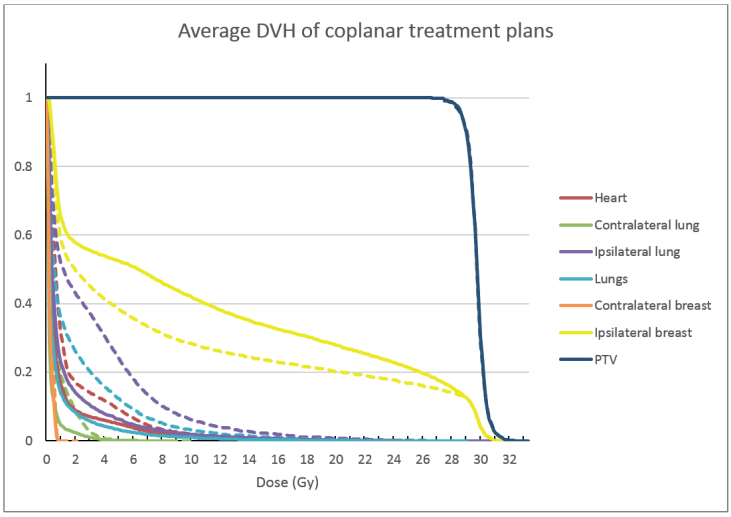

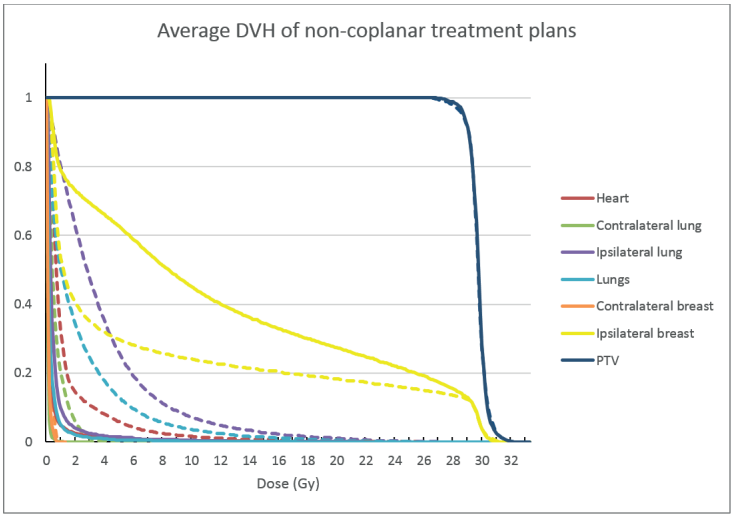

Figure 2 Average DVHs for the different treatment plans. Coplanar VMAT plans are shown in [**A**], non-coplanar CyberKnife (CK) plans are shown in [**B**]. The solid lines show the results for the plan that fully prioritizes lung sparing. The dashed lines show the result of the treatment plan that fully prioritizes breast sparing.

Table 2 Dose parameters and toxicity risks

	Coplanar			Non-coplanar		
	Breast sparing	**Equal priorities**	**Lung sparing**	**Breast sparing**	**Equal priorities**	**Lung sparing**
PTV coverage (%)	95.9 (95.6 – 96.1)	95.9 (95.7 – 96.0)	96.5 (96.0 – 96.9)	95.7 (95.4 – 96.1)	95.5 (95.2 – 95.9)	96.8 (96.5 – 97.4)
Lungs mean dose (Gy)	1.9 (1.6 – 2.2)	1.4 (1.0 – 1.6)	0.4 (0.3 – 0.8)	2.2 (2.0 – 2.5)	1.1 (0.7 – 1.2)	0.3 (0.2 – 0.4)
Ipsilateral breast mean dose (Gy)	8.0 (6.8 – 9.7)	8.4 (7.0 – 10.1)	11.5 (8.4 – 12.9)	7.3 (5.4 – 8.7)	8.2 (6.2 – 9.4)	12.4 (9.6 – 13.7)
Non-target breast tissue mean dose (Gy)	4.8 (4.1 – 5.7)	5.1 (4.4 – 6.2)	8.3 (6.2 – 9.4)	3.7 (2.6 – 4.5)	4.4 (3.5 – 5.5)	9.8 (7.5 – 10.5)
Heart mean dose (Gy)						
- Left-sided cases	2.3 (1.7 – 3.3)	1.8 (1.2 – 3.3)	0.6 (0.2 – 2.6)	2.0 (1.5 – 3.0)	1.2 (0.5 – 2.8)	0.3 (0.1 – 1.3)
- Right-sided cases	0.6 (0.6 – 0.7)	0.6 (0.5 – 0.6)	0.4 (0.2 – 0.5)	0.7 (0.6 – 0.7)	0.5 (0.5 – 0.7)	0.1 (0.1 – 0.2)
EAR secondary lung cancer	11.3 (9.7 – 13.3)	8.8 (6.9 – 9.9)	3.2 (2.4 – 5.3)	13.7 (12.7 – 15.1)	7.2 (5.6 – 8.4)	2.1 (1.5 – 2.6)
Breast fibrosis risk (%)	7.7 (6.3 – 8.6)	7.7 (6.3 – 8.6)	8.2 (6.6 – 9.1)	7.6 (6.2 – 8.6)	7.5 (6.2 – 8.5)	8.0 (6.5 – 8.9)

All data is shown as median (interquartile range). EAR Excess Absolute Risk per 10,000 patient years

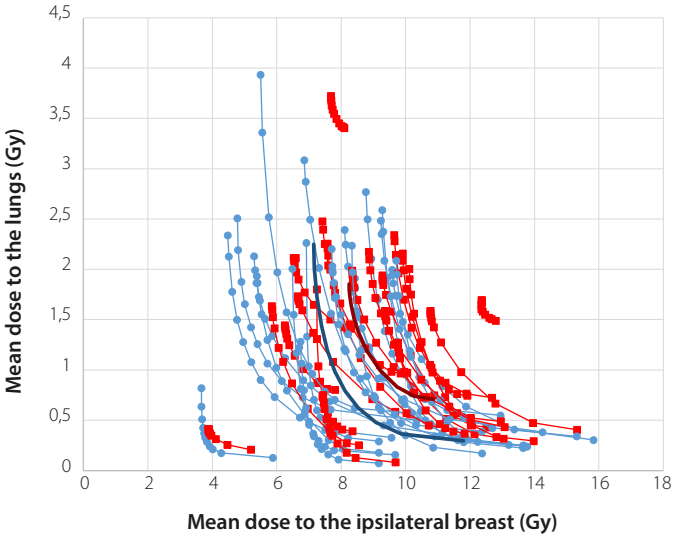

Figure 3 Pareto fronts of the mean doses to the ipsilateral breast and lungs. Non-coplanar CyberKnife (CK) plans are shown in blue circles, coplanar VMAT plans are shown in red squares. The thick line shows the mean per technique.

Table 3 Comparison of coplanar and non-coplanar techniques

	Coplanar	Non-coplanar	Wilcoxon signed rank test
PTV coverage (%)	95.9	95.6	$p < 0.001$
Lungs mean dose (Gy)	1.3	0.9	$p < 0.001$
Ipsilateral breast mean dose (Gy)	9.0	8.3	$p < 0.001$
Non-target breast tissue mean dose (Gy)	5.6	4.7	$p < 0.001$
Heart mean dose (Gy)	0.65	0.63	$p < 0.001$
EAR secondary lung cancer	8.3	6.3	$p < 0.001$
Breast fibrosis risk (%)	8.0	7.7	$p < 0.001$

Median values over all plans for all cases per technique. EAR Excess Absolute Risk per 10,000 patient years

Figure 3 shows the Pareto-fronts of all patients of the trade-off between mean lung dose and mean ipsilateral breast dose. The non-coplanar plans systematically resulted in lower doses to both lungs and ipsilateral breast tissue (Table 3, Wilcoxon signed rank test $p < 0.001$). The Pareto-fronts did not cross for any patient, meaning that for a given dose to one organ, the dose to the other organ was higher in the coplanar treatment plan in all cases.

Table 4 Dose parameters and toxicity risks for left-sided and right-sided tumor location

	Coplanar				Non-coplanar			
	Breast sparing		Lung sparing		Breast sparing		Lung sparing	
	Left-sided	Right-sided	Left-sided	Right-sided	Left-sided	Right-sided	Left-sided	Right-sided
PTV coverage (%)	95.9 (95.8 – 96.5)	95.9 (95.6 – 96.1)	96.7 (96.3 – 97.3)	96.1 (95.9 – 96.9)	95.6 (95.4 – 96.3)	95.7 (95.4 – 95.9)	97.2 (96.4 – 97.6)	96.8 (96.6 – 96.9)
Lungs mean dose (Gy)	1.8 (1.5 – 2.1)	1.9 (1.6 – 2.3)	0.4 (0.3 – 1.1)	0.5 (0.4 – 0.8)	2.2 (2.0 – 2.5)	2.2 (2.0 – 2.6)	0.3 (0.2 – 0.4)	0.3 (0.2 – 0.3)
Ipsilateral breast mean dose (Gy)	8.3 (6.2 – 9.9)	7.7 (7.4 – 9.3)	11.8 (8.3 – 12.9)	11.2 (9.7 – 12.9)	7.7 (5.1 – 9.0)	6.8 (5.5 – 8.4)	12.4 (9.2 – 13.9)	12.4 (9.7 – 13.7)
Non-target breast tissue mean dose (Gy)	4.1 (3.0 – 6.3)	4.9 (4.5 – 5.6)	8.2 (4.8 – 9.7)	8.3 (7.2 – 9.4)	3.5 (2.0 – 4.7)	3.8 (2.9 – 4.4)	8.9 (6.0 – 10.6)	9.9 (7.7 – 10.5)
Heart mean dose (Gy)	2.3 (1.7 – 3.3)	0.6 (0.6 – 0.7)	0.6 (0.2 – 2.6)	0.4 (0.2 – 0.5)	2.0 (1.5 – 3.0)	0.7 (0.6 – 0.7)	0.3 (0.1 – 1.3)	0.1 (0.1 – 0.2)
EAR secondary lung cancer	10.8 (9.5 – 12.5)	11.8 (9.6 – 14.3)	2.9 (2.1 – 6.3)	3.5 (2.7 – 5.5)	13.8 (12.7 – 15.0)	13.5 (12.6 – 16.1)	2.1 (1.4 – 3.0)	2.1 (1.7 – 2.2)
Breast fibrosis risk (%)	8.5 (6.0 – 9.0)	6.9 (6.3 – 8.5)	8.7 (6.2 – 9.2)	7.1 (6.8 – 8.9)	8.4 (5.8 – 8.8)	6.8 (6.2 – 8.4)	8.7 (6.1 – 9.2)	7.1 (6.5 – 8.8)

All data is shown as median (interquartile range). EAR Excess Absolute Risk per 10,000 patient years

In Table 4, the dose parameters are reported for the left-sided and right-sided case separately. Using the unrelated samples Mann-Whitney U test, there were no significant differences between the two groups except for the mean heart dose. The mean heart dose was higher for the left-sided cases for both techniques and for both the lung sparing plan and the breast sparing plan.

Figure 4 details the comparison of the breast sparing plan on the x-axis and the lung sparing plan on the y-axis per individual patient. A point below the unity line means that the lung sparing plan had a lower value than the breast sparing plan. The coplanar plans are shown as circles and the non-coplanar plans as squares. Figure 4(a) shows that the

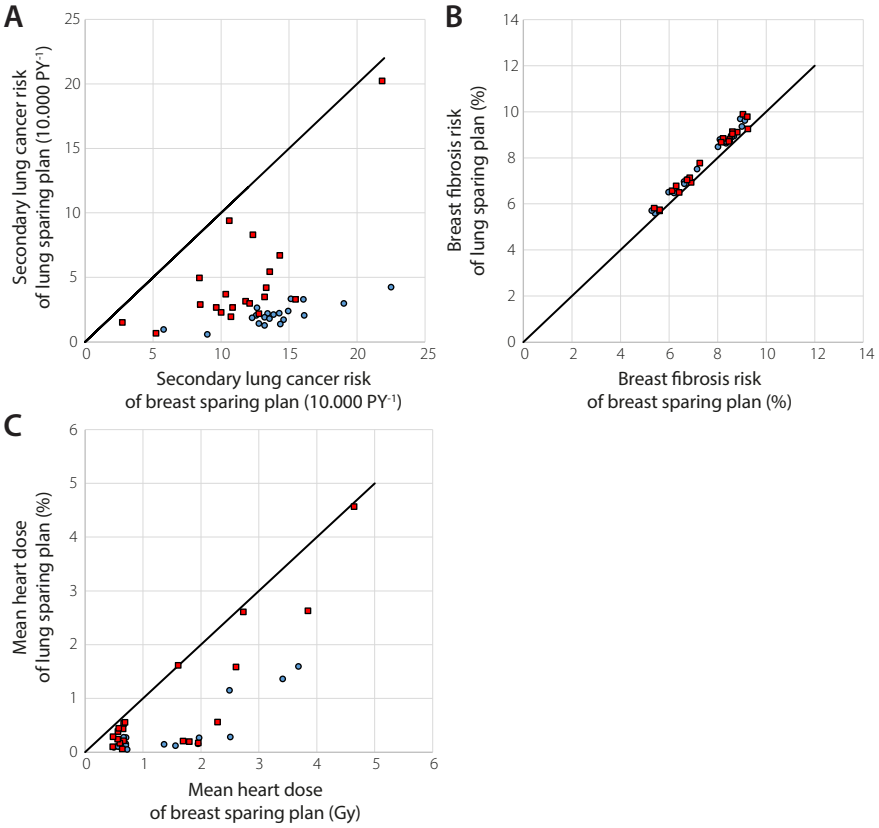

Figure 4 Scatterplots of the maximum breast sparing plans versus the maximum lung sparing plans. Figure **A** shows the secondary lung cancer risk, figure **B** the breast fibrosis risk and figure **C** the mean heart dose. Non-coplanar CyberKnife (CK) plans are shown in blue circles, coplanar VMAT plans are shown in red squares. Data points below the unity line indicate an advantage for the dose plan on the vertical axis.

absolute secondary lung cancer risks were lower for the non-coplanar technique than for the coplanar technique. The fact that the squares are at a larger distance from the unity line suggests that the differences between the lung sparing and breast sparing plans were larger for the non-coplanar technique. The breast fibrosis risks (Figure 4(b)) are close to the unity line for both techniques.

The dose to the heart was also reduced in the lung sparing plans without any specific constraint to do so. The difference in mean heart dose for the left-sided cases was 1.7 Gy and 1.2 Gy for the non-coplanar and coplanar techniques respectively. For the right-sided cases, the difference in mean heart dose was 0.5 Gy and 0.2 Gy respectively. The comparison is shown in Figure 4(c).

Discussion

This study shows that it is possible to dramatically reduce the mean lung dose and hence the risk of secondary lung cancer for APBI by giving a higher priority to lung sparing. The median risk reduction was five-fold, with a range of 1.1 to 14.8 folds. This translates into a median absolute risk reduction of 11.6 cases per 10,000 patient years for the non-coplanar technique and 8.1 for the coplanar technique, which is highly clinically relevant, as these patients are expected to survive several decades. The mortality of lung cancer is about 80% [31]. Multiplying the absolute risk reduction by 0.8 shows that minimizing the lung dose could theoretically reduce the overall mortality of early-stage breast cancer patients with 9.3 persons per 10,000 patient years for the non-coplanar technique and with 6.5 persons per 10,000 patient years for the coplanar technique.

Shifting the dose away from the lungs resulted in a higher dose to the ipsilateral non-target breast tissue. However, the increase in mean breast dose of 3.5 and 5.1 Gy translated into a small increase in the risk of breast fibrosis of 0.5 and 0.4%-point for the coplanar and non-coplanar technique, which is not clinically relevant. The limited increase in the calculated fibrosis risk could be explained by the NTCP model used, and notably the n parameter of 0.06 used in the model of Avanzo et al. [30]. This value means that the risk of fibrosis is defined primarily by the high dose volume. The planning constraints that affect the high dose volume are the PTV constraints. These constraints were kept constant for the plans with different priorities in our study. This resulted in plans with very small differences in the dose to the PTV and consequently in the risk of fibrosis. The differences between the plans with the different priorities were in the intermediate and low dose regions, and these regions have a very limited effect in the fibrosis model.

The Avanzo model for breast fibrosis is the only published model addressing APBI. One weakness of this model is the limited data on which it is based as well as the lack of external validation. However, other models of fibrosis for WBI also found that this risk mainly depends on the high dose region [32, 33]. Using the WBI fibrosis model of Mukesh et al. resulted in absolute fibrosis risks of about 17%, but the differences between the breast sparing plans and the lung sparing plans remained very small [32].

An important finding of this study is that the use of non-coplanar beams always resulted in a more favorable dose distribution, as shown in Figure 2. In this study we used CyberKnife stereotactic radiotherapy, which provides more degrees of freedom in treatment planning than coplanar VMAT. The Pareto fronts of the two techniques did not cross for any patient, and the non-coplanar technique always had the lowest doses and lowest risks of secondary lung cancer and breast fibrosis. The non-coplanar technique also had a wider front, showing a larger dynamic range for sparing of specific organs. The difference between the techniques was statistically significant, as is shown in Table 3. The PTV coverage was slightly closer to 95% for the non-coplanar technique. The aim of our automated planning technique was to get a coverage of 95%, but not higher. This means that a coverage closer to 95% is in fact a better result than a higher coverage. The non-coplanar technique has more freedom to get a coverage that is close to the requested value and to reduce doses to other organs.

Incidentally, we found that optimizing lung sparing also resulted in lower doses to the heart. The mean heart dose in the lung sparing plans for the left-sided cases was on average 1.7 and 1.2 Gy lower than in the breast sparing plan for the non-coplanar and coplanar techniques respectively. This is clinically significant following the model published by Darby et al. who reported a linear dose-response relationship between mean heart dose and cardiovascular events without a threshold. This means that optimizing lung sparing would also result in a lower risk of cardiovascular events [34-36].

There are some limitations in the present study. We did not compare all possible external beam APBI techniques. For example, 3D-conformal APBI is often used, but we have chosen to use only the coplanar and non-coplanar techniques with the highest conformality. 3D-conformal APBI would have resulted in an artificially increased dose to the ipsilateral non-target breast tissue. Intuitively there are concerns that the lung dose might be higher with VMAT compared to 3D-conformal RT. However, Essers et al. showed that the lung dose would be lower with VMAT when using partial arcs [37]. In our study, the optimizer was free to select from all available beam angles, and it chose only partial arcs for the lung sparing plans and not for the breast sparing plans. This is in agreement with the conclusion of Essers et al.

We have chosen to use Erasmus-iCycle because it can generate true bias-free comparisons using exactly the same wish-list for all plans without any human interference. Treatment plans created in Erasmus-iCycle are based on fluence map optimization. They need to be converted into segmented dose plans before the plan is deliverable to a real patient. With the right algorithm, the difference between fluence map optimized plans and segmented plans is small [38]. The VMAT and CK would need to be converted using different treatment planning software with different dose calculation algorithms. This could influence the results. The dose parameters for our plans with equal priorities are comparable to the dose levels reported in literature [23].

We used the full model of Schneider et al. for the calculation of the secondary lung cancer risk [5]. This model takes into account cell killing and fractionation effects and uses the full dose distribution in the organ. It is specifically created for radiotherapy patients, but it is based on limited epidemiological data. The BEIR VII model is based on more extensive epidemiological data, but this model is made for radiation protection purposes and intended for use in low dose exposures only [4]. Using this model would result in the same conclusion, that prioritizing lung sparing reduces the secondary cancer risk. For this model, the reduction for non-coplanar CK is 8.9-fold and for coplanar VMAT 3.9-fold, compared to 6.5-fold and 3.5-fold respectively for the Schneider model.

In conclusion, the risk of secondary lung cancer of external beam APBI can be greatly reduced by prioritizing lung sparing during treatment planning. The associated increase in breast dose did not lead to a relevant increase in fibrosis risk. Lung sparing also resulted in a lower mean heart dose. Thus, prioritizing lung sparing could increase the overall survival of early-stage breast cancer patients by reducing mortality due to secondary lung cancer and cardiovascular toxicity. The use of non-coplanar beams resulted in both a lower secondary lung cancer risk and a lower fibrosis risk which suggests that it should be favored for breast APBI.

References

[1] Surveillance, Epidemiology, and End Results (SEER) Program (www.seer.cancer.gov) SEER*Stat Database: Incidence - SEER 18 Regs Research Data + Hurricane Katrina Impacted Louisiana Cases, Nov 2016 Sub (2000-2014) <Katrina/Rita Population Adjustment> - Linked To County Attributes - Total U.S., 1969-2015 Counties, National Cancer Institute, DCCPS, Surveillance Research Program, released April 2017, based on the November 2016 submission.

[2] Taylor C, Correa C, Duane FK, et al. Estimating the Risks of Breast Cancer Radiotherapy: Evidence From Modern Radiation Doses to the Lungs and Heart and From Previous Randomized Trials. J Clin Oncol. 2017;35:1641-9.

[3] Hoekstra N, Fleury E, Merino Lara TR, et al. Long-term risks of secondary cancer for various whole and partial breast irradiation techniques. Radiotherapy and Oncology. 2018.

[4] National Research Council. Health risks from exposure to low levels of ionizing radiation: BEIR VII phase 2: National Academies Press; 2006.

[5] Schneider U, Sumila M, Robotka J. Site-specific dose-response relationships for cancer induction from the combined Japanese A-bomb and Hodgkin cohorts for doses relevant to radiotherapy. Theoretical Biology and Medical Modelling. 2011;8:27.

[6] Smith BD, Arthur DW, Buchholz TA, et al. Accelerated partial breast irradiation consensus statement from the American Society for Radiation Oncology (ASTRO). Int J Radiat Oncol Biol Phys. 2009;74:987-1001.

[7] Polgar C, Van Limbergen E, Potter R, et al. Patient selection for accelerated partial-breast irradiation (APBI) after breast-conserving surgery: recommendations of the Groupe Europeen de Curietherapie-European Society for Therapeutic Radiology and Oncology (GEC-ESTRO) breast cancer working group based on clinical evidence (2009). Radiother Oncol. 2010;94:264-73.

[8] American Society of Breast Surgeons. Consensus Statement for Accelerated Partial Breast Irradiation. 2011; https://www.breastsurgeons.org/new_layout/about/statements/PDF_Statements/APBI.pdf.

[9] Correa C, Harris EE, Leonardi MC, et al. Accelerated Partial Breast Irradiation: Executive summary for the update of an ASTRO Evidence-Based Consensus Statement. Pract Radiat Oncol. 2017;7:73-9.

[10] Hepel JT, Arthur D, Shaitelman S, et al. American Brachytherapy Society consensus report for accelerated partial breast irradiation using interstitial multicatheter brachytherapy. Brachytherapy. 2017;16:919-28.

[11] Shah C, Vicini F, Shaitelman SF, et al. The American Brachytherapy Society consensus statement for accelerated partial-breast irradiation. Brachytherapy. 2018;17:154-70.

[12] Polgar C, Fodor J, Major T, Sulyok Z, Kasler M. Breast-conserving therapy with partial or whole breast irradiation: ten-year results of the Budapest randomized trial. Radiother Oncol. 2013;108:197-202.

[13] Rodriguez N, Sanz X, Dengra J, et al. Five-year outcomes, cosmesis, and toxicity with 3-dimensional conformal external beam radiation therapy to deliver accelerated partial breast irradiation. Int J Radiat Oncol Biol Phys. 2013;87:1051-7.

[14] Livi L, Meattini I, Marrazzo L, et al. Accelerated partial breast irradiation using intensity-modulated radiotherapy versus whole breast irradiation: 5-year survival analysis of a phase 3 randomised controlled trial. Eur J Cancer. 2015;51:451-63.

[15] Strnad V, Ott OJ, Hildebrandt G, et al. 5-year results of accelerated partial breast irradiation using sole interstitial multicatheter brachytherapy versus whole-breast irradiation with boost after breast-conserving surgery for low-risk invasive and in-situ carcinoma of the female breast: a randomised, phase 3, non-inferiority trial. Lancet. 2016;387:229-38.

[16] Vicini FA, Cecchini RS, White JR, et al. Long-term primary results of accelerated partial breast irradiation after breast-conserving surgery for early-stage breast cancer: a randomised, phase 3, equivalence trial. Lancet. 2019.

[17] Whelan TJ, Julian JA, Berrang TS, et al. External beam accelerated partial breast irradiation versus whole breast irradiation after breast conserving surgery in women with ductal carcinoma in situ and node-negative breast cancer (RAPID): a randomised controlled trial. Lancet. 2019.

[18] Oliver M, Chen J, Wong E, Van Dyk J, Perera F. A treatment planning study comparing whole breast radiation therapy against conformal, IMRT and tomotherapy for accelerated partial breast irradiation. Radiother Oncol. 2007;82:317-23.

[19] Pignol JP, Keller BM, Ravi A. Doses to internal organs for various breast radiation techniques--implications on the risk of secondary cancers and cardiomyopathy. Radiat Oncol. 2011;6:5.

[20] Donovan EM, James H, Bonora M, Yarnold JR, Evans PM. Second cancer incidence risk estimates using BEIR VII models for standard and complex external beam radiotherapy for early breast cancer. Med Phys. 2012;39:5814-24.
[21] Qiu JJ, Chang Z, Horton JK, Wu QR, Yoo S, Yin FF. Dosimetric comparison of 3D conformal, IMRT, and V-MAT techniques for accelerated partial-breast irradiation (APBI). Med Dosim. 2014;39:152-8.
[22] Rault E, Lacornerie T, Dang HP, et al. Accelerated partial breast irradiation using robotic radiotherapy: a dosimetric comparison with tomotherapy and three-dimensional conformal radiotherapy. Radiat Oncol. 2016;11:29.
[23] Stelczer G, Major T, Meszaros N, Polgar C, Pesznyak C. External beam accelerated partial breast irradiation: dosimetric assessment of conformal and three different intensity modulated techniques. Radiol Oncol. 2019;53:123-30.
[24] Breedveld S, Storchi PR, Voet PW, Heijmen BJ. iCycle: Integrated, multicriterial beam angle, and profile optimization for generation of coplanar and noncoplanar IMRT plans. Med Phys. 2012;39:951-63.
[25] Voet PWJ, Dirkx MLP, Breedveld S, Al-Mamgani A, Incrocci L, Heijmen BJM. Fully Automated Volumetric Modulated Arc Therapy Plan Generation for Prostate Cancer Patients. International Journal of Radiation Oncology*Biology*Physics. 2014;88:1175-9.
[26] Hissoiny S, Ozell B, Bouchard H, Despres P. GPUMCD: A new GPU-oriented Monte Carlo dose calculation platform. Med Phys. 2011;38:754-64.
[27] National Surgical Adjuvant Breast and Bowel Project and Radiation Therapy Oncology Group. NSABP B-39/RTOG 0413: A randomized phase III study of conventional whole breast irradiation versus partial breast irradiation for women with stage 0, I, or II breast cancer. 2007; http://www.rtog.org/members/protocols/0413/0413.pdf.
[28] Obayomi-Davies O, Kole TP, Oppong B, et al. Stereotactic Accelerated Partial Breast Irradiation for Early-Stage Breast Cancer: Rationale, Feasibility, and Early Experience Using the CyberKnife Radiosurgery Delivery Platform. Front Oncol. 2016;6:129.
[29] Rahimi A, Thomas K, Spangler A, et al. Preliminary Results of a Phase 1 Dose-Escalation Trial for Early-Stage Breast Cancer Using 5-Fraction Stereotactic Body Radiation Therapy for Partial-Breast Irradiation. Int J Radiat Oncol Biol Phys. 2017;98:196-205 e2.
[30] Avanzo M, Stancanello J, Trovò M, et al. Complication probability model for subcutaneous fibrosis based on published data of partial and whole breast irradiation. Physica Medica. 2012;28:296-306.
[31] Surveillance, Epidemiology, and End Results (SEER) Program (www.seer.cancer.gov) SEER*Stat Database: Incidence - SEER 18 Regs Research Data + Hurricane Katrina Impacted Louisiana Cases, Nov 2015 Sub (1973-2013 varying) - Linked To County Attributes - Total U.S., 1969-2014 Counties, National Cancer Institute, DCCPS, Surveillance Research Program, released April 2016, based on the November 2015 submission.
[32] Mukesh MB, Harris E, Collette S, et al. Normal tissue complication probability (NTCP) parameters for breast fibrosis: pooled results from two randomised trials. Radiother Oncol. 2013;108:293-8.
[33] Hammer C, Maduro JH, Bantema-Joppe EJ, et al. Radiation-induced fibrosis in the boost area after three-dimensional conformal radiotherapy with a simultaneous integrated boost technique for early-stage breast cancer: A multivariable prediction model. Radiotherapy and Oncology. 2017;122:45-9.
[34] Darby SC, Ewertz M, McGale P, et al. Risk of ischemic heart disease in women after radiotherapy for breast cancer. N Engl J Med. 2013;368:987-98.
[35] van den Bogaard VA, Ta BD, van der Schaaf A, et al. Validation and Modification of a Prediction Model for Acute Cardiac Events in Patients With Breast Cancer Treated With Radiotherapy Based on Three-Dimensional Dose Distributions to Cardiac Substructures. J Clin Oncol. 2017;35:1171-8.
[36] Jacobse JN, Duane FK, Boekel NB, et al. Radiation Dose-Response for Risk of Myocardial Infarction in Breast Cancer Survivors. Int J Radiat Oncol Biol Phys. 2019;103:595-604.
[37] Essers M, Osman SO, Hol S, Donkers T, Poortmans PM. Accelerated partial breast irradiation (APBI): are breath-hold and volumetric radiation therapy techniques useful? Acta Oncol. 2014;53:788-94.
[38] Schipaanboord BWK, Breedveld S, Rossi L, Keijzer M, Heijmen BJM. Automated prioritised 3D dose-based MLC segment generation for step-and-shoot IMRT. Phys Med Biol. 2019.

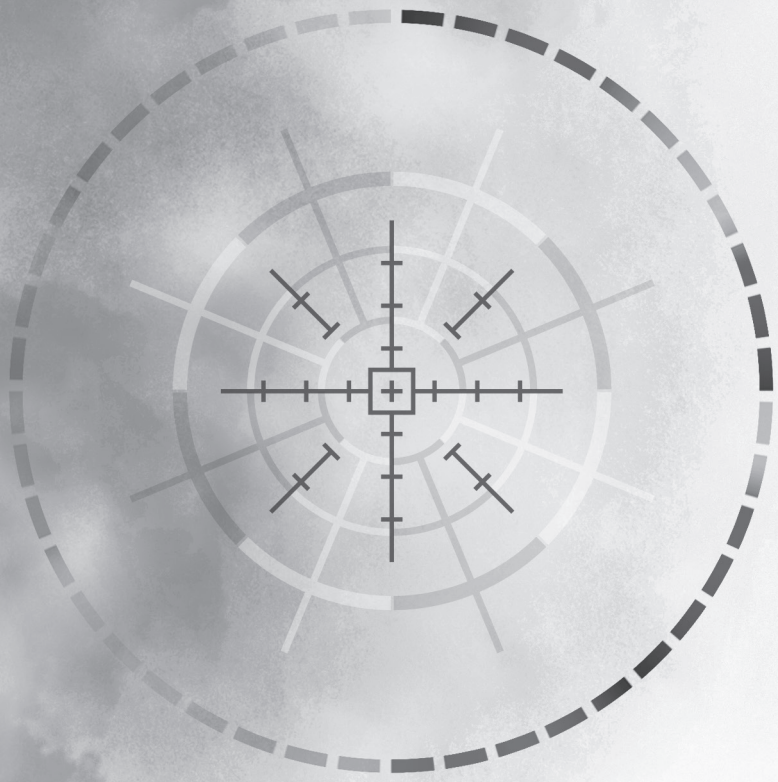

4

Intrafraction motion during partial breast irradiation

Published as
Intrafraction motion during partial breast irradiation depends on treatment time
Nienke Hoekstra, MD[1]; Steven Habraken, PhD[1]; Annemarie Swaak - Kragten, MD[1]; Mischa Hoogeman, PhD[1]; Jean-Philippe Pignol, MD, PhD[2];

1. Erasmus MC Cancer Institute, Department of Radiation Oncology, PO Box 2040, 3000 CA Rotterdam, The Netherlands
2. Dalhousie University, Department of Radiotherapy, 5820 University Avenue, Halifax NS B3H1V7, Canada

Radiotherapy and Oncology (2021), doi: 10.1016/j.radonc.2021.03.029

Abstract

Introduction – As the prognosis of early-stage breast cancer patients is excellent, prevention of radiation-induced toxicity has become crucial. Reduction of margins compensating for intrafraction motion reduces non-target dose. We assessed motion of the tumor bed throughout APBI treatment fractions and calculated CTV-PTV margins for breathing and drift.

Methods – This prospective clinical trial included patients treated with APBI on a Cyberknife with fiducial tracking. Paired orthogonal kV images made throughout the entire fraction were used to extract the tumor bed position. The images used for breathing modelling were used to calculate breathing amplitudes. The margins needed to compensate for breathing and drift were calculated according to Engelsman and Van Herk respectively.

Results – Twenty-two patients, 110 fractions and 5087 image pairs were analyzed. The margins needed for breathing were 0.3 – 0.6 mm. The margin for drift increased with time after the first imaging for positioning. For a total fraction duration up to 8 min, a margin of 1.0 mm is sufficient. For a fraction of 32 min, 2.5 mm is needed. Techniques that account for breathing motion can reduce the margin by 0.1 mm. There was a systematic trend in the drift in the caudal, medial and posterior direction. To compensate for this, 0.7 mm could be added to the margins.

Conclusions – The margin needed to compensate for intrafraction motion increased with longer fraction duration due to drifting of the target. It doubled for a fraction of 24 min compared to 8 min. Breathing motion has a limited effect.

Introduction

Accelerated partial breast irradiation (APBI) is an alternative to whole breast irradiation after lumpectomy for low risk breast cancer patients selected according to several international guidelines [1-6]. There is a tendency to reduce the number of treatment fractions for APBI from ten to five, or even down to single fraction treatments [7-14]. Hypofractionation has the advantage of convenience both for the patient and the radiotherapy facility, but could create challenges for the treatment delivery. Due to the reduced number of fractions, there is a possibly larger impact of a geographical miss of the target, with hence a potential increase in the risk of local recurrence. Most current hypofractionated external beam APBI (EB-APBI) protocols use daily online positioning verification and correction based on cone beam CT or kV imaging, or more recently MR imaging [13, 15-17]. The motion that occurs after this setup and during the treatment delivery is often not considered. It is currently unclear what the magnitude of intrafraction motion is, and thus which safety margins should be used to compensate for intrafraction motion during EB-APBI. This safety margin is used to expand the clinical target volume (CTV) and create the planning target volume (PTV) according to the ICRU report 50 [18]. In short, it is called the PTV margin.

When treating small volumes like in APBI, every additional millimeter expansion of the PTV leads to a large increase in the volume irradiated, and to a higher dose in the surrounding healthy tissues. This increases the risk of toxicity and radiation-induced mortality, partially offsetting its survival benefit [19-21]. This is especially relevant for early-stage breast cancer patients, because of their excellent long-term breast-cancer specific survival. Using a PTV margin that is as small as possible is important to reduce radiation induced mortality. On the other hand, if the PTV margin used is too small, the consequence could be a higher risk of local recurrence and eventually a higher breast-cancer mortality.

The intrafraction motion of the breast can be complex, as it is a non-rigid organ and it is affected by breathing motion as well as slight changes in arm position and patient's muscular relaxation. There are some studies comparing pretreatment and post treatment imaging, but these analyses do not give information on the motion during treatment delivery [22-24]. Other studies only investigated breathing motion [24-26]. There are also studies that use a superficial surrogate for the motion of the tumor bed, using surface scanning techniques or LEDs on the skin of the patient [27, 28]. These studies provide information on the motion during treatment delivery, but only of these surrogates and not of the actual target, which is the tumor bed. Acharya et al. reported on MR imaging of the tumor bed during APBI delivery [29]. The cine MR imaging is 2D, which means that there is no information about the left-right motion. The calculated margins are based on the total treatment times for their patient group, and they do not provide a method to

adapt the margins for a possible difference in treatment time. Treatment time influences intrafraction motion and varies substantially between techniques (e.g. flattening filter free VMAT versus pencil beam scanning protons).

In this prospective clinical study, we assessed the intrafraction motion of the tumor bed during EB-APBI, based on fiducials inside or very close to the tumor bed and using kV imaging throughout the entire fraction. To this end, we analyzed clinical data of a cohort of patients treated with Cyberknife APBI. We calculated treatment time-dependent PTV margins in 3 dimensions based on the Van Herk margin recipe and distinguished breathing motion from drift [30].

Materials and Methods

Twenty-two patients treated with APBI at Erasmus MC, Rotterdam the Netherlands, were included in this study, as part of a prospective clinical trial registered in the Netherlands Trial Register under NL6802. All patients provided written informed consent and were treated with 5 daily fractions of 5.7 Gy on a Cyberknife. Eligible patients were at least 50 years of age, had a pTis, pT1 or pT2 tumor of less than 3 cm, were pN0 for invasive disease and were treated with lumpectomy with negative margins (negative at ink for invasive disease, at least 2 mm for DCIS). Patients had at least three surgical clips placed in the tumor bed made of tantalum (any size) or titanium (at least 1 cm). Exclusion criteria were lobular carcinoma, presence of lympho-vascular infiltration, extensive intraductal component, multifocal or multicentric disease, neoadjuvant chemotherapy, distant metastasis or prior thoracic radiotherapy. In addition, all patients had three gold fiducial markers of 3 mm length placed inside the breast tissue at approximately 2 cm from the tumor bed under ultrasound guidance.

Patients were positioned supine in a vacuum mattress with the ipsilateral arm raised above the head. A planning CT scan was made with 1-1.5 mm slice thickness. The tumor bed was delineated using the seroma, postoperative changes, surgical clips and preoperative information. The CTV was created applying a uniform expansion of 10 to 15 mm to the tumor bed, excluding the thoracic wall and skin. An expansion of 5 mm was used to create the PTV. Treatment plans were made following our local clinical protocol, including digitally reconstructed radiographs (DRRs) for patient positioning. Patients were treated using the Synchrony® real-time motion synchronization technology (Accuray Inc., Sunnyvale USA). The details of this imaging protocol have been published previously [31]. In brief, two orthogonal kV images are acquired to reconstruct the 3D position of fiducials. The position of the target is calculated based on the position of the fiducials. In this study, either the surgical clips or the interstitial gold markers were used. The Synchrony system

tracks breathing motion using three optical markers placed on the abdomen of the patient. These markers are the termination of optical fibers that transmit the signal of LEDs. A stereo camera system measures the 3D position of the markers continuously. The Synchrony system creates a correlation model between the motion of the optical markers and the motion of the fiducials based on kV images that sample the entire breathing cycle. Throughout the entire treatment fraction, the model is updated with sets of 3 pairs of kV images at regular intervals. The imaging interval can be adapted by the RTTs during treatment delivery based on observed patient's motion and their clinical expertise. The most common interval used was 150 seconds, with the three kV images made one second apart.

We extracted the 3D position of the target center of mass at each kV image pair for all patients and all fractions. The magnitude of breathing motion was calculated from the minimum and maximum center of mass position of the images that were used for the breathing correlation model, as the system ensures that it samples the entire breathing cycle during the modelling phase. The method by Engelsman et al., which is based on the Van Herk margin recipe, was used to calculate the margin needed to compensate for breathing motion:

Margin = 0.7 * σ , with σ = 0.4 * amplitude [30, 32].

To apply this method to a population instead of an individual patient, we first calculated the random error σ of breathing per patient, which is 0.4 * amplitude, and then calculated the root mean squared of all the errors for the population. This value was multiplied by 0.7 to calculate the margin.

The next step was to calculate the drift of the tumor bed during the entire treatment fraction. The mean center of mass position of the breathing model was used as the reference to calculate any displacement during the treatment fraction. The images were binned into 2 minute intervals, starting at the first image pair used for the breathing model. We calculated the mean and standard deviations of the center of mass displacements of all image pairs per patient and per bin. We used this to calculate the mean of means (M), systematic error (Σ) and random error (σ). Using the Van Herk formula, we calculated the margins needed to compensate for systematic and random intrafraction motion [30]. This resulted in a margin for each time bin separately. To obtain a margin that was valid for a given fraction duration as a whole, we calculated the cumulative running average for all bins up to and including the given time bin.

The Σ and σ are used in the margin calculation, whereas M is not. We analyzed M and its standard error separately. This metric would show a trend in the drift in one direction. To

calculate the standard error, we divided the standard deviation by the number of fractions with data in each bin. We did not use the number of image pairs per bin, as the measurements within one fraction are strongly correlated.

The Synchrony algorithm ensures that the entire breathing cycle is sampled throughout the fraction. This means that breathing motion is included in our analysis of the drift. We subtracted the breathing motion error from the combined error to estimate the margin for drift only. This margin would apply to techniques that account for breathing motion but not for drift, e.g. breath hold or gating techniques. We used the Van Herk formula for the combination of different random errors, which means that the different random errors were subtracted quadratically [30].

All margin calculations were done for a target surrounded by breast tissue and a prescription isodose level of 95%.

Data extraction and calculations were done in Python version 3.5 (Python Software Foundation, Beaverton, USA) with the use of the packages Numpy and Pandas.

Results

Twenty-two patients were included in this study. Table 1 shows the patient characteristics. All patients were treated with APBI in 5 fractions to a total of 28.5 Gy. For one patient, the data of one fraction was missing. For another patient, a fraction was delivered in 2 subfractions over 2 days. Thus, there were 110 fractions available for analysis.

The mean duration of a treatment fraction, starting from the first images, was 26 min and the median was 25 min (range 11 – 47 min, 5^{th} percentile 16 min, 95^{th} percentile 36 min). In 15 fractions, the breathing model had to be rebuild at least once, due to patient movement or technical issues. The length of time that a breathing model was in use was on average 22 min with a median of 23 min (range 3 – 35 min). In total, 5039 image pairs were made, giving an average of 46 images pairs per fraction.

The average amplitude of the breathing motion of the tumor bed is shown in Table 2. The breathing amplitudes of the individual patients for each fraction are available in supplementary material table S1. The breathing motion was smallest in the lateromedial direction and of similar magnitude in the craniocaudal and anteroposterior directions. Margins between 0.3 and 0.6 mm are required to compensate for breathing motion.

Table 1 Patient characteristics.

		Range or percentage
Age (years)	Mean 63	50 - 84
Body mass index	Mean 27.7	22.3 - 40
Breast cup size		
A	1	4
B	7	27
C	5	19
D	5	19
E or more	4	15
Tumor laterality		
Left	9	41
Right	13	59
Affected quadrant		
Upper outer	13	59
Lower outer	1	5
Upper inner	6	27
Lower inner	0	0
Multiple quadrants	2	9
Tracking method		
Surgical clips	16	73
Interstitial markers	6	27

Table 2 Breathing amplitudes and required margins in craniocaudal, lateromedial and anteroposterior directions.

	Breathing amplitude (mm)		Margin (mm)
	Median	Interquartile range	
Craniocaudal	1.4	1.0 – 2.0	0.6
Lateromedial	0.6	0.4 – 1.0	0.3
Anteroposterior	1.5	1.0 – 2.2	0.6

Figure 1 shows the mean deviation M (fig. 1a), systematic error Σ (fig. 1b) and random error σ (fig. 1c) of the motion of the center of mass per time bin. This analysis includes all intrafraction motion, so both drift and breathing motion. Interestingly, the values increased with the time elapsed since the start of the fraction, mainly for M and Σ. After more than 30 min of treatment, there was limited data, which is also reflected by the increased error bars. The margin needed to compensate for intrafraction motion, calculated per time bin, also increased with fraction duration (fig. 2). The values of M, Σ, σ and the calculated margins per time bin can also be found in the table in supplementary material table S2.

a

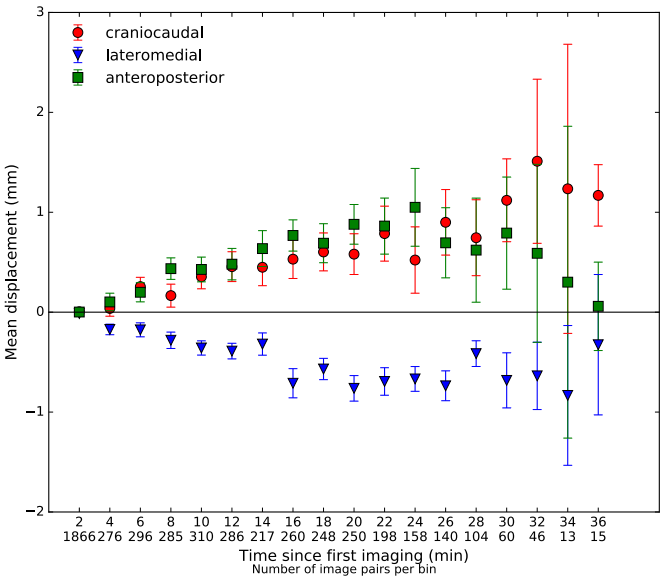

b

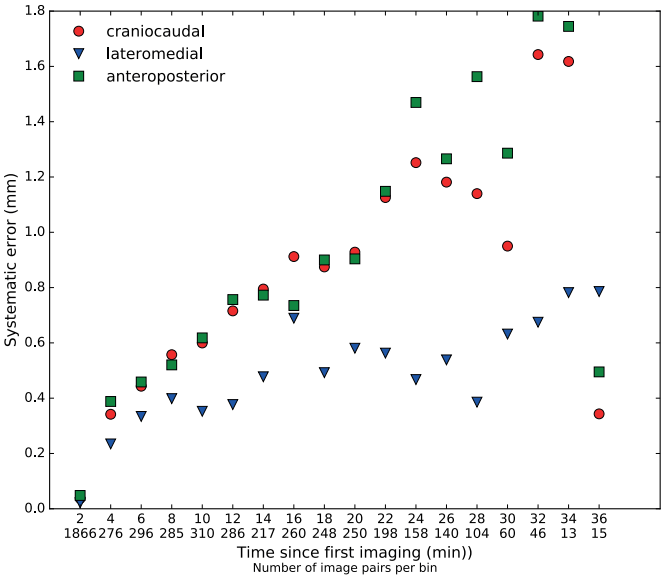

Figure 1 Mean of means M (**a**), systematic error Σ (**b**) and random error σ (**c**) of the intrafraction motion for each 2-minute time bin. The bars in fig. 1a depict 2 standard errors. A positive value in fig. 1a is a displacement in the caudal, lateral and posterior direction.

C

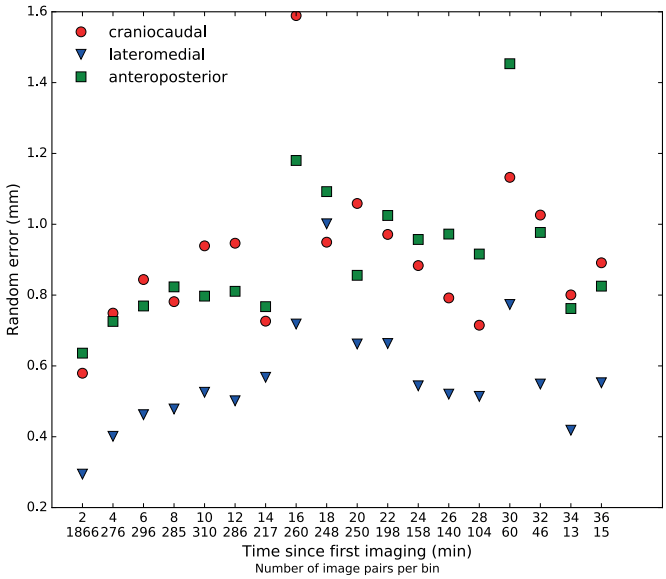

Figure 1 Continued.

In clinical practice, the PTV margin is defined for the entire fraction instead of being variable over time. The single PTV margin is shown in figure 3. It is the cumulative running average of the margins per bin up to and including the given fraction duration. The margin increases with time, from 1.0 mm if the fraction is delivered in 8 min, to 2.0 mm for a fraction of 24 min and to more than 2.5 for a fraction of 32 min or more.

Figure 3 also shows that the margin is very similar for the craniocaudal and anteroposterior direction, but smaller for the lateromedial direction. The margin in the lateromedial direction is about half as large as the margin in the other directions.

The systematic and random errors are translated into the required PTV margin, but the overall mean M is not used in this calculation. Taking a closer look at M, figure 1a shows that there was a significant deviation from the zero position in all directions. On average, patients drifted 0.7 mm in the caudal direction, 0.7 mm in the medial direction and 0.8 mm in the posterior direction during treatment. This drift could be included by the addition of 0.7 mm in the caudal and medial direction and 0.8 min in the posterior direction. That would result in asymmetric margins. For example, for a treatment of 20 min the margin would be 1.8 mm cranially, 2.5 mm caudally, 1.5 mm laterally, 2.2 medially, 1.7 mm anteriorly and 2.5 mm posteriorly.

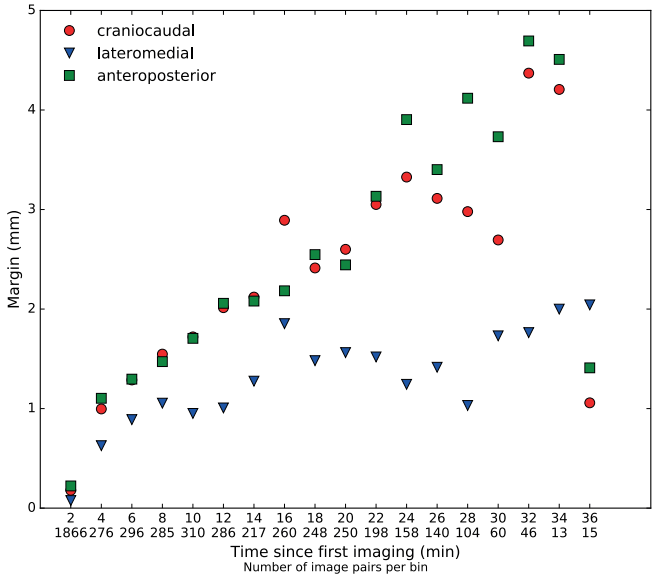

Figure 2 Margin required for each time bin to compensate for intrafraction motion. The upper row of values along the X-axis shows the time elapsed since the first imaging for set-up. The lower row shows the number of image pairs analyzed in each time bin.

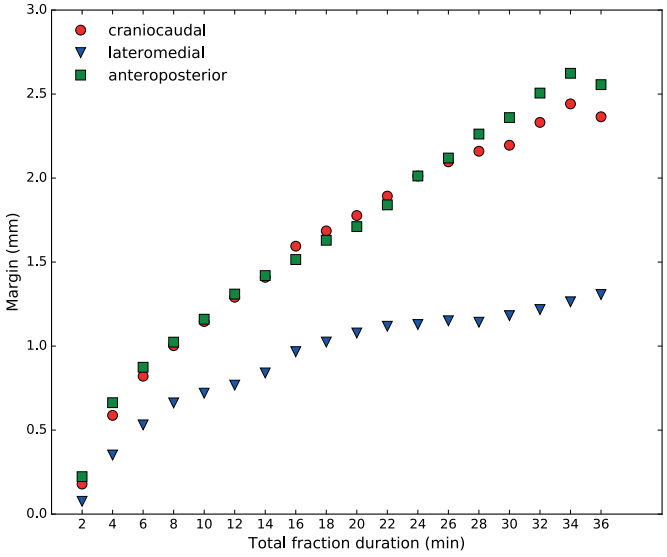

Figure 3 Margin required per total fraction duration to compensate for intrafraction motion.

The average margin from Figure 3 includes the compensation for breathing motion. Some radiotherapy techniques already account for breathing motion, including breath-hold irradiation and gating, but not for drift. In these situations, the breathing error can be subtracted from the total random error using the Van Herk rules for combining different random errors [30]. The results for the cumulative running average of the required margins are shown in figure 4. The margin excluding breathing motion is on average only 0.1 mm smaller than the margin including breathing motion, with a maximum of 0.16 mm for the longest treatment times in the anteroposterior direction.

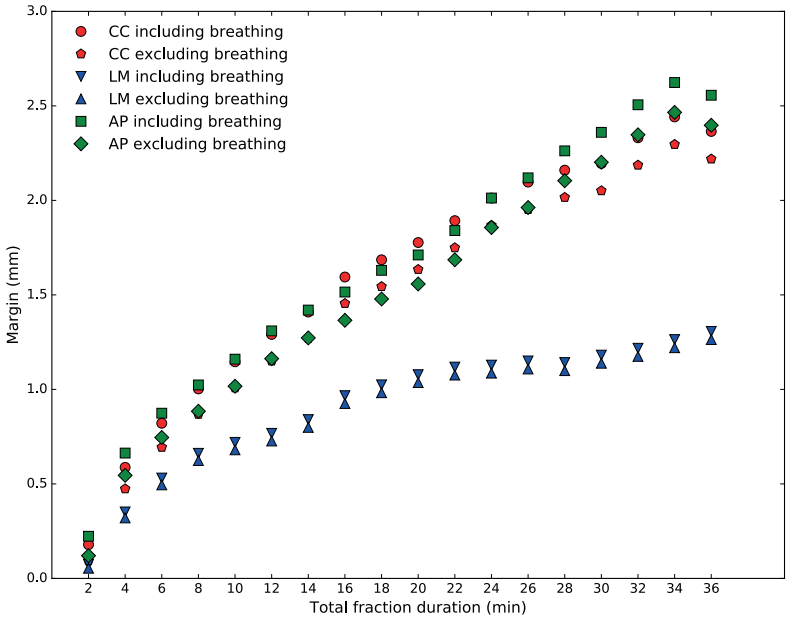

Figure 4 Margin required per total fraction duration to compensate for intrafraction motion. CC = craniocaudal, LM = lateromedial, AP = anteroposterior.

Discussion

This study showed that the margin accounting for intrafraction motion during EB-APBI is highly dependent on treatment time. The shorter the time interval between imaging and the end of irradiation, the smaller the margin required. For a fraction of up to 8 min, a PTV margin of 1.0 mm is sufficient, whereas a fraction of 32 min or more requires a margin of 2.5 mm. This is an additional reason to keep the fraction duration as short as possible, next to patient comfort and logistical reasons.

The duration of a fraction is mainly based on two aspects, the set-up time and the treatment delivery time. The set-up time includes the time for imaging, the evaluation of the images, and the application of the calculated corrections. It depends on the protocol used, for example kV imaging or CBCT and offline or online matching. Using a less sophisticated protocol can save time, but one needs to keep in mind that it could result in a lower accuracy. The margin for interfraction motion might increase, mitigating the benefit of a reduced time for positioning. The solution could be an automated set-up calculation and correction, as this should be both accurate and fast.

The treatment delivery time depends on the planning technique and the treatment machine. Regarding the choice for a technique, there is also a trade-off to keep in mind. A more sophisticated dose plan might result in lower doses to non-target tissues. For APBI, it has been shown that a non-coplanar beam setup resulted in lower doses to surrounding organs than a coplanar beam setup [33]. On the other hand, a more sophisticated dose plan often has a longer beam-on time and a longer gantry or couch movement time. The treatment machine also has an important effect on the treatment delivery time. Pencil-beam scanning proton therapy has a relatively long treatment time, but very low doses to organs-at-risk. A conventional linac is faster with flattening filter free dose delivery than without. To combine speed with conformity, the use of non-coplanar arcs or even hyperarcs could be of great benefit. The Cyberknife has a long treatment time, due to the large number of non-coplanar beams and the robot travelling time. As the Cyberknife can track and trail the target during treatment delivery, the increased drift is continuously corrected and the prolonged treatment time does not require a larger margin.

To the best of our knowledge, our study is the first to show the increase in drift over time during treatment for breast cancer patients. Lovelock et al. investigated intrafraction motion in prostate cancer patients and found an increase in margin of 2 mm per 5 min, starting from the time of the imaging procedure [34]. Wang et al. report a time-dependent increase in 3D-vector for intracranial treatments [35]. Hoogeman et al. published on both intracranial treatments and spine treatments [36]. They concluded that the systematic error of intrafraction motion depended on the time between localizations. For breast cancer patients, no other time-resolved analysis has been published.

We found a systematic drift in the caudal, medial and posterior directions. This mean deviation M is not addressed in the margin recipe as proposed by Van Herk. He assumed that M would be zero. The best way to deal with such a systematic drift would be to change the isocenter of the treatment to the new target location. Certain techniques like the CyberKnife and the MRIridian are able to track and trail the target. For techniques that cannot track the target, an additional margin is necessary. We calculated that this additional margin should be 0.7 mm in the caudal and medial direction and 0.8 mm in the posterior

direction. It is unclear why this drift occurs, but it is evident that the human body is not rigid over time. During treatment delivery, patients might slide downwards in the vacuum mattress, breathe differently, relax muscles or shift the ipsilateral arm which is raised above the head. This could all influence the position of the tumor bed.

Our results do also apply to other treatments than APBI. The motion patterns will probably be the same for whole breast irradiation with a tumor bed boost. The fields or arcs of a simultaneous boost are often given after the whole breast fields, which means that the time since start of treatment is longest. Also, protons treatments are increasingly used for complex cases, often requiring whole breast irradiation, nodal irradiation and a boost on the tumor bed. The total treatment time with pencil-beam scanning is long. The margins for the PTV of the boost should take the intrafraction motion into account.

The margins reported in this study are small with differences in PTV margins in the order of one millimeter. It is unsure whether a clinical benefit could be expected from such small differences. For example, the IMPORT LOW trial, which uses a very crude way to deliver partial breast irradiation, reports good cosmetic outcomes [37]. Thus, it is unclear whether a small margin reduction for a highly conformal technique could lead to a measurable benefit in a clinical trial. In the setting of a clinical trial, the number of patients and the length of follow-up are limited, so the absolute numbers of patients with long-term toxicity within a trial will be very small. After widespread adoption of APBI for this patient group with a long life expectancy, the absolute numbers will increase, making minor benefits also relevant. It is also important to see the small difference in margin in the light of the small volumes treated in APBI. For example, for a 2 cm sphere, a millimeter margin leads to a 33% volume increase in the PTV. Treating this much larger PTV will result in higher doses to the healthy tissues surrounding the target and in higher risks of long term toxicity. This may become clinically important with the more accelerated dose fractionations used in recent trials, even down to a single fraction treatment [9-14]. Moreover, following the ALARA principle ("as low as reasonably achievable"), one should aim to reduce the not-target dose as much as possible.

Acharya et al. reported a study on cine MR imaging during APBI delivery [29]. They found that a margin of 0.7 mm was required to cover 90% of the cavity volume for 90% of the time. This value was an average over 30 patients. The mean treatment time in their cohort was 12.7 min. We found a margin of 1.4 mm for a treatment time of 12 to 14 min. The difference might be explained by a difference in margin definition. We used the formula by Van Herk, which requires at least 90% of the patients to receive at least 95% of the prescribed dose in the CTV [30]. Both the required volume and the proportion of the population are higher in our analysis than the values used by Acharya et al., namely 95% versus 90% and 90% versus 50% respectively. The average margin of 0.7 mm of Acharya et al. would result in only half of the patients meeting a minimum coverage of 90%.

Our analysis is based on the motion of fiducials that are in the tumor bed. There is a lot of debate on the accuracy of the delineation of the tumor bed. This is especially true in the case of full thickness closure. The use of MR for delineation did not improve the interobserver agreement [38]. The study by Acharya et al. defined the tumor bed motion on 2D cine MRI, while our study is an analysis of the motion of the fiducial markers in three dimensions [29]. The 3D position of the fiducials can be calculated with high accuracy. Assuming that they are good surrogates for the tumor bed within a single fraction, this results in an accurate measurement of tumor bed motion. Our study does not focus on tumor bed definition, only on its motion. A drawback of our method is that there can be motion of the fiducials relative to the tumor bed. This has been shown for the interval between simulation and the first fraction, and the magnitude of this motion is related to the length of the interval [23, 39]. For the very short time scale of intrafraction motion, the displacement of fiducials with respect to the tumor bed is expected to be negligible. The analysis is done relative to the position at the start of treatment after the initial alignment. Because the patient is not repositioned during treatment, there is no influence of repositioning or interfraction motion in our analysis. To calculate a margin that compensates for both intrafraction and interfraction motion, a linear combination of these margins would result in an overestimation. The systematic and random errors of each component should be combined quadratically in the van Herk formula. The systematic and random errors for each time bin in this study are provided in the supplementary materials.

In our study, patients were positioned in a vacuum mattress. Another option for patient positioning is the use of a chest board. The magnitude of drift can differ between different positioning devices. Hubie et al. found the accuracy of a vacuum mattress to be better than that of a chest board, but the differences were not statistically significant [40]. Thus, a definitive conclusion cannot be drawn at this point.

The median breathing amplitude in this study was small, 1.4 mm in craniocaudal direction, 0.6 mm in lateromedial direction and 1.5 mm in anteroposterior direction. This is similar to the results of other studies [25, 26, 28]. These studies do not report a margin for breathing motion. Applying the calculation as published by Engelsman, the margins in these studies would be similar to our results [32].

Another interesting finding of our study was that the margin for techniques that already account for breathing motion, e.g. breath hold and gating, is only 0.1 mm smaller than for techniques that do not account for breathing. The random error of breathing motion was subtracted quadratically from the total error according to the Van Herk formula, resulting in a very small difference [30]. This indicates that efforts trying to reduce intrafraction motion would better be aimed at reducing drift than at accounting for breathing motion.

Still, the use of deep inspiration breath hold has other advantages than reducing breathing motion, such as a lower dose to heart and lungs.

The required margin does not linearly depend on treatment time, as can be seen in Figure 2 and 3. After an initial steep increase, the dependence flattens. This might be explained by the patients tending to relax and settle down on the treatment couch. The time spent on the couch before the first imaging might influence the drift. This time is not included in our analysis. In 15 out of 110 fractions, the breathing model was rebuilt during treatment delivery. In some cases, the patient was repositioned and therefore we expect no difference with motion after the initial setup. In other cases, the patient was not repositioned, which could lead to a smaller drift after the model rebuild. Overall, this could lead to a slightly smaller drift calculated for the entire patient population.

The use of kV images throughout the fraction warrants a consideration of the associated imaging dose. The imaging dose of an orthogonal kV image pair is about 0.01 cGy [41]. With an average number of image pairs per fraction of 46, the total imaging dose is below 0.5 cGy. With a prescription dose of 5.7 Gy per fraction, the imaging dose contribution is only 0.01%. Also, a decrease in margin will result in lower doses in surrounding tissues, and the benefit is expected to be much larger than the additional imaging dose. The steepness of the drift is highest in the first part of treatment and quite stable in the second part. It would be most efficient to use a slightly shorter imaging interval in the first part of treatment, but imaging throughout the fraction will remain necessary.

Conclusion

For APBI, the CTV to PTV margin is strongly influenced by the target drifting over time. The margin required to compensate for intrafraction motion increases from 1.0 mm for a fraction of 8 min, to more than 2.5 mm for a fraction of 32 min. We recommend to keep the time between set-up and end of treatment as short as possible to avoid geographical miss. If a short treatment time is not feasible, the margin should be increased or the drifting should be corrected for. Therefore, it is important to consider treatment time when developing and implementing more conformal irradiation techniques. Breathing motion has a limited influence on the intrafraction motion.

Acknowledgements

We would like to thank Liesbeth Boersma and Karolien Verhoeven (Department of Radiation Oncology (Maastro Clinic), GROW, University Hospital Maastricht, Maastricht, The Netherlands) for our valuable discussions and their contributions to the manuscript.

References

[1] American Society of Breast Surgeons. Consensus Statement for Accelerated Partial Breast Irradiation. 2011; https://www.breastsurgeons.org/new_layout/about/statements/PDF_Statements/APBI.pdf.

[2] Correa C, Harris EE, Leonardi MC, et al. Accelerated Partial Breast Irradiation: Executive summary for the update of an ASTRO Evidence-Based Consensus Statement. Pract Radiat Oncol. 2017;7:73-9.

[3] Hepel JT, Arthur D, Shaitelman S, et al. American Brachytherapy Society consensus report for accelerated partial breast irradiation using interstitial multicatheter brachytherapy. Brachytherapy. 2017;16:919-28.

[4] Polgar C, Van Limbergen E, Potter R, et al. Patient selection for accelerated partial-breast irradiation (APBI) after breast-conserving surgery: recommendations of the Groupe Europeen de Curietherapie-European Society for Therapeutic Radiology and Oncology (GEC-ESTRO) breast cancer working group based on clinical evidence (2009). Radiother Oncol. 2010;94:264-73.

[5] Shah C, Vicini F, Shaitelman SF, et al. The American Brachytherapy Society consensus statement for accelerated partial-breast irradiation. Brachytherapy. 2018;17:154-70.

[6] Smith BD, Arthur DW, Buchholz TA, et al. Accelerated partial breast irradiation consensus statement from the American Society for Radiation Oncology (ASTRO). Int J Radiat Oncol Biol Phys. 2009;74:987-1001.

[7] Vicini FA, Cecchini RS, White JR, et al. Long-term primary results of accelerated partial breast irradiation after breast-conserving surgery for early-stage breast cancer: a randomised, phase 3, equivalence trial. Lancet. 2019;394:2155-64.

[8] Whelan TJ, Julian JA, Berrang TS, et al. External beam accelerated partial breast irradiation versus whole breast irradiation after breast conserving surgery in women with ductal carcinoma in situ and node-negative breast cancer (RAPID): a randomised controlled trial. Lancet. 2019;394:2165-72.

[9] Mouawad M, Biernaski H, Brackstone M, et al. DCE-MRI assessment of response to neoadjuvant SABR in early stage breast cancer: Comparisons of single versus three fraction schemes and two different imaging time delays post-SABR. Clinical and Translational Radiation Oncology. 2020;21:25-31.

[10] Horton JK, Blitzblau RC, Yoo S, et al. Preoperative Single-Fraction Partial Breast Radiation Therapy: A Novel Phase 1, Dose-Escalation Protocol With Radiation Response Biomarkers. Int J Radiat Oncol Biol Phys. 2015;92:846-55.

[11] Guidolin K, Yaremko B, Lynn K, et al. Stereotactic image-guided neoadjuvant ablative single-dose radiation, then lumpectomy, for early breast cancer: the SIGNAL prospective single-arm trial of single-dose radiation therapy. Curr Oncol. 2019;26:e334-e40.

[12] Charaghvandi KR, Van't Westeinde T, Yoo S, et al. Single dose partial breast irradiation using an MRI linear accelerator in the supine and prone treatment position. Clin Transl Radiat Oncol. 2019;14:1-7.

[13] Kennedy WR, Thomas MA, Stanley JA, et al. Single-Institution Phase 1/2 Prospective Clinical Trial of Single-Fraction, High-Gradient Adjuvant Partial-Breast Irradiation for Hormone Sensitive Stage 0-I Breast Cancer. International Journal of Radiation Oncology, Biology, Physics. 2020;107:344-52.

[14] Grendarova P, Roumeliotis M, Quirk S, et al. One-Year Cosmesis and Fibrosis From ACCEL: Accelerated Partial Breast Irradiation (APBI) Using 27 Gy in 5 Daily Fractions. Pract Radiat Oncol. 2019;9:e457-e64.

[15] Quirk S, Grendarova P, Craighead P, et al. Results of the ACCEL trial: Dosimetry in accelerated partial breast irradiation. Radiotherapy and Oncology. 2020;147:50-5.

[16] Livi L, Meattini I, Marrazzo L, et al. Accelerated partial breast irradiation using intensity-modulated radiotherapy versus whole breast irradiation: 5-year survival analysis of a phase 3 randomised controlled trial. Eur J Cancer. 2015;51:451-63.

[17] Lozza L, Fariselli L, Sandri M, et al. Partial breast irradiation with CyberKnife after breast conserving surgery: a pilot study in early breast cancer. Radiat Oncol. 2018;13:49.

[18] International Commission on Radiation Units and Measurements. ICRU Report 50: Prescribing, Recording, and Reporting Photon Beam Therapy. 1993.

[19] Darby SC, Ewertz M, McGale P, et al. Risk of ischemic heart disease in women after radiotherapy for breast cancer. N Engl J Med. 2013;368:987-98.

[20] Taylor C, Correa C, Duane FK, et al. Estimating the Risks of Breast Cancer Radiotherapy: Evidence From Modern Radiation Doses to the Lungs and Heart and From Previous Randomized Trials. J Clin Oncol. 2017;35:1641-9.

[21] Hoekstra N, Fleury E, Merino Lara TR, et al. Long-term risks of secondary cancer for various whole and partial breast irradiation techniques. Radiotherapy and Oncology. 2018.
[22] Cai G, Hu WG, Chen JY, et al. Impact of residual and intrafractional errors on strategy of correction for image-guided accelerated partial breast irradiation. Radiat Oncol. 2010;5:96.
[23] Park CK, Pritz J, Zhang GG, Forster KM, Harris EE. Validating fiducial markers for image-guided radiation therapy for accelerated partial breast irradiation in early-stage breast cancer. Int J Radiat Oncol Biol Phys. 2012;82:e425-31.
[24] Yue NJ, Goyal S, Zhou J, Khan AJ, Haffty BG. Intrafractional target motions and uncertainties of treatment setup reference systems in accelerated partial breast irradiation. Int J Radiat Oncol Biol Phys. 2011;79:1549-56.
[25] Ding Y, Li J, Wang W, et al. Displacement of the lumpectomy cavity defined by surgical clips and seroma based on 4D-CT scan for external-beam partial breast irradiation after breast-conserving surgery: a comparative study. Br J Radiol. 2013;86:20130416.
[26] van Heijst TC, Philippens ME, Charaghvandi RK, et al. Quantification of intra-fraction motion in breast radiotherapy using supine magnetic resonance imaging. Phys Med Biol. 2016;61:1352-70.
[27] Reitz D, Carl G, Schonecker S, et al. Real-time intra-fraction motion management in breast cancer radiotherapy: analysis of 2028 treatment sessions. Radiat Oncol. 2018;13:128.
[28] Ricotti R, Ciardo D, Fattori G, et al. Intra-fraction respiratory motion and baseline drift during breast Helical Tomotherapy. Radiother Oncol. 2017;122:79-86.
[29] Acharya S, Fischer-Valuck BW, Mazur TR, et al. Magnetic Resonance Image Guided Radiation Therapy for External Beam Accelerated Partial-Breast Irradiation: Evaluation of Delivered Dose and Intrafractional Cavity Motion. Int J Radiat Oncol Biol Phys. 2016;96:785-92.
[30] van Herk M. Errors and margins in radiotherapy. Semin Radiat Oncol. 2004;14:52-64.
[31] Hoogeman M, Prevost JB, Nuyttens J, Poll J, Levendag P, Heijmen B. Clinical accuracy of the respiratory tumor tracking system of the cyberknife: assessment by analysis of log files. Int J Radiat Oncol Biol Phys. 2009;74:297-303.
[32] Engelsman M, Sharp GC, Bortfeld T, Onimaru R, Shirato H. How much margin reduction is possible through gating or breath hold? Phys Med Biol. 2005;50:477-90.
[33] Hoekstra N, Habraken S, Swaak-Kragten A, Breedveld S, Pignol JP, Hoogeman M. Reducing the Risk of Secondary Lung Cancer in Treatment Planning of Accelerated Partial Breast Irradiation. Front Oncol. 2020;10:1445.
[34] Lovelock DM, Messineo AP, Cox BW, Kollmeier MA, Zelefsky MJ. Continuous monitoring and intrafraction target position correction during treatment improves target coverage for patients undergoing SBRT prostate therapy. Int J Radiat Oncol Biol Phys. 2015;91:588-94.
[35] Wang CW, Lin YC, Tseng HM, et al. Prolonged treatment time deteriorates positioning accuracy for stereotactic radiosurgery. PLoS One. 2015;10:e0123359.
[36] Hoogeman MS, Nuyttens JJ, Levendag PC, Heijmen BJ. Time dependence of intrafraction patient motion assessed by repeat stereoscopic imaging. Int J Radiat Oncol Biol Phys. 2008;70:609-18.
[37] Coles CE, Griffin CL, Kirby AM, et al. Partial-breast radiotherapy after breast conservation surgery for patients with early breast cancer (UK IMPORT LOW trial): 5-year results from a multicentre, randomised, controlled, phase 3, non-inferiority trial. The Lancet. 2017;390:1048-60.
[38] den Hartogh MD, van den Bongard HJ, Davidson MT, et al. Full-thickness closure in breast-conserving surgery: the impact on radiotherapy target definition for boost and partial breast irradiation. A multimodality image evaluation. Ann Surg Oncol. 2014;21:3774-9.
[39] Yue NJ, Haffty BG, Kearney T, Kirstein L, Chen S, Goyal S. Tracking the dynamic seroma cavity using fiducial markers in patients treated with accelerated partial breast irradiation using 3D conformal radiotherapy. Med Phys. 2013;40:021717.
[40] Hubie C, Shaw M, Bydder S, et al. A randomised comparison of three different immobilisation devices for thoracic and abdominal cancers. J Med Radiat Sci. 2017;64:90-6.
[41] Stelczer G, Tatai-Szabo D, Major T, et al. Measurement of dose exposure of image guidance in external beam accelerated partial breast irradiation: Evaluation of different techniques and linear accelerators. Phys Med. 2019;63:70-8.

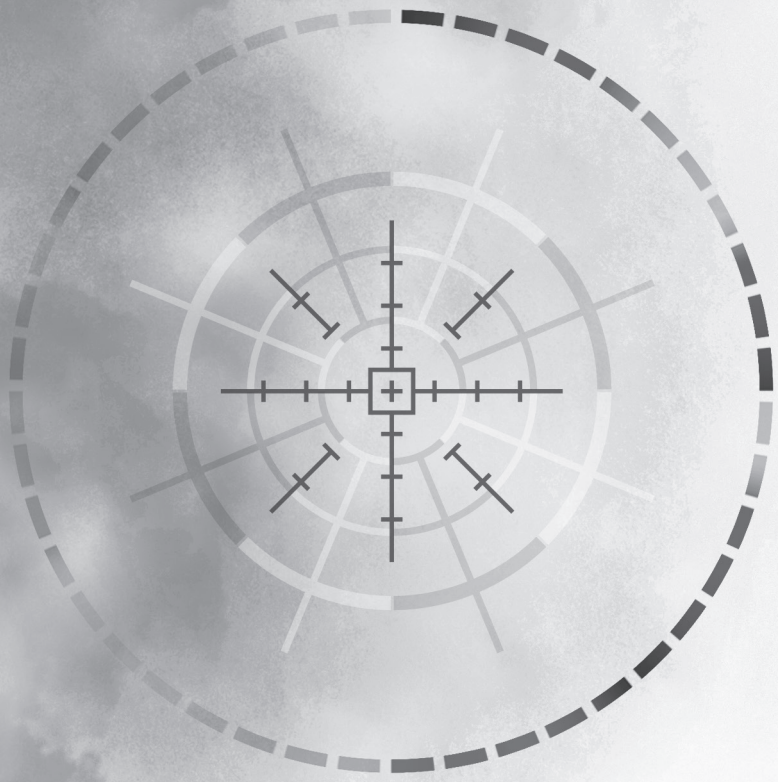

5

Interfraction motion of partial breast irradiation

Published as
Fiducial marker motion relative to the tumor bed has a significant impact on PTV margins in partial breast irradiation
Nienke Hoekstra, MD[1]; Steven Habraken, PhD[1]; Annemarie Swaak - Kragten, MD[1]; Jean-Philippe Pignol, MD, PhD[2]; Mischa Hoogeman, PhD[1]

1. Erasmus MC Cancer Institute, Department of Radiation Oncology, PO Box 2040, 3000 CA Rotterdam, The Netherlands
2. Dalhousie University, Department of Radiotherapy, 5820 University Avenue, Halifax NS B3H1V7, Canada

Radiotherapy and Oncology (2021), doi: 10.1016/j.radonc.2021.07.020

Abstract

Introduction – With the introduction of accelerated partial breast irradiation (APBI) and the trend of reducing the number of fractions, the geometric accuracy of treatment delivery becomes critical. APBI patient setup is often based on fiducials, as the seroma is frequently not visible on pretreatment imaging. We assessed the motion of fiducials relative to the tumor bed between planning CT and treatment, and calculated margins to compensate for this motion.

Methods – cohort of seventy patients treated with APBI on a Cyberknife was included. Planning and in-room pretreatment CT scans were registered on the tumor bed. Residual motion of the centers of mass of surgical clips and interstitial gold markers was calculated. We calculated the margins required per desired percentage of patients with 100% CTV coverage, and the systematic and random errors for fiducial motion.

Results – For a single fraction treatment, a margin of 1.8 mm would ensure 100% CTV coverage in 90% of patients when using surgical clips for patient set-up. When using interstitial markers, the margin should be 2.2 mm. The systematic and random errors were 0.46 mm for surgical clip motion and 0.60 mm for interstitial marker motion. No clinical factors were found predictive for fiducial motion.

Conclusions – Fiducial motion relative to the tumor bed between planning CT and APBI treatment is non-negligible and should be included in the PTV margin calculation to prevent geographical miss. Systematic and random errors of fiducial motion were combined with other geometric uncertainties to calculate comprehensive PTV margins for different treatment techniques.

Introduction

Adjuvant radiotherapy remains a cornerstone in the treatment of early-stage breast cancer, reducing the local recurrence risk and increasing the overall survival [1]. Hypofractionated treatment schedules result in similar local recurrence risks for early-stage breast cancer as conventional fractionation [2, 3]. The reduced number of hospital visits and the shorter overall treatment time are more convenient for patients and radiotherapy institutions. The trend towards even more ultra-hypofractionated regimens is still ongoing, with trials currently investigating treatment schedules for accelerated partial breast irradiation (APBI) with a single fraction [4-8]. The first examples of single-fraction APBI (SF-APBI) techniques in clinical use were intraoperative radiotherapy and permanent seed implants [9-12]. These techniques require specialized equipment and training. External beam radiotherapy techniques have the advantage of being non-invasive and more widely available. However, the major concern with external beam SF-APBI is the accurate localization of the target during treatment. Missing the target could result in an increased risk of local recurrence, because the random errors between fractions are not averaged, but contribute to the systematic error in a single fraction treatment. Therefore, a high geometric accuracy combined with the use of an adequate margin from clinical target volume (CTV) to planning target volume (PTV) is essential.

Another challenge for the use of SF-APBI for early-stage breast cancer is the use of full thickness closure after breast-conserving surgery. While suturing the glandular tissue after tumor removal leads to a smaller seroma cavity and lower risk of complications, the smaller seroma is often not visible on the images used for patient setup and target localization for radiotherapy [13, 14]. Radiopaque fiducial markers inserted in or close to the tumor bed are often used instead. However, little is known about the possibility of motion between the fiducials and the tumor bed. To avoid a geographical miss and an increased risk of local recurrence, the motion of the fiducials relative to the tumor bed should be quantified and included in the PTV margin calculation.

The choice of a CTV to PTV margin for use in clinical practice is a trade-off between the risk of a geographical miss and the doses to surrounding healthy tissues. The balance depends on the prognosis of the treated patient group and the toxicity profile of the treatment. With the current highly conformal APBI techniques, dose to surrounding tissues is reduced and local recurrence risks are low [15-18]. Therefore, it would be interesting to see the effect of varying the PTV margin on the probability of geographical miss.

The main goal of this study is to determine adequate CTV to PTV margins for external beam APBI. The motion of surgical clips and interstitial gold markers relative to the tumor bed was measured in a large cohort of patients using in-room diagnostic quality CT scans.

Next, we calculated the PTV margin needed to compensate for this motion in a single fraction treatment as a function of the risk of geographical miss. In addition, we generalized our results to comprehensive PTV margins for different APBI techniques to be used in clinical practice.

Materials and Methods

Patients and procedures

Patients treated with APBI on a CyberKnife at Erasmus MC between November 2018 and March 2021 were included. Patients with at least 3 titanium surgical clips in the tumor bed were eligible for this study. The insertion of surgical clips in the walls of the tumor bed during lumpectomy is a standard procedure for all patients undergoing breast conserving surgery. The aim of the use of surgical clips is to increase the accuracy and reproducibility of the tumor bed delineation for radiotherapy. The standard surgical procedure was a closed-cavity technique. Patients were treated with 5 fractions of 5.2 to 5.7 Gy in one week. All patients had 2 to 3 gold markers inserted postoperatively into the breast around the tumor bed under ultrasound guidance. We refer to these as interstitial markers. The local Medical Ethics Committee of Erasmus MC, Rotterdam the Netherlands approved the exempt of ethics review and informed consent for this analysis of anonymized patient data (MEC-2020-0415).

Patients were positioned on a vacuum mattress with the ipsilateral arm raised. According to our clinical protocol, all patients had both a planning CT scan (Siemens Somatom Confidence) and a diagnostic-quality in-room CT scan (Siemens Somatom Definition AS) in treatment position before the first fraction. The in-room CT scan was acquired with a CT-on-rails scanner integrated with a CyberKnife [19]. The robotic treatment couch is shared between the CT scanner and the CyberKnife system, so that the patient can remain in treatment position on the treatment coach between image acquisition and the treatment. The obtained CT scan can be used to offset the treatment center to align with soft tissue targets, to perform online adaptive treatments, or to verify the position of implanted markers relative to e.g. the tumor bed, as done in this study. Identical acquisition parameters were used for the planning and in-room CT scans. The slice thickness was 1 – 1.5 mm. All CT scans were acquired during voluntary exhalation to decrease variation due to breathing motion. The tumor bed was delineated by the treating radiation oncologist bearing in mind all preoperative and postoperative information and physical examination, paying careful attention to the surgical clip positions and the postoperative changes on the planning CT scan. The tumor bed was expanded with a 10 to 15 mm uniform margin to create the CTV, depending on the resection margins.

CT analysis

The planning CT scan and the in-room CT scan were registered based on the delineation of the tumor bed using MIM software (version 6.9.3). A 5 mm isotropic margin was added to create the registration volume. All automated registrations were checked visually by a single trained observer. There were sufficient anatomical landmarks visible within this area to perform an accurate registration, including but not limited to seroma, postoperative changes and glandular tissue. In case of a suboptimal registration, the two CT scans were first registered on the PTV or CTV and then on the registration volume. This was repeated until an adequate registration was obtained. As quality assurance, the registration procedure was repeated with an isotropic expansion of 4 and 6 mm in a random sample of 10 patients. For this random sample, the registration procedure was repeated by a different observer using the default 5 mm expansion to quantify interobserver variation. Finally, we selected the patients with the 10% highest fiducial motion errors in the default analysis and repeated the registration procedure for these cases to test the intraobserver variability in the worst case scenario.

The fiducials were manually delineated by the observer who also performed the registrations, using a lower threshold of 400 HU. In the tumor bed aligned CT scans, we determined the distance between the fiducials in the planning CT and the in-room CT scan for each of the 3 main directions separately. Next, we calculated for each patient the residual distance of the center of mass (CoM) of all surgical clips and of all interstitial markers together. This distance is the error in patient setup for the tumor bed when it is based either on the CoM of the surgical clips or interstitial markers.

CTV to PTV margin calculation for fiducial-based patient set-up

The percentage of patients without any loss of coverage, i.e. without any deviation from the prescribed dose, was calculated as a function of the PTV margin, simulating a patient-setup based on the CoM of the surgical clips or the interstitial markers. The margin was defined as a uniform three-dimensional expansion of the CTV. Here, we calculated the margins required for the setup errors in the CoM of the surgical clips and interstitial markers relative to the tumor bed only. The common approach is to calculate the standard deviation of the error distributions and to use for example the Van Herk margin recipe, which provides a margin for adequate treatment in 90% of the patients [20]. Because the underlying assumption of a Gaussian distribution was not fully satisfied in this study and because we wanted to calculate the margin as a function of the percentage of patients without coverage loss, we used sampling of the error distributions instead. Bootstrapping with replacement was used to reduce bias in the calculation of the margins. For each percentage of patients without coverage loss, the average margin over the bootstrap samples was calculated.

Comprehensive CTV to PTV margin calculation

Next, we generalized the margin calculation by also including other error sources and calculating the single-fraction margin for two commonly used APBI techniques: 1) VMAT-APBI on a conventional radiation treatment unit with patient-setup based on surgical clips using cone beam CT and 2) CyberKnife-APBI with real-time respiratory tracking based on interstitial markers. As the real-time tracking algorithm does not reliably track most types of surgical clips, interstitial gold markers are used in our and other institutions [21-24]. To calculate the single-fraction margins for these two techniques, technique-specific systematic and random errors, expressed as 1 standard deviation of a Gaussian distribution, were taken from literature. For VMAT-APBI, these are beam isocenter accuracy, couch accuracy, and intrafraction motion (Table 1) [25-29]. For CyberKnife-APBI, this is the CyberKnife total system error, which combines imaging and beam adjustment errors. If only tolerance values were available, half the tolerance value was taken as standard deviation of the error distribution. In case the error has been separated in a random and systematic component, both errors were combined by adding the standard deviations in quadrature for the single-fraction treatment margin. This is in accordance with the methodology presented by de Boer et al. to convert systematic and random errors for conventionally fractionated treatments to hypofractionated schedules [30]. To calculate the systematic margin for VMAT-APBI, the drift, beam and couch error distributions and the systematic breathing error distribution were sampled together with the error distribution of the surgical-clip-based patient setup and summed. Next, we calculated the random margin to account for intrafraction breathing motion by multiplying the random breathing error with 0.7. This describes the dose blurring by breathing motion. Following the methodology of Van Herk this random margin was added linearly to the systematic margin to calculate the total margin [20]. For CyberKnife-ABPI, a similar procedure was followed to calculate the systematic margin, but as CyberKnife compensates for breathing motion by real-time tracking, this random error was not added.

Finally, we generalized our margin calculation to fractionated treatments. Although the underlying assumption of a Gaussian distribution was not fully satisfied in this study, we calculated the systematic error (Σ) and of the random error (σ) for both fiducial-based patient-setup methods. As our results are based on a single fraction per patient, we had to estimate the contribution of systematic and random errors. We assumed an equal magnitude of systematic and random errors based on literature, so $\Sigma \approx \sigma$ [31]. Next, we converted the single fraction errors into errors of fractionated treatment using the method proposed by De Boer et al. [30].

Factors predictive for fiducial motion

We compared the distributions of the residual errors of the surgical clips and interstitial markers with the two-sample Kolmogorov Smirnov test. To assess whether there are clinical

Table 1 Overview of systematic and random errors for various geometric uncertainties of external beam APBI.

Geometric uncertainty		Systematic error Σ (mm)	Random error σ (mm)
Intrafraction motion	Breathing motion [25]	0.7*	0.7
	Drift [25]	0.49	0.28
Beam accuracy	Conventional treatment unit [26, 27]	0.5	-
Couch accuracy	Conventional treatment couch [26, 27]	0.5	0.5
Total system error	Cyberknife fiducial tracking [28, 29]	0.23	-

Reported values are for conventionally fractionated treatments.
* Applicable for the situation of a free breathing planning CT scan with a scanning time much shorter than the breathing cycle time.

or treatment factors associated with the magnitude of the fiducial motion, we tested a possible correlation with breast size, tumor bed size and the interval between planning CT and first fraction. To this end, the Pearson correlation coefficient was calculated, after visual inspection of scatterplots to exclude other types of correlation than a linear correlation. All analyses were done with Python version 3.5. A p-value of < 0.01 was considered significant because of multiple testing.

Results

In total, 70 patients were included in this study. Patient characteristics are shown in Table 2. Thirty-nine patients had a left-sided breast cancer and 31 patients had a right-sided tumor. The median interval between planning CT scan and first fraction CT scan was 14.5 days (IQR 11 – 17 days). For three patients, the anatomical changes noticed on the first fraction in-room CT images were so large that a new treatment plan was requested. The in-room CT images were used or this new plan and these three patients were treated with a delay of 3, 3 and 10 days. For each of those 3 patients, an additional in-room CT scan was acquired at the delivery of the first fraction. We used the first and second in-room CT scan for the analysis.

The median number of surgical clips was five (range 3 – 8). All but two patients had three interstitial gold markers inserted in the breast around the surgical cavity and the other two patients had 2 markers.

Table 2 Characteristics of included patients and their treatments.

	Number or median	Percentage or range
Laterality		
· Left-sided	39	56%
· Right-sided	31	44%
Interval planning – first fraction (days)	14.5	3 - 24
Number of surgical clips		
· 3	2	3%
· 4	13	19%
· 5	49	70%
· 6	3	4%
· 7	1	1%
· 8	2	3%
Number of interstitial markers		
· 2	2	3%
· 3	68	97%
Ipsilateral breast volume (cc)	873	166 – 2743
Tumor bed volume (cc)	9.5	0.9 – 41.1

The distributions of the displacements of all individual fiducials are shown in Figure 1. Both the one-dimensional displacements per fiducial and the combined three-dimensional displacements for the CoM per fiducial type are shown. The distributions of the 3D-displacements were statistically significantly different for the surgical clips and the interstitial markers (2-sample Kolmogorov Smirnov test $p < 0.001$). The quality assurance of the CT registration procedure showed good intraobserver and interobserver reproducibility (supplementary material Table S1). The absolute differences between the means and standard deviations of the original and quality assurance data were always smaller than 0.2 mm, and the large majority of differences was below 0.1 mm.

We calculated the PTV margin required for each percentage of patients without any CTV coverage loss based on the CoM motion of either the surgical clips or the interstitial markers (Figure 2). To fully cover the CTV of 90% of patients, a margin of 1.8 mm was required when using surgical clips for patient positioning, and a margin of 2.2 mm when interstitial markers were used. Increasing this percentage to 95% of patients resulted in a margin of 2.4 mm for the surgical clips and of 2.6 mm for the interstitial markers.

We calculated comprehensive PTV margins for the two SF-APBI treatment techniques, VMAT-APBI and CyberKnife-APBI. In Figure 3, the required PTV margins as a function of coverage are shown including all relevant geometric errors for both SF-APBI techniques.

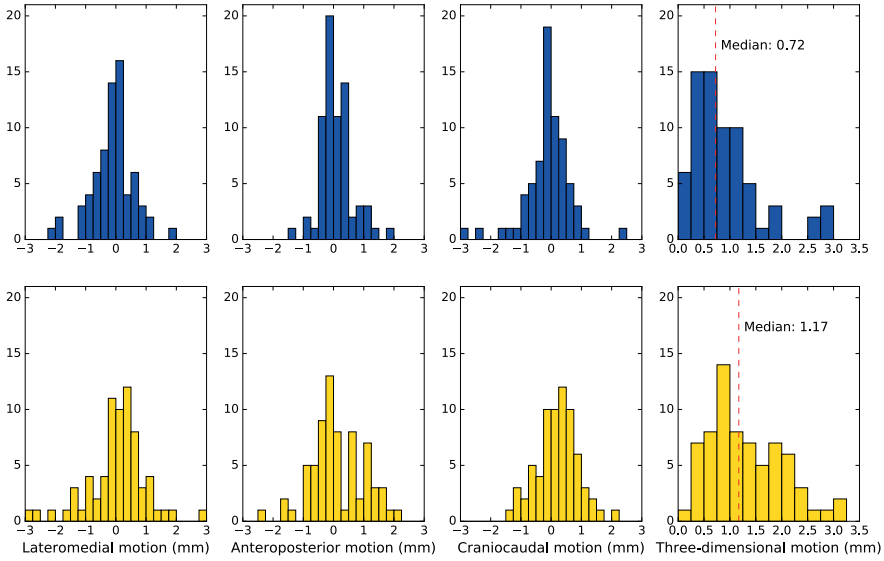

Figure 1 Histograms of the surgical clips (top row) and interstitial markers (bottom row) center of mass displacements. Positive values for the one-dimensional displacements indicate motion in the lateral, posterior and cranial directions.

To ensure full coverage in 90% of patients, the margin for CyberKnife SF-APBI should be 2.3 mm and for VMAT SF-APBI 4.0 mm.

To calculate PTV margins for fractionated treatments, the systematic error Σ and random error σ of fiducial motion were calculated. For the surgical clips, Σ and σ for a conventionally fractionated treatment were 0.46 mm. The interstitial markers had larger Σ and σ of 0.60 mm. The PTV margin accounting for fiducial motion only was calculated according to Van Herk, ensuring at least 95% CTV coverage in 90% of patients [20]. The margin should be 1.6 mm when using surgical clips and 2.1 mm when using the interstitial markers for a single-fraction treatment. These margins are slightly smaller than the margins calculated for 100% CTV coverage in 90% of patients in our single fraction analysis, which were 1.8 mm for the surgical clips and 2.2 mm for the interstitial markers (Figure 2).

Using this calculation method, the comprehensive PTV margins for single-fraction treatment should be 3.9 mm for VMAT-APBI and 2.2 mm with CyberKnife-APBI. For a 5-fraction treatment schedule, the margins should be 3.8 mm for VMAT-APBI and 2.1 mm with CyberKnife-APBI.

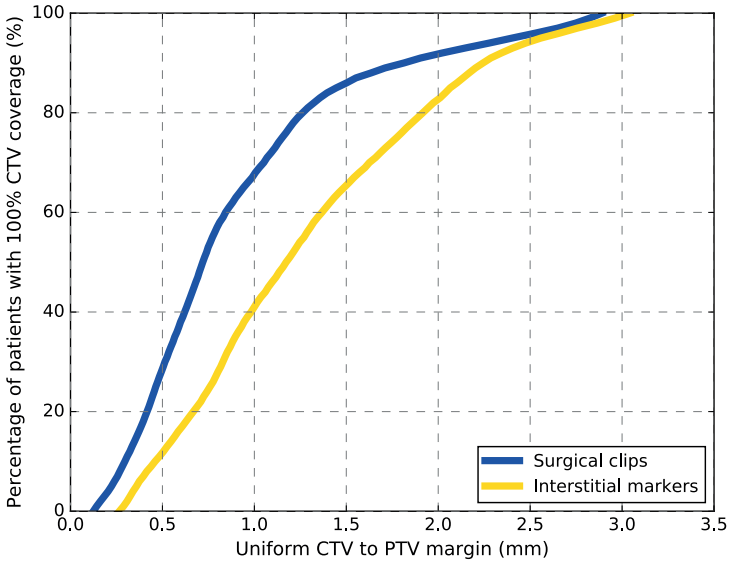

Figure 2 Percentage of patients with 100% CTV coverage per uniform CTV to PTV margin, accounting for fiducial motion of surgical clips or interstitial markers center of mass.

There was a statistically significant but weak correlation between the distance of an individual fiducial to the tumor bed CoM and its displacement. For the surgical clips, the Pearson correlation coefficient r was 0.27 ($p < 0.001$) and for the interstitial markers, it was 0.34 ($p < 0.001$). There was also a significant but weak correlation between the length of the time interval between planning CT scan and treatment and the 3D error for the CoM of surgical clips (Pearson's $r = 0.32$, $p = 0.007$), but not for the interstitial markers. Conversely, there was a statistically significant correlation between ipsilateral breast volume and the 3D error of the interstitial markers (Pearson's $r = 0.46$, $p < 0.001$), but not for the surgical clips. The tumor bed volume and the 3D CoM error were not correlated for either of the two types of fiducials.

Discussion

This study showed that there is significant motion of fiducials relative to the tumor bed between the planning CT and the treatment fraction. As the seroma is frequently not visible on patient or target setup imaging and the fiducials are used as a surrogate of target localization, this motion should be included in the calculation of the PTV margins to reduce the risk of geographical miss.

To generalize our results to fractionated treatment schedules, we propose a value of 0.46 mm for the systematic and random error for positioning based on surgical clips. For the interstitial markers, this value is 0.60 mm. The motion of fiducials relative to the tumor bed is only one source of uncertainty in the delivery of external beam APBI. Comparing our calculated values for fiducial motion with the other relevant uncertainties from Table 1 shows that for VMAT-APBI the surgical clip motion error is of the same magnitude as the other errors and thus should not be ignored. The interstitial marker motion is much larger than the total system error of CyberKnife-APBI and will dominate the PTV margin calculation for CyberKnife-APBI.

The values of the systematic and random errors for geometric uncertainties as shown in Table 1 and calculated in this analysis allow for the calculation of the required PTV margin for a large variety of techniques and fractionation schedules. An institution can select the uncertainties present in their treatment technique and sum them quadratically to calculate a comprehensive PTV margin. It is important to keep in mind that these values may differ between institutions and depend for example on the quality assurance program. Table 1 serves as an indication of the likely magnitude of the various errors based on literature.

The reported systematic and random errors can also be used to calculate the PTV margin for a sequentially delivered tumor bed boost if the alignment is based on fiducials. If the boost is delivered as a simultaneous integrated boost (SIB), the patient positioning is often performed on the thoracic wall or breast contour instead of on fiducials. An additional geometrical uncertainty should be included to account for the motion of the tumor bed relative to the thoracic wall or breast contour. In a review on setup using cone-beam CT, large variations are shown for the registration errors using different registration methods and different patient positioning devices [31]. The systematic error for thoracic wall and/or soft tissue registration ranged from 1.3 to 5.7 mm. For the random error, the range was 2.2 to 4.1 mm. These values are much larger than the values reported in Table 1 for the other uncertainties and will dominate the PTV margin calculation. Using a value of 3 mm for both the systematic and random error results in a required PTV margin of 10 mm for the tumor bed in a conventionally fractionated SIB treatment.

The range of fiducial motion in our patient cohort was large. The motion of the surgical clips CoM ranged from 0.1 to 2.9 mm. For most patients, an additional margin of 1 mm is sufficient to account for fiducial motion, while for 5% of them a margin larger than 2.5 mm is required. This suggests that the use of individualized PTV margins is warranted. Importantly, we did not find strong predictive factors for a larger CoM motion. There were some significant correlations, for the ipsilateral breast volume, the interval between simulation and treatment, and the distance between the fiducial and the tumor bed, but the predictive power was low. This means that, based on our results, it is not possible to

define an individualized PTV margin for a given patient at the time of treatment planning. However, like the plan-of-the-day concept recommended for cervical and bladder cancer, a solution could be the creation of a library of plans with different PTV margins [32]. At time of treatment, the fiducial motion could be assessed based on 3D imaging for setup, and the plan with the smallest adequate PTV margin could be chosen for delivery.

If such individualized PTV margins are not practically feasible, it is necessary to define the required proportion of patients with 100% CTV coverage. In the commonly used Van Herk formula, this percentage is chosen at 90% [20]. For contemporary APBI techniques, it is important to reconsider the trade-off between the proportion of patients with 100% CTV coverage and the doses to surrounding healthy tissues. On one hand, the rate of local recurrences after APBI is low but not negligible at around 4% at 10 years [17, 18, 33]. The dose to surrounding tissues is dramatically reduced compared to whole breast irradiation. A millimetric increase of margins may not result in a clinically detectable increase in toxicity but could reduce the local recurrence rate. On the other hand, patients treated with APBI have a very long life expectancy and the risk of late treatment-induced mortality has become more important [34, 35]. There are good salvage treatments for patients experiencing a local breast cancer recurrence, but not for radiation-induced lung cancer. Allowing for a lower percentage of patients with 100% CTV coverage might result in less treatment-related deaths. Our results enable the selection of a PTV margin for every desired percentage of patients with 100% CTV coverage. The trade-off between the percentage of patients with 100% CTV coverage and the CTV to PTV expansion is visualized in Figure 3.

Our study shows that interstitial gold markers present a larger motion than surgical clips. The reason for this difference is unclear. The interstitial markers were inserted just outside the tumor bed, while the surgical clips are inside the tumor bed. This larger distance to the tumor bed CoM may partially explain the large difference, as there is a weak correlation between distance and the magnitude of the motion. Another possibility is that the surgical clips might be more firmly anchored in the tissue, as they are mechanically stapled into the walls of the lumpectomy cavity. Conversely, interstitial markers are inserted into fatty tissue through a needle and not firmly attached to the tissue. The surgical clips were per definition situated within the tumor bed and thus in the area used for the registration of the planning CT and in-room CT. The impact of these clips on the registration was probably small. Every registration was visually inspected for the correct alignment of the tumor bed. Also, the surgical clips represented only a small volume relative to the total registration area.

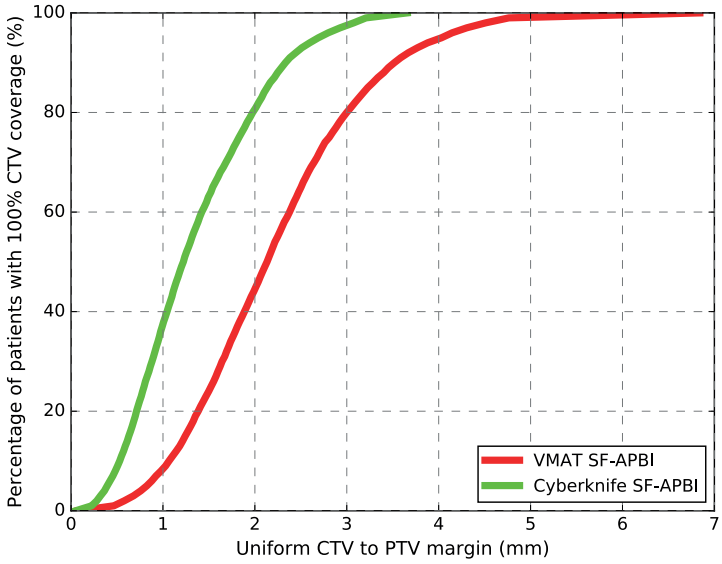

Figure 3 Percentage of patients with 100% CTV coverage per uniform CTV to PTV margin, including all geometric uncertainties of two treatment techniques: VMAT SF-APBI on a conventional linac with positioning based on the surgical clips on cone beam CT, and CyberKnife SF-APBI with real-time tracking based on interstitial markers.

In conclusion, our study showed that the motion of fiducials relative to the tumor bed occurring between planning CT and treatment is clinically significant and should be included in the PTV margin calculation. The comprehensive PTV margin for a single-fraction treatment including fiducial motion is 2.3 mm for CyberKnife-APBI and 4 mm for VMAT-APBI.

References

[1] Early Breast Cancer Trialists' Collaborative G, Darby S, McGale P, et al. Effect of radiotherapy after breast-conserving surgery on 10-year recurrence and 15-year breast cancer death: meta-analysis of individual patient data for 10,801 women in 17 randomised trials. Lancet. 2011;378:1707-16.

[2] Haviland JS, Owen JR, Dewar JA, et al. The UK Standardisation of Breast Radiotherapy (START) trials of radiotherapy hypofractionation for treatment of early breast cancer: 10-year follow-up results of two randomised controlled trials. Lancet Oncol. 2013;14:1086-94.

[3] Whelan TJ, Pignol JP, Levine MN, et al. Long-term results of hypofractionated radiation therapy for breast cancer. N Engl J Med. 2010;362:513-20.

[4] Mouawad M, Biernaski H, Brackstone M, et al. DCE-MRI assessment of response to neoadjuvant SABR in early stage breast cancer: Comparisons of single versus three fraction schemes and two different imaging time delays post-SABR. Clinical and Translational Radiation Oncology. 2020;21:25-31.

[5] Horton JK, Blitzblau RC, Yoo S, et al. Preoperative Single-Fraction Partial Breast Radiation Therapy: A Novel Phase 1, Dose-Escalation Protocol With Radiation Response Biomarkers. Int J Radiat Oncol Biol Phys. 2015;92:846-55.

[6] Guidolin K, Yaremko B, Lynn K, et al. Stereotactic image-guided neoadjuvant ablative single-dose radiation, then lumpectomy, for early breast cancer: the SIGNAL prospective single-arm trial of single-dose radiation therapy. Curr Oncol. 2019;26:e334-e40.

[7] Charaghvandi KR, Van't Westeinde T, Yoo S, et al. Single dose partial breast irradiation using an MRI linear accelerator in the supine and prone treatment position. Clin Transl Radiat Oncol. 2019;14:1-7.

[8] Kennedy WR, Thomas MA, Stanley JA, et al. Single-Institution Phase 1/2 Prospective Clinical Trial of Single-Fraction, High-Gradient Adjuvant Partial-Breast Irradiation for Hormone Sensitive Stage 0-I Breast Cancer. International Journal of Radiation Oncology, Biology, Physics. 2020;107:344-52.

[9] Vaidya JS, Bulsara M, Baum M, et al. Long term survival and local control outcomes from single dose targeted intraoperative radiotherapy during lumpectomy (TARGIT-IORT) for early breast cancer: TARGIT-A randomised clinical trial. Bmj. 2020;370:m2836.

[10] Veronesi U, Orecchia R, Maisonneuve P, et al. Intraoperative radiotherapy versus external radiotherapy for early breast cancer (ELIOT): a randomised controlled equivalence trial. Lancet Oncol. 2013;14:1269-77.

[11] Crook J, Hilts M, Batchelar D, et al. Permanent breast seed implant for partial breast radiotherapy after partial mastectomy for favorable breast cancer: Technique, results, and applications to various seroma presentations. Brachytherapy. 2019;18:510-20.

[12] Pignol JP, Caudrelier JM, Crook J, McCann C, Truong P, Verkooijen HA. Report on the Clinical Outcomes of Permanent Breast Seed Implant for Early-Stage Breast Cancers. Int J Radiat Oncol Biol Phys. 2015;93:614-21.

[13] Indelicato D, Grobmyer SR, Newlin H, et al. Association between operative closure type and acute infection, local recurrence, and disease surveillance in patients undergoing breast conserving therapy for early-stage breast cancer. Surgery. 2007;141:645-53.

[14] Mukesh MB, Barnett G, Cumming J, et al. Association of breast tumour bed seroma with post-operative complications and late normal tissue toxicity: results from the Cambridge Breast IMRT trial. Eur J Surg Oncol. 2012;38:918-24.

[15] Quirk S, Grendarova P, Craighead P, et al. Results of the ACCEL trial: Dosimetry in accelerated partial breast irradiation. Radiotherapy and Oncology. 2020;147:50-5.

[16] Qiu JJ, Chang Z, Horton JK, Wu QR, Yoo S, Yin FF. Dosimetric comparison of 3D conformal, IMRT, and V-MAT techniques for accelerated partial-breast irradiation (APBI). Med Dosim. 2014;39:152-8.

[17] Whelan TJ, Julian JA, Berrang TS, et al. External beam accelerated partial breast irradiation versus whole breast irradiation after breast conserving surgery in women with ductal carcinoma in situ and node-negative breast cancer (RAPID): a randomised controlled trial. Lancet. 2019;394:2165-72.

[18] Vicini FA, Cecchini RS, White JR, et al. Long-term primary results of accelerated partial breast irradiation after breast-conserving surgery for early-stage breast cancer: a randomised, phase 3, equivalence trial. Lancet. 2019;394:2155-64.

[19] Papalazarou C, Klop GJ, Milder MTW, et al. CyberKnife with integrated CT-on-rails: System description and first clinical application for pancreas SBRT. Med Phys. 2017;44:4816-27.

[20] van Herk M. Errors and margins in radiotherapy. Semin Radiat Oncol. 2004;14:52-64.
[21] Seiler S, Rahimi A, Choudhery S, et al. Ultrasound-Guided Placement of Gold Fiducial Markers for Stereotactic Partial-Breast Irradiation. AJR Am J Roentgenol. 2016;207:685-8.
[22] Lozza L, Fariselli L, Sandri M, et al. Partial breast irradiation with CyberKnife after breast conserving surgery: a pilot study in early breast cancer. Radiat Oncol. 2018;13:49.
[23] Obayomi-Davies O, Kole TP, Oppong B, et al. Stereotactic Accelerated Partial Breast Irradiation for Early-Stage Breast Cancer: Rationale, Feasibility, and Early Experience Using the CyberKnife Radiosurgery Delivery Platform. Front Oncol. 2016;6:129.
[24] Rahimi A, Thomas K, Spangler A, et al. Preliminary Results of a Phase 1 Dose-Escalation Trial for Early-Stage Breast Cancer Using 5-Fraction Stereotactic Body Radiation Therapy for Partial-Breast Irradiation. Int J Radiat Oncol Biol Phys. 2017;98:196-205 e2.
[25] Hoekstra N, Habraken S, Swaak – Kragten A, Hoogeman M, Pignol J-P. Intrafraction motion during partial breast irradiation depends on treatment time. Radiotherapy and Oncology. 2021.
[26] American Association of Physicists in Medicine. Quality assurance for image-guided radiation therapy utilizing CT-based technologies: A report of the AAPM TG-179. 2012.
[27] Seravalli E, van Haaren PM, van der Toorn PP, Hurkmans CW. A comprehensive evaluation of treatment accuracy, including end-to-end tests and clinical data, applied to intracranial stereotactic radiotherapy. Radiother Oncol. 2015;116:131-8.
[28] Pantelis E, Moutsatsos A, Antypas C, et al. On the total system error of a robotic radiosurgery system: phantom measurements, clinical evaluation and long-term analysis. Phys Med Biol. 2018;63:165015.
[29] Nano TF, Capaldi DPI, Yeung T, Chuang CF, Wang L, Descovich M. Technical Note: Performance of CyberKnife(®) tracking using low-dose CT and kV imaging. Med Phys. 2020;47:6163-70.
[30] de Boer HC, Heijmen BJ. A protocol for the reduction of systematic patient setup errors with minimal portal imaging workload. Int J Radiat Oncol Biol Phys. 2001;50:1350-65.
[31] Batumalai V, Holloway L, Delaney GP. A review of setup error in supine breast radiotherapy using cone-beam computed tomography. Med Dosim. 2016;41:225-9.
[32] Heijkoop ST, Langerak TR, Quint S, et al. Clinical implementation of an online adaptive plan-of-the-day protocol for nonrigid motion management in locally advanced cervical cancer IMRT. Int J Radiat Oncol Biol Phys. 2014;90:673-9.
[33] Meattini I, Marrazzo L, Saieva C, et al. Accelerated Partial-Breast Irradiation Compared With Whole-Breast Irradiation for Early Breast Cancer: Long-Term Results of the Randomized Phase III APBI-IMRT-Florence Trial. J Clin Oncol. 2020:JCO2000650.
[34] Taylor C, Correa C, Duane FK, et al. Estimating the Risks of Breast Cancer Radiotherapy: Evidence From Modern Radiation Doses to the Lungs and Heart and From Previous Randomized Trials. J Clin Oncol. 2017;35:1641-9.
[35] Hoekstra N, Fleury E, Merino Lara TR, et al. Long-term risks of secondary cancer for various whole and partial breast irradiation techniques. Radiotherapy and Oncology. 2018.

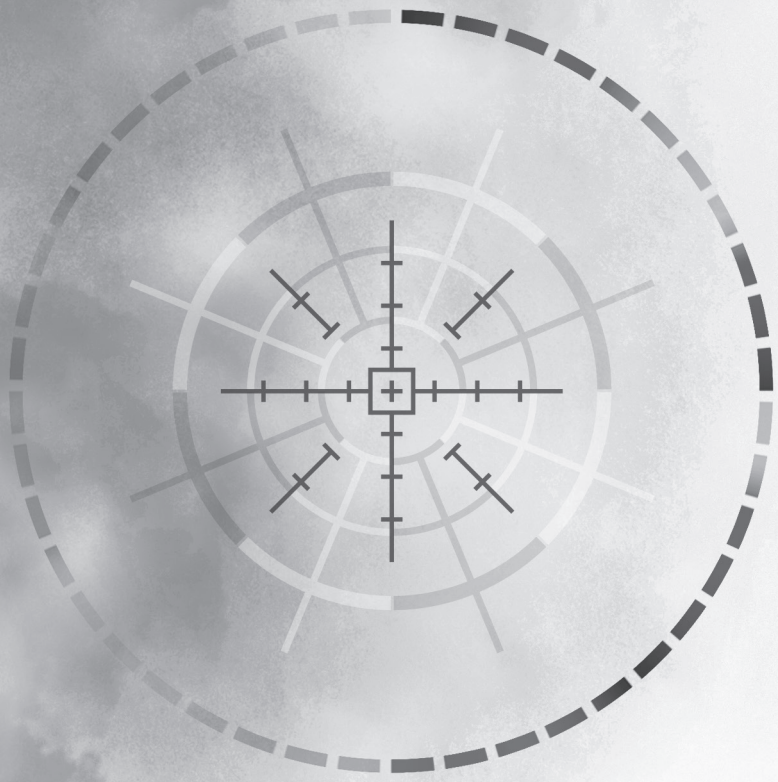

6

Improving the delineation of the tumor bed

Published as

Injection of radiopaque hydrogel at time of lumpectomy improves the target definition for adjuvant radiotherapy

Gerson M. Struik[1,2], MD; Nienke Hoekstra[2], MD ; Taco M. Klem[1], MD, PhD; Ali Ghandi[3], MD; Gerda M. Verduijn[2], MD; Annemarie T. Swaak-Kragten, MD[2]; Alja Schoonbeek[2], MD; Kim C. de Vries[2], MD; Margriet A. Sattler[2], MD, PhD; Kees Verhoef[4], MD, PhD; Erwin Birnie[5], PhD; Jean-Philippe Pignol[2,6], MD, PhD

1. Franciscus Gasthuis and Vlietland, Department of Surgery, Rotterdam, the Netherlands
2. Erasmus MC, Department of Radiation Oncology, Rotterdam, the Netherlands
3. Franciscus Gasthuis and Vlietland, Department of Radiology, Rotterdam, the Netherlands
4. Erasmus MC, Department of Surgery, Rotterdam, the Netherlands
5. Franciscus Gasthuis and Vlietland, Department of Statistics and Education, Rotterdam, the Netherlands,
6. Dalhousie University, Department of Radiation Oncology, Halifax, Nova Scotia, Canada

Radiotherapy and Oncology 131 (2019) 8–13
Doi: 10.1016/j.radonc.2018.11.003

Abstract

Background and purpose – During oncoplastic breast-conserving surgery (BCS), the surgical cavity is closed to reduce seroma formation. This makes the radiotherapy target definition using clips challenging, leading to poor inter-observer agreement and potentially geographical misses. We hypothesize that injecting a radiopaque hydrogel in the lumpectomy cavity before closure improves radiotherapy target definition and agreement between observers.

Materials and methods – Women undergoing BCS in a single university hospital were prospectively accrued in the study. Three to 9 ml of iodined PolyEthylene Glycol (PEG) hydrogel and clips were inserted in the lumpectomy cavity. A CT-scan was performed at 4 to 6 weeks. CT images of BCS patients with standard clips only were used as control group, matched on age, specimen weight, and distance between clips. Six radiation oncologists delineated the tumor bed volumes and rated the cavity visualization score (CVS). The primary endpoint was the agreement between observers measured using a Conformity Index (Cx).

Results – Forty-two patients were included, 21 hydrogel procedures and 21 control, resulting in 315 observer pairs. The feasibility of the intervention was 100%. The median Cx was higher in the intervention group (Cx=0.70, IQR [0.54-0.79]) than in the control group (Cx=0.54, IQR [0.42-0.66]), $p<0.001$, as were the CVS (3.5 [2.5-4.5] versus 2.5 [2-3.5], $p<0.001$). The rate of surgical site infections was similar to literature.

Conclusions – The use of radiopaque PEG enables to identify the lumpectomy cavity, resulting in a high inter-observer agreement for radiotherapy target definition. This intervention is easy to perform and blends well into current practice.

Introduction

For localized cancers, breast-conserving therapy (BCT), including limited surgery and adjuvant whole breast radiotherapy, is equivalent to mastectomy in regard to oncologic outcomes while enabling breast preservation [2]. Oncoplastic techniques have been increasingly used worldwide to improve cosmesis [3-5]. Those techniques involve, at minimum, a simple volume displacement (level 1 oncoplastic technique), as the breast parenchyma is approximated to close the lumpectomy cavity [6]. In so doing, the seroma is limited in size, and it often becomes invisible on a CT-scan. Eventually this technique creates challenges for tumor bed delineation at the time of adjuvant radiotherapy planning [7]. Accurate tumor bed delineation to target breast radiotherapy is particularly critical for accelerated partial breast irradiation (APBI) or when a boost dose is required. During APBI, only the part of the breast immediately surrounding the tumor bed is irradiated [8-12]. Also, young or high-risk patients are benefiting from a boost dose to the tumor bed after or during whole breast radiotherapy [13].

Inaccurate target definition carries the risk of a radiation geographical miss, which, in turn, might lead to an increased risk of local recurrence, especially for APBI. Furthermore, if the tumor bed delineation is enlarged due to uncertainties, there is an increased risk of toxicity [14-16]. Finally, if the target cannot be appropriately defined, some patients may be declined for patient-friendly APBI techniques [16-20]. Traditionally, surgical clips are placed at the time of surgery to guide the tumor bed delineation. However, a recent study by den Hartogh shows that radiotherapy target definition using clips has poor inter-observer agreement in patients following oncoplastic surgery [7]. Thus, the attempt to improve surgical outcome by performing oncoplastic techniques might impair radiotherapy treatment outcomes.

A recent development in radiation oncology is the use of temporary injectable hydrogels. Among others, polyethylene glycol (PEG) radiopaque hydrogel is successfully used as a spacer to remove critical structures from the high dose area, such as the rectum in prostate radiotherapy [21]. Also, PEG hydrogel has been proposed as a tissue marker [22].

Ciernik et al. tested a PEG hydrogel marker to visualize the cavity after lumpectomy and suggested a high level of inter-observer agreement for target delineation [23]. The marker contains PEG with less than 1% iodine, and this material has a high imaging contrast on CT, MRI and, to a lesser extent, on ultrasound up to 3 months. Reabsorption and clearance takes place approximately 7 months after implantation.

We report a prospective clinical cohort study testing the radiopaque hydrogel to improve radiotherapy target definition following oncoplastic breast conserving surgery. Our aim was to assess if the injection in the lumpectomy cavity before closure was safe, feasible, and increased inter-observer agreement for the radiotherapy target definition.

Patients and methods

Study population

The study design was a prospective intervention cohort study with a matched control group. The study was approved by the Erasmus MC research ethic board and registered at the Netherlands Trial Register (NTR-6610).

Eligible patients included women with a diagnosis of breast cancer or DCIS planned for breast-conserving surgery, with full-thickness closure corresponding to level 1 oncoplastic breast surgery, and adjuvant radiotherapy. Patients with oncoplastic surgery of level 2 or more (volume replacement), pre-operative indication for adjuvant chemotherapy, or an allergy for PEG or iodine were excluded. Selected patients were included after written informed consent was obtained.

Treatments

Surgical procedures were performed in a single large secondary teaching hospital in Rotterdam, the Netherlands (Franciscus Gasthuis and Vlietland). After tumor resection and hemostasis were achieved, five surgical clips were placed, according to standard protocol, to define the cavity walls: including one positioned deep toward the fascia pectoralis and four in each radial direction [24]. Subsequently, any undermining of the fibroglandular tissue from the pectoralis muscle and/or skin was performed. Then, 3 to 9 ml of radiopaque PEG hydrogel (TraceIT©, Augmenix Inc, Bedford, MA) was instilled in the cavity and coated onto the tumor cavity walls with the fingertips. The cavity was closed following oncoplastic protocol with the suture of at least one deep, glandular, layer and closure of the most superficial layer and the skin. The amount of product used was recorded and ease of use scored using the System Usability Scale (SUS) [25]. This 10 question 5-point scale is a simple and reliable tool to measure usability of new technology or products, and has been used in medical research[26]. After referral to radiation oncology, a standard CT-simulation for radiotherapy planning purpose was acquired with images of 2.5 mm thickness and a resolution of 1 x 1 mm^2 at 120 kilovoltpeak (kVp). The surgical scar and the glandular tissue were marked on the skin with a CT compatible wire.

Patients treated with the hydrogel were matched 1:1 with a cohort of patients treated by the same team of surgeons also performing a level 1 oncoplastic surgery with placement

of five surgical clips [24], but without instillation of the hydrogel. Matching was performed on factors known to influence interobserver variability of target definition and/or cavity visibility, ensuring similar resected specimen weight and maximum distance between clips (as predictors of target volume)[27-30], and age (below or above 70 years) as surrogate for breast composition[30].

Target volume delineation

Anonymized CT image sets of both group of patients were transferred to a MIM Symphony 6.6 imaging station (MIM Software Inc, Cleveland,OH). Six experienced and senior radiation oncologists delineated the target volumes in a random sequence and were blinded for each other's contours, by making the sets of CT-images available to each radiation oncologist separately (Fig. 1). Each patient's pre-operative information and imaging, surgical report and pathology report were available.

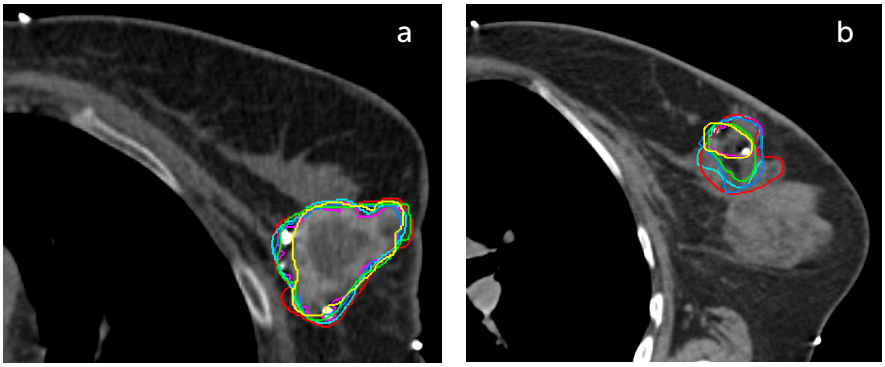

Figure 1a and 1b Example of tumor bed delineation on CT with (**a**) and without (**b**) hydrogel.

For the patients in the intervention group, the radiation oncologists were asked to contour the tumor bed with the following instruction: "*Please contour the tumor bed volume as usual, using information of the CT density (including the hydrogel) and the clips*". For the control group, the radiation oncologists were asked to delineate using the following instruction: "*Please contour the tumor bed volume as usual, using information of the CT density and the clips*". Additionally, all six radiation oncologists were asked to rate the cavity visualization score (CVS) [27, 31]and record the time needed for contouring per patient. The CVS is a metric assessing the visibility of the lumpectomy cavity on CT on a 5-point scale ranging from "no cavity visible" (CVS 1) to "homogeneous cavity with clearly identified margins" (CVS 5) (fig. 2). It is commonly used in studies on target definition [7, 32].

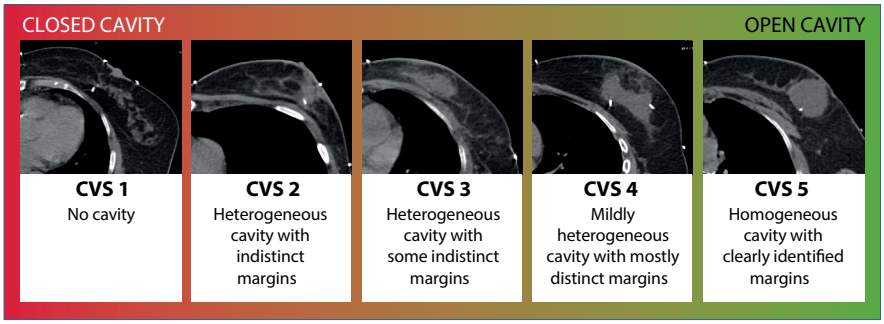

Figure 2 Cavity Visualisation Score. All example CT-images are captured from patients in the control group of this study.

Analysis

The primary outcome measure was the Conformity Index (Cx), defined by the ratio between the volume of agreement of the defined target volumes divided by the encompassing volume for each observer pair [7]. Secondary outcome measures included the distance between the center of mass of the target volumes (dCOM), the target volumes in cc, the CVS[27, 31], the feasibility of hydrogel injection, adverse events, and ease of use.

A sample size of 21 patients times 6 observers was calculated, leading to 315 observer pairs in both the intervention and control group. Based on an expected SD in Cx of 0.19 [7, 33], alpha=0.05 and beta =0.2, this sample size would make it possible to detect an effect size of 0.044 of the primary outcome (Cx) with 95% confidence. Even for a subgroup analysis (alpha=0.025) on CVS≤3 with an expected number of n=10 patients in each group the detectable effect size would be 0.068, which was deemed acceptable.

For the primary outcome measure, we reported median values and accompanying interquartile ranges (IQRs) and, as Shapiro–Wilk normality tests showed this variable was not normally distributed, assessed significance using a Mann-Whitney U-test.

Descriptive statistics were used for the analysis of secondary endpoints, assuming independency of groups. Differences between groups were also assessed using a Mann-Whitney U-test. Multiple linear regression analysis testing the factors influencing the Cx included the following independent variables: group (intervention versus control), mean target volume, CVS per observer pair, and the matching factors as described above. The effect modification was modelled as an interaction effect of group (intervention versus control) times target volume. The feasibility of the hydrogel marker injection and adverse events were described as percentages. IBMM SPSS Statistics version 24 was used with two-sided p-values below 0.05 considered statistically significant.

Results

Twenty-four patients were included in the interventional group. Three patients were excluded because they had positive margins on the pathology report and they had a second surgery for re-excision. In these three cases , during re-excision the hydrogel was clearly identifiable, being solid in the surgical cavity and easy to remove. In the control group we randomly matched 21 patients out of 100 possible controls. Patient characteristics are detailed in Table 1. The groups were well balanced in regard to tumor diameter, histology, resected specimen weight, and maximum distance between clips. In the intervention group, patients were 5 years younger, leading to potentially more dense breasts.

Table 1 Patient characteristics between groups.

	Intervention group (hydrogel+clips) n=21	**Control group (clips only) n=21**
Age, years	57 [50-64]	62 [50-65]
Microscopic tumor diameter in mm	14.5 [12-18]	15 [9.5-21]
Resected specimen weight in grams	42 [28-66]	45 [35-61]
Histology	19 ductal carcinoma 1 DCIS 1 mucinous carcinoma	15 ductal carcinoma 4 DCIS 1 lobular carcinoma 1 apocrine carcinoma
Laterality	5 Left 16 Right	9 Left 12 Right
Interval between surgery and CT-simulation in days	39 [31-46]	36 [24-55]
Maximum distance between surgical clips on CT in mm	46 [39-52]	45 [31-55]

Data are presented as median values, and inter-quartile ranges within brackets.

The use of hydrogel was technically feasible in all patients. The product was easy to use, with a median SUS score of 100 (IQR [96-100]). Two patients (9.5%) in the intervention group developed a superficial surgical site infection, and two patients (9.5%%) had clinically apparent seroma formation, all being grade 1-2 out of 5 according to the Clavien Dindo classification [34].

Patients in the intervention group had their CT-simulation performed at a median of 39 days post-surgery (IQR [31-46]). For most patients, the hydrogel was easily identified in the surgical cavity on the radiotherapy planning CT. The occurrence of seroma in some cases caused dilution of the hydrogel or, in other cases, formation of a level of hydrogel, not completely filling up the cavity (Fig. 3).

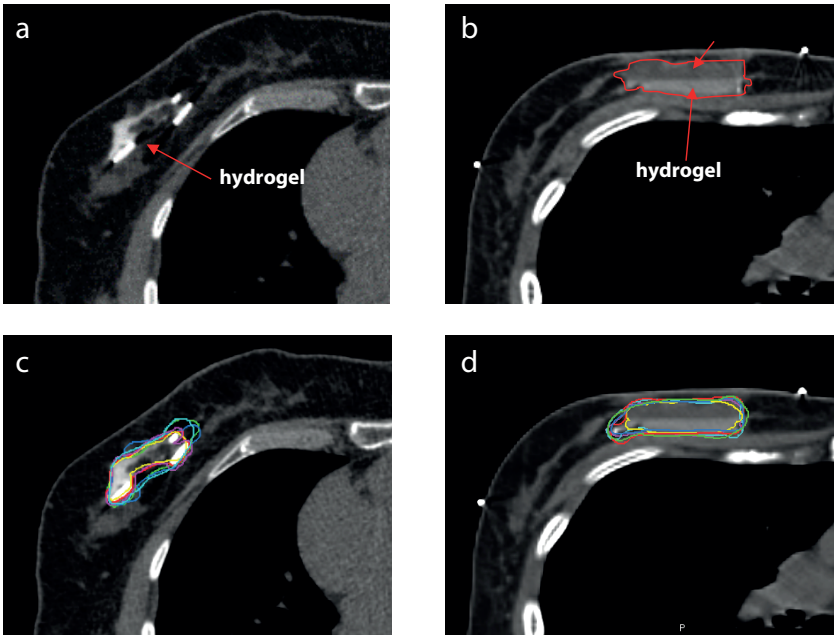

Figure 3 Example of case without natural seroma (**a**) and a case with natural seroma (**b**), showing some dilution and formation of a level of hydrogel, not completely filling up the cavity (shown in red) and the resulting six contours for both cases (**c** and **d**).

The median conformity index was higher in the intervention group, with a Cx of 0.70 (IQR [0.54-0.79]), compared to the control group, with a Cx of 0.54 (IQR [0.42-0.66]), suggesting that the target delineation was less variable in the presence of hydrogel ($p<0.001$). On the other-hand, contouring in the presence of hydrogel took slightly more time - 5 minutes instead of 4 ($p<0.001$) – and also led to target volumes two and a half times larger being contoured - 26.2 cc instead of 10.2cc ($p<0.001$).

Multiple linear regression analysis showed that the adjusted Beta coefficient was 0.09 (95% CI [0.05 - 0.17]) for group and 0.002 (95% CI [0.001 - 0.004]) for mean target volume, meaning that both the presence of hydrogel and of a large target volume were significantly

Table 2 Results for various radiotherapy target delineation metrics.

	Intervention group (hydrogel + clips) n=315**	**Control group (clips only) n=315****	**P-value***
Cx	0.70 [0.54-0.79]	0.54 [0.42-0.66]	<0.001
CVS	3.5 [2.5-4.5]	2.5 [2-3.5]	<0.001
dCOM in mm	2.0 [1.1-4.3]	3.1 [1.6-5.3]	<0.001
Target volume in cc	26.2 [15.1-43.8])	10.2 [5.8-22.9]	<0.001
Time needed for delineation in minutes	5 [4-7]	4 [3-5]	<0.001.

Data are presented as median values with inter-quartile ranges within brackets. * Mann-Whitney-U-test, ** n= number of observer pairs.

associated with a better Cx. Adding the interaction term of intervention times target volume to the model showed that the increase in Cx per unit volume is larger in the presence of gel (adjusted Beta coefficient was 0.005 (95% CI [0.004 - 0.006]). meaning that with every 2cc larger volume, the presence of gel, leads to an extra 0.01 increase of Cx. Mean CVS per observer pair was eventually excluded from the model as variable group is positively correlated with a CVS (Spearman's correlation coefficient 0.326, p<0.001). This is logical since the intervention is intended to increase the seroma visibility.

The effect of the intervention was strongest in the matched group of patients with a CVS ≤3 in the control group (median Cx 0.67 with hydrogel and clips versus 0.49 with clips alone, p<0.001), meaning in the group of patients where the seroma was difficult to identify, compared to the group of patients with a CVS>3 in the control group (median Cx 0.74 versus 0.68, p<0.001).

Discussion

This study demonstrates that using a hydrogel loaded with iodine during lumpectomy cavity closure, reduces the variability of target contouring in a population of well trained and highly specialized radiation oncologists.

We report on a simple surgical intervention adding to other solutions to improve radiotherapy target definition for breast cancer patients, including the use of clips, 3D ultrasound or MR image fusion or simulation. Since inter-observer variability is indicative of the difficulty to accurately define the treatment target volumes among practitioners,

those studies examining these options have used the conformity index (Cx) as a measure of accuracy in defining the target volume[29]. Our results compare well with other studies using standardized contouring protocols and surgical clips, which is the current gold standard in radiotherapy [16]. Previous studies evaluating the interobserver agreement for delineation with clips found comparable Cx to the one we reported here for the control group, between 0.56 to 0.61 [28, 29, 35]. Another study reports a higher agreement using gold fiducial markers, with a Cx of 0.70[32]. However, none of these studies were performed in a context of a level 1 oncoplastic intervention. A study by Den Hartogh showed that radiotherapy target definition using clips alone for patients with full thickness closure (FTC) has a much poorer inter-observer agreement, with a median Cx of 0.44 [7].

The significantly higher Cx in our intervention group than in our control group can probably be explained by the also significantly higher CVS (3.5 versus 2.5 respectively). The median CVS score of 2.5 (heterogeneous cavity with no to minimal distinct margins) in our control group seems intuitively higher than expected. However, a median CVS score of 3 was found in the study by den Hartogh et al. after FTC [7]. This means that a FTC not always translates into a loss of cavity. In several cases in our study the full-thickness closure was limited to a single suture, which could be the explanation of the existence of a visible seroma. The high conformity index found in our intervention group, where all patients had oncoplastic intervention, should be considered as a good result for improving the quality of the radiation treatment. The larger median target volume found in the intervention group (26.2 versus 10.2cc) did not alone explain the difference in Cx, since the regression analysis adjusting for target volume showed that the use of hydrogel was an independent factor of improved Cx. The hydrogel itself accounted for a 9% increase in Cx on average, which is clinically relevant. Interestingly, although the hydrogel itself adds some volume (3 to 9cc in this study) which may preserve part of the seroma, the median target volume in our intervention group, 26.2cc, is comparable to the 23cc found in the study by den Hartogh[7]. In those cases with a relatively large seroma, the visualization was however facilitated by the presence of radio-opaque gel on the border of the seroma. Finally, the effect of hydrogel on mean target volumes and consequent planned target volumes (PTVs) could be more formally concluded in a randomized controlled trial or a comparison within the same patient.

The hydrogel injection intervention was found feasible, safe and easy to perform. The rate of infection (9.5%) and the formation of a clinically apparent seroma (9.5%) after injection of hydrogel was comparable to the literature for breast-conserving surgery [36-39].

A higher Cx results in a lower risk of geographical miss of the administered radiotherapy, which, in turn, may result in a better outcome in term of local control. Additionally, with less inter-observer variability, smaller margins accounting for delineation variation could

be used. This could reduce radiotherapy related toxicity, such as skin effects and breast fibrosis, and compensate for the possibly larger volume delineated when using a hydrogel injection. Also, as shown in figure 1, some observers have smaller volume contoured compared to other. This would mean a lower volume treated using APBI and potentially an improvement of the treatment tolerance. Furthermore, by helping target definition in patients with low CVS, more patients may be eligible for more patient friendly APBI techniques as patients with a poorly defined cavity are generally excluded [16-18, 40, 41]. A gel with good MRI visibility could also be very useful in an era when new machines, including the MR-linac, are used for improved image guided radiotherapy (IGRT)[42].

An important caveat in breast radiotherapy target definition is the fact that the tumor bed needs treatment and does not necessarily match the lumpectomy cavity. The discussion about the volume to be treated lead the GEC-ESTRO to develop complex contouring guidelines and recommends using the exact microscopic surgical margins in all directions to realize the volume expansion from seroma to clinical target volume (CTV). The hydrogel helps to better define the lumpectomy cavity, but still the contouring guidelines should be followed.

A limitation of the intra-operative injection of the hydrogel is that in 9 out of 21 cases the seroma as defined by the gel showed some leveling with fluid or dilution resulting in imprecise contours. Since the CT scan was performed on average 5.5 weeks after the surgery, we assume that post-operative healing, inflammation and fluid production may have deteriorated the visibility of the gel. In such cases the observers have unanimously incorporated the diluted cavity into the target volume.

In our study, patients with a CVS ≤3 had the most benefit from the hydrogel. To better select patients with a low CVS, that could benefit from a hydrogel injection, a future direction would be to change the timing of the intervention to the moment of radiotherapy planning when the healing process is largely completed. This would also partly resolve some of the limitations caused by dilution of the gel as described above.

In conclusion, this study shows that the use of a radiopaque hydrogel during BCS enables breast surgeons to clearly demarcate the lumpectomy cavity, resulting in a high inter-observer agreement of radiotherapy target definition. This intervention is easy to perform and can easily blend into standard practice.

Acknowledgements

The author wants to acknowledge the support of Peter van Gelder for proofreading the manuscript and Bas Schipaanboord for technical support analyzing the contours in MIM. The study was supported by a grant in kind from Augmenix Inc.

References

[1] American Society of Breast Surgeons. Consensus Statement for Accelerated Partial Breast Irradiation. 2011; https://www.breastsurgeons.org/new_layout/about/statements/PDF_Statements/APBI.pdf.

[2] Group EBCTC, Darby S, McGale P, et al. Effect of radiotherapy after breast-conserving surgery on 10-year recurrence and 15-year breast cancer death: meta-analysis of individual patient data for 10,801 women in 17 randomised trials. Lancet. 2011;378:1707-16.

[3] Asgeirsson KS, Rasheed T, McCulley SJ, Macmillan RD. Oncological and cosmetic outcomes of oncoplastic breast conserving surgery. Eur J Surg Oncol. 2005;31:817-23.

[4] Driul L, Bernardi S, Bertozzi S, Schiavon M, Londero AP, Petri R. New surgical trends in breast cancer treatment: conservative interventions and oncoplastic breast surgery. Minerva Ginecol. 2013;65:289-96.

[5] Kim MK, Kim T, Moon HG, et al. Effect of cosmetic outcome on quality of life after breast cancer surgery. Eur J Surg Oncol. 2015;41:426-32.

[6] Chatterjee A, Dayicioglu D, Khakpour N, Czerniecki BJ. Oncoplastic Surgery: Keeping It Simple With 5 Essential Volume Displacement Techniques for Breast Conservation in a Patient With Moderate- to Large-Sized Breasts. Cancer Control. 2017;24:1073274817729043.

[7] den Hartogh MD, van den Bongard HJ, Davidson MT, et al. Full-thickness closure in breast-conserving surgery: the impact on radiotherapy target definition for boost and partial breast irradiation. A multimodality image evaluation. Ann Surg Oncol. 2014;21:3774-9.

[8] Consensus Statement for Accelerated Partial Breast Irradiation. 2011; https://www.breastsurgeons.org/new_layout/about/statements/PDF_Statements/APBI.pdf.

[9] Correa C, Harris EE, Leonardi MC, et al. Accelerated Partial Breast Irradiation: Executive summary for the update of an ASTRO Evidence-Based Consensus Statement. Pract Radiat Oncol. 2017;7:73-9.

[10] Polgar C, Van Limbergen E, Potter R, et al. Patient selection for accelerated partial-breast irradiation (APBI) after breast-conserving surgery: recommendations of the Groupe Europeen de Curietherapie-European Society for Therapeutic Radiology and Oncology (GEC-ESTRO) breast cancer working group based on clinical evidence (2009). Radiother Oncol. 2010;94:264-73.

[11] Shah C, Vicini F, Wazer DE, Arthur D, Patel RR. The American Brachytherapy Society consensus statement for accelerated partial breast irradiation. Brachytherapy. 2013;12:267-77.

[12] Shaitelman SF, Lin HY, Smith BD, et al. Practical Implications of the Publication of Consensus Guidelines by the American Society for Radiation Oncology: Accelerated Partial Breast Irradiation and the National Cancer Data Base. Int J Radiat Oncol Biol Phys. 2016;94:338-48.

[13] Bartelink H, Maingon P, Poortmans P, et al. Whole-breast irradiation with or without a boost for patients treated with breast-conserving surgery for early breast cancer: 20-year follow-up of a randomised phase 3 trial. Lancet Oncol. 2015;16:47-56.

[14] Borger JH, Kemperman H, Smitt HS, et al. Dose and volume effects on fibrosis after breast conservation therapy. Int J Radiat Oncol Biol Phys. 1994;30:1073-81.

[15] den Hartogh MD, van Asselen B, Monninkhof EM, et al. Excised and irradiated volumes in relation to the tumor size in breast-conserving therapy. Breast Cancer Res Treat. 2011;129:857-65.

[16] Strnad V, Hannoun-Levi JM, Guinot JL, et al. Recommendations from GEC ESTRO Breast Cancer Working Group (I): Target definition and target delineation for accelerated or boost Partial Breast Irradiation using multicatheter interstitial brachytherapy after breast conserving closed cavity surgery. Radiother Oncol. 2015;115:342-8.

[17] Wang L, Ding GX. The accuracy of the out-of-field dose calculations using a model based algorithm in a commercial treatment planning system. Phys Med Biol. 2014;59:N113-28.

[18] Major T, Gutierrez C, Guix B, van Limbergen E, Strnad V, Polgar C. Recommendations from GEC ESTRO Breast Cancer Working Group (II): Target definition and target delineation for accelerated or boost partial breast irradiation using multicatheter interstitial brachytherapy after breast conserving open cavity surgery. Radiother Oncol. 2016;118:199-204.

[19] Ott OJ, Strnad V, Hildebrandt G, et al. GEC-ESTRO multicenter phase 3-trial: Accelerated partial breast irradiation with interstitial multicatheter brachytherapy versus external beam whole breast irradiation: Early toxicity and patient compliance. Radiother Oncol. 2016;120:119-23.

[20] Vicini F, Shah C, Tendulkar R, et al. Accelerated partial breast irradiation: An update on published Level I evidence. Brachytherapy. 2016;15:607-15.
[21] Hamstra DA, Mariados N, Sylvester J, et al. Continued Benefit to Rectal Separation for Prostate Radiation Therapy: Final Results of a Phase III Trial. International Journal of Radiation Oncology • Biology • Physics. 2017;97:976-85.
[22] Bair RJ, Bair E, Viswanathan AN. A radiopaque polymer hydrogel used as a fiducial marker in gynecologic-cancer patients receiving brachytherapy. Brachytherapy. 2015;14:876-80.
[23] Ciernik IF, Voss H, Wosle M. Standardization of the target volume for boost or partial breast radiation therapy after lumpectomy of breast cancer. Int J Radiat Oncol Biol Phys. 2014;89:690-1.
[24] Kirby AN, Jena R, Harris EJ, et al. Tumour bed delineation for partial breast/breast boost radiotherapy: what is the optimal number of implanted markers? Radiother Oncol. 2013;106:231-5.
[25] Brooke J. SUS - A quick and dirty usability scale. In: P. W. Jordan BT, B. A. Weerdmeester, A. L. McClelland, editor. Usability evaluation in industry. London: Taylor and Francis; 1996. p. 189-94.
[26] Pei Y-C, Chen J-L, Wong AMK, Tseng KC. An Evaluation of the Design and Usability of a Novel Robotic Bilateral Arm Rehabilitation Device for Patients with Stroke. Frontiers in Neurorobotics. 2017;11:36.
[27] Landis DM, Luo W, Song J, et al. Variability among breast radiation oncologists in delineation of the postsurgical lumpectomy cavity. Int J Radiat Oncol Biol Phys. 2007;67:1299-308.
[28] Petersen RP, Truong PT, Kader HA, et al. Target volume delineation for partial breast radiotherapy planning: clinical characteristics associated with low interobserver concordance. Int J Radiat Oncol Biol Phys. 2007;69:41-8.
[29] Yang TJ, Tao R, Elkhuizen PHM, van Vliet-Vroegindeweij C, Li G, Powell SN. Tumor bed delineation for external beam accelerated partial breast irradiation: A systematic review. Radiotherapy and Oncology. 2013;108:181-9.
[30] Kader HA, Truong PT, Pai R, et al. When is CT-based postoperative seroma most useful to plan partial breast radiotherapy? Evaluation of clinical factors affecting seroma volume and clarity. Int J Radiat Oncol Biol Phys. 2008;72:1064-9.
[31] Smitt MC, Birdwell RL, Goffinet DR. Breast electron boost planning: comparison of CT and US. Radiology. 2001;219:203-6.
[32] Shaikh T, Chen T, Khan A, et al. Improvement in Interobserver Accuracy in Delineation of the Lumpectomy Cavity Using Fiducial Markers. International Journal of Radiation Oncology • Biology • Physics. 2010;78:1127-34.
[33] Wan X, Wang W, Liu J, Tong T. Estimating the sample mean and standard deviation from the sample size, median, range and/or interquartile range. BMC medical research methodology. 2014;14:135.
[34] Dindo D, Demartines N, Clavien PA. Classification of surgical complications: a new proposal with evaluation in a cohort of 6336 patients and results of a survey. Ann Surg. 2004;240:205-13.
[35] Atrchian S, Sadeghi P, Cwajna W, et al. Improvement of consistency in delineating breast lumpectomy cavity using surgical clips. J Surg Res. 2018;221:30-4.
[36] Williams N, Sweetland H, Goyal S, Ivins N, Leaper DJ. Randomized trial of antimicrobial-coated sutures to prevent surgical site infection after breast cancer surgery. Surg Infect (Larchmt). 2011;12:469-74.
[37] Degnim AC, Throckmorton AD, Boostrom SY, et al. Surgical site infection after breast surgery: impact of 2010 CDC reporting guidelines. Ann Surg Oncol. 2012;19:4099-103.
[38] Panhofer P, Ferenc V, Schutz M, et al. Standardization of morbidity assessment in breast cancer surgery using the Clavien Dindo Classification. Int J Surg. 2014;12:334-9.
[39] Struik GM, Vrijland WW, Birnie E, Klem TM. A randomized controlled trial on the effect of a silver carboxymethylcellulose dressing on surgical site infections after breast cancer surgery. PLoS One. 2018;13:e0195715.
[40] Edmundson GK, Vicini FA, Chen PY, Mitchell C, Martinez AA. Dosimetric characteristics of the MammoSite RTS, a new breast brachytherapy applicator. International Journal of Radiation Oncology • Biology • Physics. 2002;52:1132-9.
[41] Pignol JP, Keller B, Rakovitch E, Sankreacha R, Easton H, Que W. First report of a permanent breast 103Pd seed implant as adjuvant radiation treatment for early-stage breast cancer. Int J Radiat Oncol Biol Phys. 2006;64:176-81.
[42] Henke LE, Contreras JA, Green OL, et al. Magnetic Resonance Image-Guided Radiotherapy (MRIgRT): A 4.5-Year Clinical Experience. Clinical Oncology. 2018;30:720-7.

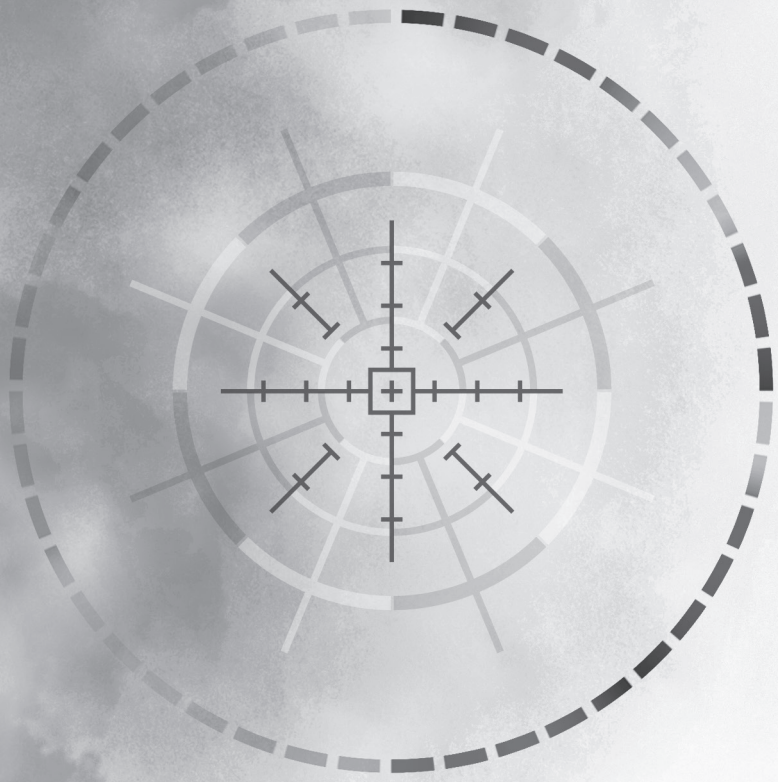

7

Discussion

Introduction

The optimal treatment for cancer patients is a delicate balance between the probability of cure and the risk of treatment-induced toxicities. Using very intensive treatments, the chance on cure can be improved, but this comes at the price of increased toxicity. The best way to improve treatment for a specific type or stage of cancer depends on the current risks of cancer-related death and severe toxicity. For the treatment of locally advanced pancreas carcinoma for example, overall survival is low and toxicity is high [1]. It is therefore warranted to find ways to safely intensify treatment. On the other hand, the chance of cure is very high for early-stage breast cancer patients [2, 3]. In this situation, treatment de-escalation would result in less toxicity for all patients, with only a small increase in the number of recurrences. It is even possible that de-escalating treatment would lead to an increased overall survival for early stage-breast cancer patients, because some of the toxicities are potentially lethal. This thesis focusses on adjuvant breast radiotherapy. The two most important and potentially lethal long-term toxicities of adjuvant breast radiotherapy are cardiovascular disease and the induction of secondary cancers [4].

In this thesis, our results on reducing the secondary cancer risks by optimized treatment planning and increasing the accuracy of treatment are discussed.

Secondary cancer risk after breast radiotherapy

To reduce the secondary cancer risk, it is important to know the magnitude of this risk. Several epidemiological studies have been published on the secondary cancer risk after adjuvant breast radiotherapy [4-7]. These studies show that there is indeed a higher risk for breast cancer patients to experience a new malignancy compared to the normal population. There are multiple possible explanations for this increased risk. It could be treatment-related, due to shared risk factors, or due to genetic susceptibility.

A large meta-analysis by Grantzau and Overgaard showed that both irradiated and non-irradiated breast cancer patients had an excess risk of second non-breast cancer compared to the general female population [5]. The risk for irradiated patients was larger than for non-irradiated patients, with a standardized incidence ratio (SIR) of 1.23 for the irradiated patients and 1.08 for the non-irradiated patients. Especially the risk of a new cancer occurring in organs adjacent to the treatment area was increased for the irradiated patients. The SIRs at ≥ 15 years after treatment were 1.91 for lung, 2.71 for esophagus and 3.15 for thyroid. This suggests that radiation is causing the increase in secondary cancer risks. The SIRs increased progressively over time after treatment for the irradiated patients,

but not for the non-irradiated patients. For lung cancer, the SIR was not significantly higher than 1 in the analysis of all studies regardless of length of follow-up. When applying a latency of ≥ 5 years after treatment, the SIR for lung cancer was 1.21 and significantly increased. After ≥ 10 years, the SIR was 1.58 and after ≥ 15 years it was 1.91.

These results are in line with the results of our phantom experiment as described in **chapter 2**. We showed that the largest part of the total secondary cancer risk after adjuvant breast radiotherapy was due to secondary lung cancer induction. The relative risk for a patient treated with whole breast radiotherapy at age 60 years in our analysis was 1.68, which is slightly lower than the SIR of 1.91 after 15 years from Grantzau et al. for patients with a median age of 56 years [5]. This could be due to improvements in radiation technique. In the Grantzau meta-analysis, patients were treated between 1935 and 2007. With the techniques available at that time, their lung mean lung dose was probably higher than in our phantom treated with a linear accelerator using 3D treatment planning and a multi-leaf collimator.

The calculated lifetime risk of secondary lung cancer mortality is high. For an early-stage breast cancer patient treated at age 50 years, we found a 2.4% absolute increase in lung cancer mortality up to the age of 80 years. This is higher than published risks on cardiovascular mortality. For example, Darby et al. calculated a 0.5% absolute excess risk of cardiovascular mortality up to the age of 80 years for the similar 50-year old patient without pre-existing cardiac risk factors [8]. In case of one or more pre-existing cardiac risk factors, for example diabetes or smoking, the cardiovascular risk of death increased to 0.7%, which is still 4 times lower than the calculated risk of secondary lung cancer mortality. In their meta-analysis, Taylor et al. found that for smoking patients receiving adjuvant breast radiotherapy, the risk of cardiovascular disease was 3-fold increased [4]. The increase in risk of secondary lung cancer was more pronounced with a 10-fold increase.

The long latency found in our study and the meta-analysis by Grantzau et al. might explain why the risk of secondary cancers has received less attention than the risk of cardiovascular disease. In our calculations, the incidence of secondary lung cancers started at least 5 years after treatment and continued to increase. The peak incidence in our analysis was found at 25 years after treatment. Darby et al. found that 44% of all major cardiovascular events occurred within 10 years after treatment [8]. Conversely, in our analysis only 7% of all secondary lung cancers occurred within 10 years. Since most clinical trials are losing power after about 10 years of follow-up and never reach 25 years of follow-up, neither those trials nor meta-analyses of those trials could capture accurately the importance of secondary lung cancer mortality over cardiac mortality.

We indeed showed that the incidence rate of secondary lung cancers continues to increase up to 25 years after treatment (**Chapter 2**, figure 2). If more patients with a longer follow-up would be included in the clinical trials, the number of secondary lung cancer cases per women-years would increase sharply. We calculated the life-time risk of secondary cancer instead of the risk up to age 80 years. With the increasing life expectancy of the entire population and the very favorable prognosis after contemporary treatment techniques, it is likely that the majority of females with early stage breast cancer will live beyond 80 years. Therefore, the incidence of secondary lung cancers after the age of 80 years has become of interest.

When predicting the risk of secondary lung cancer for a patient treated today, it is important to take into the account the limitations of the data from clinical trials and registry studies. Next to the bias linked to patient selection, the dramatic reduction in lung doses and the lower rates of smoking in the population will have a major impact on this risk. A consequence of the long latency of secondary cancer induction is that it is practically infeasible to conduct a randomized clinical trial on reducing the secondary cancer risk. First, the number of included patients would need to be very high, as the event rate is low, and the follow-up would need to be at least 30 years. Second, by that time, the techniques investigated are outdated. The use of models to calculate risks of new techniques is the only way to predict the associated reductions in secondary cancer risks. The main advantage of using a model is that it enables a comparison of different treatment techniques knowing the lung dose distributions for the same patients. On the other hand, these models bear various uncertainties and the calculated absolute excess risks of secondary lung cancer must be interpreted with caution. These uncertainties have very limited impact on the relative comparison of different treatment techniques.

For a patient group with such an excellent prognosis as the early-stage breast cancer patients, it is very important to apply the ALARA principle (as low as reasonably achievable) and to reduce the dose to healthy tissues as much as possible. One way to do this is to optimize the treatment planning technique, as is discussed in **chapter 3**. Another way is to reduce the volume treated, by increasing the accuracy of treatment preparation and delivery. This is discussed in **chapters 4, 5, and 6**.

Reducing the secondary lung cancer risk by optimized treatment planning

An example of a comparison of different treatment techniques aiming to reduce the secondary lung cancer risk is reported in **chapter 3**. For this comparison, we generated treatment plans for early-stage breast cancer patients using the Erasmus-iCycle treatment planning software. Erasmus-iCycle is a fully automated multicriteria prioritized optimizer which generates plans of consistent and high quality. As there is no subjective human involvement in the planning, this system is highly suited for unbiased comparisons between treatment techniques. We compared treatment plans varying the priority given to two opposite planning aims, reducing either the dose to the lungs or the dose to the ipsilateral non-target breast tissue (NTBT). When prioritizing sparing of the lungs, an average 5-fold decrease in secondary lung cancer risk was found compared to prioritizing NTBT sparing. As expected, there was an increased dose to the breast with prioritizing lung sparing, but this would correspond to an absolute increase in breast fibrosis risk of only 0.5%. The use of a non-coplanar beam setup resulted in lower doses to both the lungs and NTBT than the use of a coplanar beam setup. This translated into lower risks of secondary lung cancer and breast fibrosis for the non-coplanar beam setup.

Prioritizing lung sparing during treatment planning is easy to implement and is feasible for every external-beam APBI treatment technique, coming at no additional costs for the treating institution. The use of a non-coplanar beam setup could reduce the secondary lung cancer risk even further. This requires additional resources, but is still a relatively easy method that could increase the overall survival of early-stage breast cancer patients.

These findings represent a paradigm shift in the planning of adjuvant breast radiotherapy and especially APBI. The current goal is mainly dose distribution conformity, assuming this leads to lower doses to all surrounding organs. Prioritizing lung sparing requires degrading treatment conformity specifically in the direction of the breast tissue, which can be done using the current high-precision treatment techniques. It is important to prevent excess toxicity in the breast, as breast fibrosis does not lead to mortality but can have a detrimental impact on the quality of life. Care should be given to limit the maximum breast dose, as this is the main factor predicting the risk of breast fibrosis [9, 10].

Geometric accuracy of external-beam APBI

An important step in reducing the dose to healthy tissues for early-stage breast cancer patients was the introduction of accelerated partial breast irradiation (APBI). The rationale for this treatment was the fact that the majority of all local recurrences occur near the surgical tumor bed [11, 12]. Several large randomized trials have demonstrated the safety and efficacy of limiting the treated volume to the tumor bed plus 1 to 2 cm margin [13-16]. The volume to be treated with radiation is called the clinical target volume (CTV) [17, 18]. As this margin from tumor bed to CTV is quite small, a major challenge in external-beam APBI is the geometric accuracy. A geographical miss could lead to a higher risk of local recurrence, as there are few fractions to compensate for this error. This is increasingly important in the context of a further reduction of the number of fractions, even down to a single fraction treatment.

The CTV is expanded with a safety margin to account for the geometric uncertainties of treatment preparation and delivery. This expansion results in the planning target volume (PTV). The choice of a CTV to PTV margin is a trade-off between the risk of a geographical miss and dose to surrounding healthy tissues. The margin is used in three dimensions, meaning it follows a cubic law, so every millimeter CTV expansion has a major impact on the treated volume. The smaller the CTV size, the greater the relative increase in treated volume. Thus, it is important to carefully consider the PTV margin used for external-beam APBI.

With respect to timing, the geometric uncertainties included in the PTV margin calculation are classically divided into interfraction and intrafraction errors. Interfraction motion mainly corresponds to errors related to patient set-up on the couch as well as possible anatomical changes, and the intrafraction error corresponds to motion during the treatment. To appropriately calculate a PTV margin, first the error distributions of the systematic and random components must be quantified. Next, the PTV margin is calculated using an appropriate algorithm, for example following the formula by van Herk [19].

The intrafraction motion during the delivery of an APBI fraction is quantified in **chapter 4**. We analyzed 110 fractions of 22 patients treated with Cyberknife APBI. Two types of motion were distinguished, i.e. breathing motion and the slow drift of the patient during the treatment fraction. The breathing motion was small and a margin of 0.3 – 0.6 mm is sufficient to compensate for it. We showed that the magnitude of the drift depended on the duration of the treatment. For a fraction of up to 8 minutes after the first imaging for patient positioning, a PTV margin of 1 mm is sufficient to compensate for intrafraction motion. For a fraction duration up to 24 minutes, 2 mm margin is required. For fractions of more than 32 minutes, a margin exceeding 2.5 mm is needed. Interestingly, we found a

systematic trend in the direction of the drift. Patients moved on average to the posterior, caudal and medial directions, probably because patients tend to relax on the couch during treatment. Such a trend is not accounted for in the margin as calculated according to the recipe of by van Herk [19], and since it is larger than the breathing motion, it should be included. Asymmetric margins could be used, expanding the target with an additional 0.7 mm in the caudal and medial direction and 0.8 mm in the posterior direction. An alternative without increasing the treated volume is to enable the beam isocenter to track and trail the target, as can be done for example with the Cyberknife technology using fiducial tracking.

The results presented in **chapter 4** are the first time-resolved analysis of intrafraction motion in breast cancer published and show that it is more important to focus on reducing fraction duration and drift than breathing motion. The finding of intrafraction motion increase with the fraction duration is an additional reason, next to patient comfort and logistical reasons, to keep the fraction as short as possible. This duration includes the time used for patient setup after the first imaging and the dose delivery time. Both of these elements could be optimized. One should keep in mind not to compromise on accuracy or dose conformity when reducing treatment time, as this would offset the benefit of a shorter fraction duration.
Next to the motion occurring during a fraction, there is also interfraction motion, which is addressed in **chapter 5**. The main goal of this study was to determine adequate CTV to PTV margins for external-beam APBI. To this end, the motion of surgical clips and interstitial gold markers relative to the tumor bed was measured in a large cohort of 70 patients using in-room diagnostic quality CT scans. Next, we calculated the PTV margin needed to compensate for this motion as a function of the risk of geographical miss for a single fraction treatment. A margin of 1.7 mm is required to ensure 100% CTV coverage in 90% of patients when using surgical clips for patient set-up. With a slightly larger margin of 2.3 mm, 95% of patients would have their CTVs fully covered.

The comprehensive PTV margin for a APBI treatment depends on the technique used, since other sources of geometric uncertainty play a role during treatment preparation and delivery. The comprehensive PTV margin for VMAT single-fraction APBI on a conventional linear accelerator with patient setup based on surgical clips and cone beam CT was calculated at 4.0 mm to ensure 100% CTV coverage in 90% of patients. For a Cyberknife single-fraction APBI using real-time tracking and the interstitial markers, it was 2.3 mm. These results were generalized to fractionated treatment schedules, using the calculated systematic and random errors of 0.46 mm for surgical clip motion and 0.60 mm for interstitial marker motion. A 3.8 mm margin is required for a 5-fraction schedule of VMAT APBI and a 2.1 mm margin for 5 fractions of Cyberknife APBI, which are slightly smaller values than for the single fraction treatments. The main reason for the smaller margin of

Cyberknife APBI compared to VMAT APBI is the use of real-time tracking for compensation of drift and breathing. Using real-time tracking on a conventional linear accelerator, for example using MLC tracking, would result in similar margins for the two treatment machines. The Cyberknife has a better machine accuracy, but the tracking based on interstitial markers has a slightly lower accuracy than tracking on the surgical clips, as is usually done on a conventional linear accelerator. The accuracy of the new real-time tracking technique on a conventional linear accelerator would need to be defined to exactly calculate the required PTV margin, but the difference compared to Cyberknife APBI will probably be small.

The choice for a PTV margin is a trade-off between the risk of geographical miss and the dose to surrounding healthy tissues. Using our results, PTV margins can be calculated varying the risk of geographical miss, defined as a CTV coverage of less than 100%. Since the current APBI techniques are highly conformal, the dose to healthy tissue is greatly reduced compared to whole breast irradiation. A small increase in PTV margin is unlikely to lead to a measurable increase in toxicity, but could lead to a lower local recurrence risk. On the other hand, it is important to keep in mind that a local recurrence after breast conserving surgery (BCS) has a good prognosis as effective salvage treatments exist [20]. Conversely, the prognosis of a radiation-induced lung cancer is poor. According to this reasoning, it would be logical to reduce the PTV margin and accept a higher risk of local recurrence. The challenge in this discussion is the absence of clinical data. The rate of local recurrences for early-stage breast cancer is so low and the occurrence of secondary lung cancer is so delayed that a clinical trial aiming at quantifying the effects of PTV margin sizes would need a very large number of patients followed for a very long follow-up time, which is practically infeasible. Our results are based on modeling and enable visualizing the trade-off between PTV margin and local recurrence, which could aid in the choice of PTV margin.

Our analyses of the interfraction and intrafraction motion could be performed because the treatment protocol included the acquisition of diagnostic-quality in-room CT scans and real-time tracking with a Cyberknife. This means that for these patients, the intrafraction motion was accounted for and the calculated margin for intrafraction motion was not relevant. However, most institutions use APBI treatment techniques without real-time tracking. We believe that it is important to generalize our data and to enable all institutions to accurately compensate for motion uncertainties in APBI. Based on the data presented in **chapter 5**, the required PTV margin can be calculated for all external-beam APBI techniques.

Delineation of the tumor bed

The target definition for APBI is done delineating the tumor bed on the planning CT scan images. It is known that this process has high interobserver variability, especially after full thickness closure [21]. This uncertainty can lead to a high risk of geographical miss and hence risk of local recurrence. Using a larger PTV margin would compensate for this uncertainty, but it also leads to a higher dose to healthy tissue. Another drawback of increasing the PTV is that it could make some patients ineligible for APBI, as there are maximum PTV volume constraints in most APBI protocols [22-25].

In **chapter 6**, an intervention to decrease the interobserver variability of tumor bed delineation is reported. An iodined hydrogel was injected into the lumpectomy cavity just before full thickness closure. Six experienced radiation oncologists delineated the tumor bed on the planning CTs of 21 patients with hydrogel and 21 historical matched controls without hydrogel. Contours were compared using the conformity index (Cx), which is the ratio between the volume of agreement divided by the total volume contoured by observers. We showed an increased Cx in the intervention group of 0.70 compared to the control group (Cx = 0.54, $p < 0.001$). Also, the cavity visualization score (CVS) was higher in the intervention group. The CVS is a score ranging from 1 to 5 with 5 representing the best visibility of the surgical cavity. The median CVS was 3.5 in the intervention group and 2.5 in the control group ($p < 0.001$). The injection of the hydrogel was feasible in all patients and easy to perform. There was no increase in postoperative infections.
The use of the hydrogel lead to a larger delineated volume, 26.2 cc in the intervention group versus 10.2 cc in the control group. This could only partially explain the increase in Cx, as the multivariate analysis showed an independent significant association of both volume and intervention with Cx. The difference in Cx between the intervention and control groups was largest when comparing the group of control patients with a CVS ≤ 3 and their matched controls. For control patients with a CVS ≥ 4, the Cx was high at 0.68. This indicates that the use of hydrogel is most efficient for patients with a low CVS. Selecting only patients with a low CVS is not possible at time of surgery. The planning CT could serve as a selection tool for the use of the hydrogel. In that situation, only patients with a CVS ≤ 3 would be referred for an injection of the hydrogel under ultrasound guidance by an experienced operator, to ensure the accurate localization of the injection within the lumpectomy cavity.

The holy grail of target definition would be to exactly localize the tumor bed during patient setup, just before treatment delivery. In a previous study it was shown that while MR imaging has superior soft tissue contrast compared to CT, the Cx of tumor bed delineation was not improved by the use of MR [21]. An intervention to make the tumor bed visible is still required. The ideal intervention would make the tumor bed clearly

visible on both the planning and pretreatment imaging, without generating artefacts. Currently, surgical clips are used to guide both delineation and patient setup. As shown in **chapter 5**, these clips can move relative to the tumor bed. Also, these clips can generate artefacts in the planning CT. The severity of the artefacts depends on the type of material (the denser, the more profound are the artefacts) and on the size of the clips (the larger, the more profound are the artefacts). Conversely, less dense and small clips are not visualized on 2D kV imaging, such as used for Cyberknife APBI. An ideal marker would completely fill the lumpectomy cavity, such that it's center of mass cannot move relative to the tumor bed. It should have a density and volume such that there is enough contrast in the 2D images without generating artefacts in the planning CT. A hydrogel containing dense particles such as iodine or gold microparticles might serve this purpose, depending on the concentration of the particles.

The future of accelerated partial breast irradiation

Since the start of the research reported in this thesis, some important studies have been published that shed a new light on the future of APBI.

The FAST and FAST-Forward trials are in fact not investigating APBI, but they are very important for the future of all breast radiotherapy regimens [26, 27]. In the FAST trial, 915 women with early-stage breast cancer were randomly assigned to whole breast irradiation (WBI) to a dose of 50 Gy in 25 fractions or 30 Gy or 28.5 Gy in 5 fractions [26]. At 10 years, the normal tissue side effects were not significantly different between the 50 Gy in 25 fractions and the 28.5 Gy in 5 fractions schedules. The 30 Gy in 5 fractions schedule resulted in worse normal tissue side effects. This trial was not powered to compare tumor control, but the rates of ipsilateral breast cancer events appeared similar.

The FAST-Forward trial on whole breast irradiation randomized more than 4000 women over three treatment arms; 40 Gy in 15 fractions over 3 weeks, 26 Gy in 5 fractions over 1 week or 27 Gy in 5 fractions over 1 week [27]. The 26 Gy in 1 week regimen was non-inferior to the three-week schedule regarding local tumor control and normal tissue side effects at 5 years. The 27 Gy in 5 fractions schedule had a higher risk of normal tissue side effects. The results of this trial were published in April 2020, at the beginning of the COVID-19 pandemic. The pandemic stimulated a fast adoption of the 26 Gy in 5 fractions schedule in order to reduce the number of hospital visits for breast cancer patients [28]. Institutions started to use this schedule for both WBI and APBI, even though there was no data on the safety and efficacy of this schedule for APBI [28].

The FAST and FAST-Forward trials provided new insights in the radiobiology of normal tissue sensitivity in breast radiotherapy [26, 27]. The findings support the ongoing reduction in the number of fractions for both WBI and APBI. APBI trials are starting to investigate single-fraction regimens [29-33]. The use of only one fraction would be more convenient for the patients and the institutions. It could also increase the use of breast conserving surgery, as patients sometimes opt for mastectomy because of the burden of protracted radiotherapy treatments. The challenge of single-fraction techniques is to ensure accuracy and precision of treatment delivery to prevent an increase in local recurrence risk.

Regarding health economics and logistics, the optimal technique for the delivery of APBI should be low-cost and widely available for large numbers of patients, because of the high incidence of early-stage breast cancer. Good early results on the local control and toxicity of proton APBI have been published [34]. However, the availability of protons is limited and the costs are substantially higher compared to photon treatments. It remains to be seen whether the higher costs translate into substantial long-term benefit. Brachytherapy has been extensively used for the delivery of APBI. The results are excellent, both for interstitial brachytherapy and permanent breast seed implants [35-38]. Yet, these techniques require specific skills and equipment, next to a large time commitment of the radiation oncologist. The number of patients that can be treated with brachytherapy might not be sufficient to treat all eligible cases. On the other hand, external-beam techniques are widely available and will probably be the mainstream APBI technique used in the majority of patients.

When deciding to use external-beam for APBI delivery, the next step is to define the optimal treatment planning technique. As shown in **chapter 3**, the use of a non-coplanar beam setup for external-beam APBI can reduce the dose to the lungs and heart, and thus the risk of radiation-induced mortality. Non-coplanar VMAT APBI would combine the advantages of the non-coplanar beam setup with the fast irradiation times of VMAT. The use of hyperarcs with simultaneous motion of the couch and gantry might lead to even lower doses to healthy tissues without increasing treatment time. Hyperarcs are available for cranial treatments but not yet for APBI [39, 40]. The Cyberknife is designed to use multiple non-coplanar beams for treatment delivery. The step-and-shoot delivery has the drawback of relatively long treatment times. If the Cyberknife could use arc delivery, treatment times would be greatly reduced. The advantage of the Cyberknife is that it can real-time track and trail the target during irradiation, mitigating patient drift. As shown in **chapter 4 and 5**, this technique requires smaller PTV margins than techniques without real-time motion tracking. From a technical point of view, Cyberknife with arc delivery and real-time tracking would be the optimal external-beam APBI technique. However, few radiotherapy institutions have access to a Cyberknife. The other way around would be to

include real-time tracking and trailing into non-coplanar VMAT. There are currently no linear accelerators capable of combining these technologies.

Finally, the option to use no radiotherapy at all needs to be considered. It has been shown that in older low-risk patients (over age 65 or 70 years) using adjuvant endocrine therapy, adjuvant radiotherapy can be omitted, as this omission resulted in a very small increase in local recurrence risk [41, 42]. It is important to note that the adherence rate to the endocrine therapy is less strict outside clinical trials [43]. The actual local recurrence rates after the omission of adjuvant radiotherapy might be higher than reported in clinical trials. Also, in some countries, such as the Netherlands, the national protocol does not advise endocrine therapy for this group of low-risk breast cancer patients [44]. There is limited evidence on the comparison of endocrine therapy alone versus radiotherapy alone. A population-based registry study reported 5-year local recurrence rates of 1.5% for whole breast radiotherapy alone and 4.2% for endocrine therapy alone, compared to 0.8% for combined treatment and 12% for no adjuvant treatment [45]. Endocrine therapy is associated with substantial short-term and long-term toxicity. Radiotherapy alone can be a very suitable option for these elderly low-risk patients, especially if APBI is used.

Conclusion

The excellent prognosis of early-stage breast cancer patients poses new challenges to the radiotherapy community. There is an urgent need to focus on reducing long-term toxicities and mortalities, even though these risks are difficult to quantify. Some changes are simple to implement, such as prioritizing lung sparing during treatment planning, and can have an impact on the overall survival of this group of patients.

References

[1] Wilmink J.W. dV-GJ, Busch O.R.,. Nieuwe richtlijn pancreascarcinoom. Nederlands Tijdschrift voor Oncologie. 2019;16:317-8.

[2] Surveillance, Epidemiology, and End Results (SEER) Program (www.seer.cancer.gov) SEER*Stat Database: Incidence - SEER 18 Regs Research Data + Hurricane Katrina Impacted Louisiana Cases, Nov 2015 Sub (1973-2013 varying) - Linked To County Attributes - Total U.S., 1969-2014 Counties, National Cancer Institute, DCCPS, Surveillance Research Program, released April 2016, based on the November 2015 submission.

[3] Integraal Kankercentrum Nederland. Cijfers over kanker. 2020; http://www.cijfersoverkanker.nl/.

[4] Taylor C, Correa C, Duane FK, et al. Estimating the Risks of Breast Cancer Radiotherapy: Evidence From Modern Radiation Doses to the Lungs and Heart and From Previous Randomized Trials. J Clin Oncol. 2017;35:1641-9.

[5] Grantzau T, Overgaard J. Risk of second non-breast cancer among patients treated with and without postoperative radiotherapy for primary breast cancer: A systematic review and meta-analysis of population-based studies including 522,739 patients. Radiother Oncol. 2016;121:402-13.

[6] Grantzau T, Overgaard J. Risk of second non-breast cancer after radiotherapy for breast cancer: A systematic review and meta-analysis of 762,468 patients. Radiotherapy and Oncology. 2015;114:56-65.

[7] Mellemkjaer L, Friis S, Olsen JH, et al. Risk of second cancer among women with breast cancer. Int J Cancer. 2006;118:2285-92.

[8] Darby SC, Ewertz M, McGale P, et al. Risk of ischemic heart disease in women after radiotherapy for breast cancer. N Engl J Med. 2013;368:987-98.

[9] Mukesh MB, Harris E, Collette S, et al. Normal tissue complication probability (NTCP) parameters for breast fibrosis: pooled results from two randomised trials. Radiother Oncol. 2013;108:293-8.

[10] Avanzo M, Stancanello J, Trovò M, et al. Complication probability model for subcutaneous fibrosis based on published data of partial and whole breast irradiation. Physica Medica. 2012;28:296-306.

[11] Fisher ER, Anderson S, Redmond C, Fisher B. Ipsilateral breast tumor recurrence and survival following lumpectomy and irradiation: pathological findings from NSABP protocol B-06. Semin Surg Oncol. 1992;8:161-6.

[12] Vicini FA, Kestin LL, Goldstein NS. Defining the clinical target volume for patients with early-stage breast cancer treated with lumpectomy and accelerated partial breast irradiation: a pathologic analysis. Int J Radiat Oncol Biol Phys. 2004;60:722-30.

[13] Vicini FA, Cecchini RS, White JR, et al. Long-term primary results of accelerated partial breast irradiation after breast-conserving surgery for early-stage breast cancer: a randomised, phase 3, equivalence trial. Lancet. 2019;394:2155-64.

[14] Whelan TJ, Julian JA, Berrang TS, et al. External beam accelerated partial breast irradiation versus whole breast irradiation after breast conserving surgery in women with ductal carcinoma in situ and node-negative breast cancer (RAPID): a randomised controlled trial. Lancet. 2019;394:2165-72.

[15] Rodriguez N, Sanz X, Dengra J, et al. Five-year outcomes, cosmesis, and toxicity with 3-dimensional conformal external beam radiation therapy to deliver accelerated partial breast irradiation. Int J Radiat Oncol Biol Phys. 2013;87:1051-7.

[16] Livi L, Meattini I, Marrazzo L, et al. Accelerated partial breast irradiation using intensity-modulated radiotherapy versus whole breast irradiation: 5-year survival analysis of a phase 3 randomised controlled trial. Eur J Cancer. 2015;51:451-63.

[17] International Commission on Radiation Units and Measurements. ICRU Report 50: Prescribing, Recording, and Reporting Photon Beam Therapy. 1993.

[18] International Commission on Radiation Units and Measurements. ICRU REPORT 62 Prescribing, Recording and Reporting Photon Beam Therapy (Supplement to ICRU Report 50) 1999.

[19] van Herk M. Errors and margins in radiotherapy. Semin Radiat Oncol. 2004;14:52-64.

[20] Federatie Medisch Specialisten. Borstkanker, Behandeling van locoregionaal recidief. 2020; https://richtlijnendatabase.nl/richtlijn/borstkanker/locoregionaal_recidief/behandeling.html.

[21] den Hartogh MD, van den Bongard HJ, Davidson MT, et al. Full-thickness closure in breast-conserving surgery: the impact on radiotherapy target definition for boost and partial breast irradiation. A multimodality image evaluation. Ann Surg Oncol. 2014;21:3774-9.

[22] Correa C, Harris EE, Leonardi MC, et al. Accelerated Partial Breast Irradiation: Executive summary for the update of an ASTRO Evidence-Based Consensus Statement. Pract Radiat Oncol. 2017;7:73-9.
[23] American Society of Breast Surgeons. Consensus Statement for Accelerated Partial Breast Irradiation. 2011; https://www.breastsurgeons.org/new_layout/about/statements/PDF_Statements/APBI.pdf.
[24] Smith BD, Arthur DW, Buchholz TA, et al. Accelerated partial breast irradiation consensus statement from the American Society for Radiation Oncology (ASTRO). Int J Radiat Oncol Biol Phys. 2009;74:987-1001.
[25] Polgar C, Van Limbergen E, Potter R, et al. Patient selection for accelerated partial-breast irradiation (APBI) after breast-conserving surgery: recommendations of the Groupe Europeen de Curietherapie-European Society for Therapeutic Radiology and Oncology (GEC-ESTRO) breast cancer working group based on clinical evidence (2009). Radiother Oncol. 2010;94:264-73.
[26] Brunt AM, Haviland JS, Sydenham M, et al. Ten-Year Results of FAST: A Randomized Controlled Trial of 5-Fraction Whole-Breast Radiotherapy for Early Breast Cancer. J Clin Oncol. 2020;38:3261-72.
[27] Brunt AM, Haviland JS, Wheatley DA, et al. Hypofractionated breast radiotherapy for 1 week versus 3 weeks (FAST-Forward): 5-year efficacy and late normal tissue effects results from a multicentre, non-inferiority, randomised, phase 3 trial. Lancet. 2020;395:1613-26.
[28] Coles CE, Aristei C, Bliss J, et al. International Guidelines on Radiation Therapy for Breast Cancer During the COVID-19 Pandemic. Clin Oncol (R Coll Radiol). 2020;32:279-81.
[29] Mouawad M, Biernaski H, Brackstone M, et al. DCE-MRI assessment of response to neoadjuvant SABR in early stage breast cancer: Comparisons of single versus three fraction schemes and two different imaging time delays post-SABR. Clinical and Translational Radiation Oncology. 2020;21:25-31.
[30] Horton JK, Blitzblau RC, Yoo S, et al. Preoperative Single-Fraction Partial Breast Radiation Therapy: A Novel Phase 1, Dose-Escalation Protocol With Radiation Response Biomarkers. Int J Radiat Oncol Biol Phys. 2015;92: 846-55.
[31] Charaghvandi KR, Van't Westeinde T, Yoo S, et al. Single dose partial breast irradiation using an MRI linear accelerator in the supine and prone treatment position. Clin Transl Radiat Oncol. 2019;14:1-7.
[32] Kennedy WR, Thomas MA, Stanley JA, et al. Single-Institution Phase 1/2 Prospective Clinical Trial of Single-Fraction, High-Gradient Adjuvant Partial-Breast Irradiation for Hormone Sensitive Stage 0-I Breast Cancer. International Journal of Radiation Oncology, Biology, Physics. 2020;107:344-52.
[33] Guidolin K, Yaremko B, Lynn K, et al. Stereotactic image-guided neoadjuvant ablative single-dose radiation, then lumpectomy, for early breast cancer: the SIGNAL prospective single-arm trial of single-dose radiation therapy. Curr Oncol. 2019;26:e334-e40.
[34] Pasalic D, Strom EA, Allen PK, et al. Proton Accelerated Partial Breast Irradiation: Clinical Outcomes at a Planned Interim Analysis of a Prospective Phase 2 Trial. International Journal of Radiation Oncology*Biology*Physics. 2021;109:441-8.
[35] Crook J, Hilts M, Batchelar D, et al. Permanent breast seed implant for partial breast radiotherapy after partial mastectomy for favorable breast cancer: Technique, results, and applications to various seroma presentations. Brachytherapy. 2019;18:510-20.
[36] Pignol JP, Caudrelier JM, Crook J, McCann C, Truong P, Verkooijen HA. Report on the Clinical Outcomes of Permanent Breast Seed Implant for Early-Stage Breast Cancers. Int J Radiat Oncol Biol Phys. 2015;93:614-21.
[37] Polgar C, Fodor J, Major T, Sulyok Z, Kasler M. Breast-conserving therapy with partial or whole breast irradiation: ten-year results of the Budapest randomized trial. Radiother Oncol. 2013;108:197-202.
[38] Polgár C, Ott OJ, Hildebrandt G, et al. Late side-effects and cosmetic results of accelerated partial breast irradiation with interstitial brachytherapy versus whole-breast irradiation after breast-conserving surgery for low-risk invasive and in-situ carcinoma of the female breast: 5-year results of a randomised, controlled, phase 3 trial. The Lancet Oncology. 2017;18:259-68.
[39] Liang J, Atwood T, von Eyben R, et al. Trajectory Modulated Arc Therapy: A Fully Dynamic Delivery With Synchronized Couch and Gantry Motion Significantly Improves Dosimetric Indices Correlated With Poor Cosmesis in Accelerated Partial Breast Irradiation. International Journal of Radiation Oncology*Biology*Physics. 2015;92:1148-56.
[40] MacDonald RL, Robar JL, Thomas CG. Overlap-guided fixed-patient support positioning optimization for cranial SRT. Med Phys. 2017;44:17-27.

[41] Hughes KS, Schnaper LA, Bellon JR, et al. Lumpectomy Plus Tamoxifen With or Without Irradiation in Women Age 70 Years or Older With Early Breast Cancer: Long-Term Follow-Up of CALGB 9343. Journal of Clinical Oncology. 2013;31:2382-7.
[42] Kunkler IH, Williams LJ, Jack WJL, Cameron DA, Dixon JM. Breast-conserving surgery with or without irradiation in women aged 65 years or older with early breast cancer (PRIME II): a randomised controlled trial. The Lancet Oncology. 2015;16:266-73.
[43] Chu QD, Zhou M, Peddi P, Medeiros KL, Wu XC. Outcomes in real-world practice are different than cooperative trial for elderly patients with early breast cancer treated with adjuvant radiation therapy. Surgery. 2018;163:1213-9.
[44] Federatie Medisch Specialisten. Borstkanker - Endocriene therapie. 2020; https://richtlijnendatabase.nl/richtlijn/borstkanker/adjuvante_systemische_therapie/endocriene_therapie.html.
[45] Dahn H, Wilke D, Walsh G, Pignol JP. Radiation and/or endocrine therapy? Recurrence and survival outcomes in women over 70 with early breast cancer after breast-conserving surgery. Breast Cancer Res Treat. 2020;182:411-20.

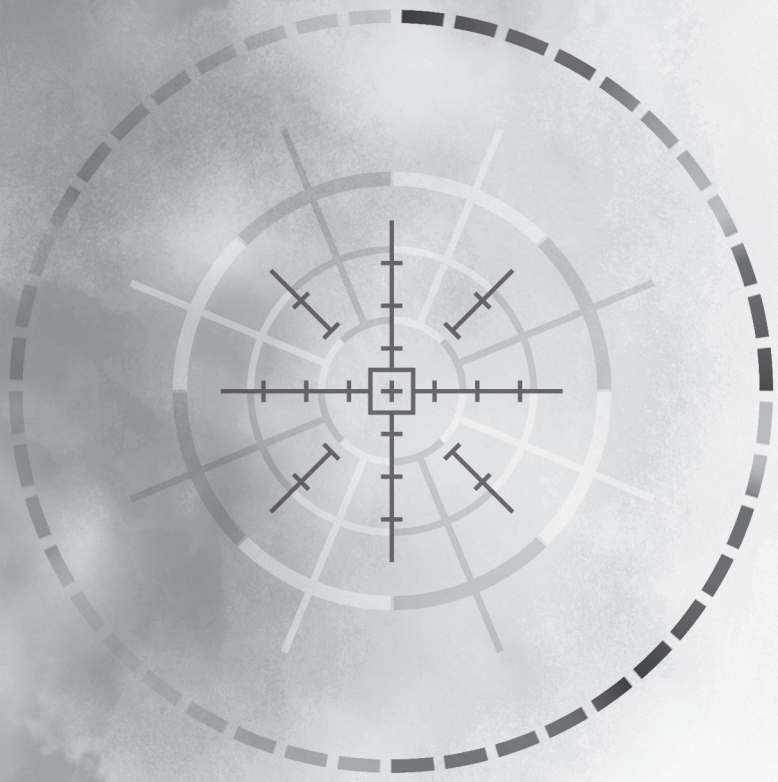

8

Summary

Breast cancer is the most common female malignancy worldwide and mainly affects woman over the age of 50 years. After the implementation of public screening programs in developed countries in the 1980s and 1990s, most breast cancers are diagnosed at an early stage. The prognosis of early-stage breast cancer is excellent, with a cancer specific survival of 99% at 5 years after diagnosis. Thus, the focus of improving breast cancer care has shifted from increasing survival to decreasing treatment-related side effects.

The two most important long-term toxicities of radiotherapy after breast conserving surgery are cardiovascular toxicity and the induction of secondary cancers. Both can lead to treatment-induced mortality. The aim of this thesis was to assess the magnitude of the secondary cancer risks of adjuvant breast radiotherapy and to investigate methods to reduce this risk.

Our first step was the assessment of the secondary cancer risks of various organs for several whole and partial breast irradiation techniques, based on dose measurements in an anthropomorphic phantom. **Chapter 2** details the experiment and the calculation of the secondary cancer risks based on the measured doses. We found that whole breast irradiation leads to the highest overall secondary cancer risk and that the use of partial breast irradiation (PBI) can reduce this risk to about a half. Brachytherapy PBI resulted in the lowest risks and VMAT PBI in the highest risks of the PBI techniques. Another striking result was that the large majority of all the secondary cancers were lung cancers, regardless of the technique used. For example, whole breast irradiation resulted in a 3.8% lifetime risk of secondary lung cancer, which was 89% of the total secondary cancer risk. As lung cancer has a mortality of about 80%, the secondary lung cancer risk translates into an excess 3% life-time mortality. This toxicity occurs at a long time interval after treatment. It starts after 5 years and continues for the remainder of life of the treated patients. The peak incidence rate in our analysis was found around 25 years after treatment. This latency is much longer than the latency of radiation-induced cardiovascular disease, which might explain why the prevention of secondary lung cancer after radiotherapy has received less attention than cardiovascular disease prevention.

The next step was to explore the possibility of reducing dose to the lungs during treatment planning, as well as the price to pay for this reduction. This is discussed in **chapter 3**. For 20 breast cancer patients, we created treatment plans using Erasmus-iCycle. Erasmus-iCycle is software creating consistent high-quality treatment plans through fully automated multicriteria prioritized optimization. The technique is hence objective and free of human biases. We generated plans that prioritized sparing of lung tissue versus sparing of healthy non-target breast tissue. The resulting dose distributions were converted into the risks of secondary lung cancer induction and the risks of breast fibrosis per treatment plan. We found on average a five-fold reduction in the risk of secondary lung cancer achieved by

prioritizing lung sparing. The price to pay is a small increase in the long-term breast fibrosis risk of about 0.5 %point. The use of non-coplanar beams lowered both the secondary cancer risks and breast fibrosis risks compared to a coplanar beam set-up. Prioritizing lung sparing also resulted in a lower mean heart dose, and thus may lead to a lower risk of cardiovascular toxicity. Based on these results, we recommended to prioritize lung sparing during treatment planning and the use of a non-coplanar beam set-up. This could improve the long-term overall survival of early-stage breast cancer patients.

The second part of this thesis focusses on the geometric accuracy of accelerated partial breast irradiation (APBI). The volume to be treated with radiation is called the clinical target volume (CTV). A safety margin is applied to this volume to compensate for geometric uncertainties that are present during the preparation and delivery of a radiation treatment. The expansion of the CTV with this margin results in the planning target volume (PTV). The selection of a PTV margin is a trade-off. The expansion needs to be sufficiently large to prevent geographical miss for most treated patients. On the other hand, a larger margin leads to a larger volume to be treated and to higher doses to surrounding healthy tissues. The margin should be as small as possible to decrease the toxicity risks of these healthy tissues. The first step towards an optimal PTV margin is the assessment of the magnitude of all geometric uncertainties of a specific radiation treatment technique. Next, the required PTV margin can be calculated using established methods. Also, an assessment of all errors shows which factors can be optimized to reduce the required PTV margin.

In **chapter 4**, our results on the motion of the tumor bed occurring during APBI delivery are shown. Based on the intrafraction motion during 110 fractions of 22 patients, we concluded that the PTV margin required to compensate for breathing is only 0.3 – 0.6 mm. A different type of intrafraction motion is drift, a gradual change in patient position due to for example sliding down or relaxing. The magnitude of patient drift increased with increasing fraction duration. A margin of 1.0 mm is sufficient for a total fraction duration up to 8 minutes after the first imaging for patient set-up. For a fraction of 32 minutes, 2.5 mm is needed. Techniques that account for breathing motion but not for drift, e.g. breath-hold or gating, can reduce these margins by 0.1 mm. There was a systematic trend in the drift in the dorsal, caudal and medial direction. This trend is not taken into account in the standard PTV margin calculation methods. To compensate for these trends, an asymmetric margin could be used with an additional 0.7 mm expansion in these directions. The most important factors to minimize the intrafraction motion margin are reducing treatment duration and drift.

In addition to the motion occurring during the fraction, the motion between subsequent fractions is another geometric uncertainty that should be included in the PTV margin calculation. This interfraction motion is discussed in **chapter 5**. As the tumor bed is often

not visible on the pre-treatment imaging used for patient positioning, fiducials are used instead. For a cohort of 70 patients, we calculated the motion of the fiducials relative to the tumor bed that occurred between planning CT and the first fraction. A margin of 1.7 mm was required to ensure 100% CTV coverage in 90% of patients when using surgical clips for patient set-up, while 2.3 mm resulted in 100% CTV coverage in 95% of patients. The range of motion among patients was large, 0.1 – 2.9 mm for the center of mass of the surgical clips. These findings strongly support the use of individualized PTV margins. Our analysis showed no clear predictive factors for personalized margins based on clinical parameters known at the time of treatment planning. Individualized PTV margins could be implemented using a library of plans with different PTV margins. At the time of treatment, fiducial motion could be assessed and the plan with the optimal margin would be selected for delivery.

The different geometric uncertainties need to be combined into one comprehensive PTV margin for the use in clinical practice. As the different contributions are not correlated, this is done quadratically summing up all the systematic and random errors and use these values in calculations such as the van Herk formula. In the discussion section of **chapter 5**, examples are shown of realistic values of the systematic and random errors for external beam APBI. Based on these values, a comprehensive PTV margin for VMAT APBI on a conventional linac would be 4.0 mm for a 5-fraction schedule. Using a Cyberknife with fiducial tracking, this margin would be 2.2 mm.

Finally, the definition of the tumor bed on a CT scan is challenging, especially after lumpectomy with full thickness closure. In such cases, the interobserver variability in the delineation of the tumor bed is high. This could lead to geographical misses during APBI and eventually a higher risk of local recurrence. In **chapter 6**, a study on the use of a radiopaque hydrogel for improved target definition is presented. In 21 breast cancer patients, 3 – 9 ml of iodined hydrogel were inserted into the lumpectomy cavity just before full thickness closure. Another 21 breast cancer patients were included as matched controls. The tumor bed was delineated on the planning CT scan by six experienced radiation oncologists. After the hydrogel injection, the median conformity index (Cx) between the delineations of the different radiation oncologists was higher (intervention group Cx 0.70, control group Cx 0.54, $p< 0.001$). Also, the cavity visualization score was higher in the intervention group than in the control group (median 3.5 versus 2.5 respectively, $p < 0.001$)). The feasibility of the procedure was 100% and the rate of surgical site infections was not different from literature. The use of a radiopaque hydrogel is a feasible and practical option to improve the target definition for APBI.

In **chapter 7**, the results and conclusions of this thesis are discussed in a broader context. The main conclusion is that secondary lung cancer induction partially offsets the survival

benefit of adjuvant breast radiotherapy. Prioritizing lung sparing during planning reduces this risk and is easy to implement at no additional costs. The use of a non-coplanar beam set-up and intrafraction motion tracking could reduce the secondary cancer risk even more.

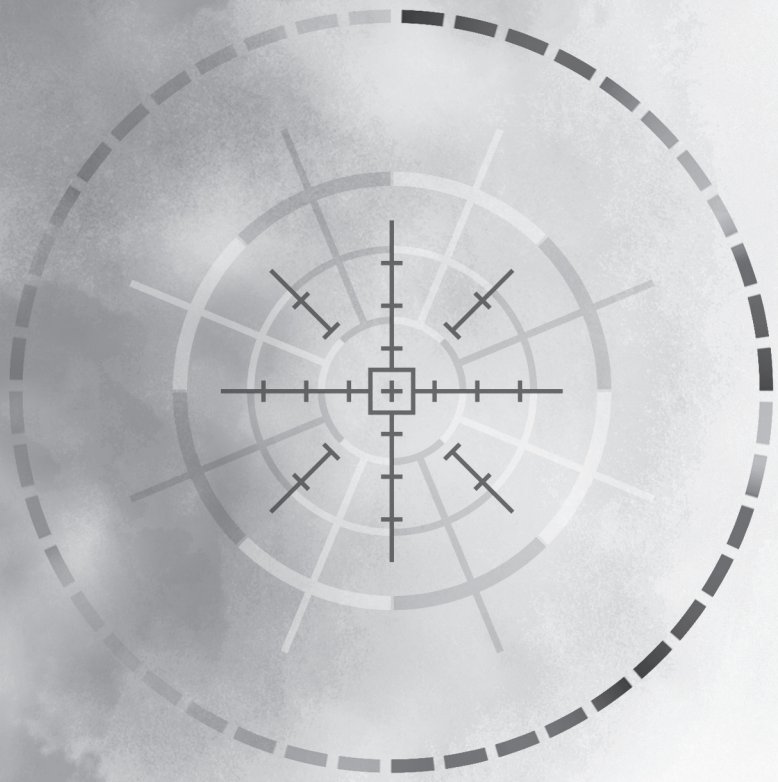

9

Nederlandse samenvatting

Borstkanker is het type kanker dat het meest voorkomt wereldwijd. Het komt met name voor bij vrouwen boven de 50 jaar. Sinds de invoering van programma's voor preventief bevolkingsonderzoek in de jaren tachtig en negentig van de vorige eeuw worden de meeste patiënten gediagnosticeerd in een vroeg stadium. De prognose van vroeg-stadium borstkanker is uitstekend, met een kankerspecifieke overleving van 99% na 5 jaar. De focus in het verbeteren van de behandeling van borstkanker is daarom verschoven van het verbeteren van de overleving naar het verminderen van de bijwerkingen van de behandeling.

De twee belangrijkste bijwerkingen op lange termijn van radiotherapie na borstsparende chirurgie zijn cardiovasculaire ziekten en de inductie van secundaire tumoren. Beiden kunnen ze leiden tot behandelingsgerelateerde mortaliteit. Het doel van dit proefschrift was het kwantificeren van de risico's op secundaire tumoren na adjuvante borstbestraling en het onderzoeken van manieren om dit risico te verminderen.

Onze eerste stap was het kwantificeren van het risico op secundaire tumoren in verschillende organen. We vergeleken meerdere technieken voor gehele of partiële borstbestraling door het meten van bestralingsdosis in een fantoom lijkend op een mens. **Hoofdstuk 2** beschrijft dit experiment en van de berekening van de secundaire tumor risico's op basis van de metingen. Uit onze resultaten bleek dat gehele borstbestraling leidt tot het hoogste totale risico op secundaire tumoren en dat partiële borstbestraling (PBI) het risico ongeveer kan halveren. Brachytherapie PBI leidde tot de laagste risico's en VMAT PBI tot de hoogste van de PBI technieken. Een andere opvallende bevinding was dat het overgrote deel van alle secundaire tumoren longtumoren betrof. Voor bijvoorbeeld de gehele borstbestraling was het totale levenslange risico op secundaire tumoren 3.8%, dat was 89% van alle secundaire tumoren. Ongeveer 80% van de longkanker patiënten overlijdt aan de ziekte, waardoor het risico op secundaire longtumoren van gehele borstbestraling zich vertaalt in een risico van 3% om te overlijden aan een bestralingsgeïnduceerde longtumor in de rest van het leven van bestraalde borstkanker patiënten. Secundaire tumoren ontstaan na een lang interval na de bestraling. De eerste secundaire tumoren ontstaan na 5 jaar en dit risico blijft bestaan voor de rest van het leven van de patiënt. In onze analyse lag de piek in incidentie van secundaire tumoren rond de 25 jaar na behandeling. Dit zou kunnen verklaren waarom er in de laatste jaren meer aandacht is geweest voor de preventie van cardiovasculaire bijwerking dan voor het voorkomen van secundaire tumoren.

De volgende stap was het onderzoeken van manieren om de bestralingsdosis van de longen te verlagen. Belangrijk daarbij was de prijs voor deze verlaging. Dit onderzoek wordt besproken in **hoofdstuk 3**. Voor 20 borstkanker patiënten werden er behandelplannen gemaakt met Erasmus iCycle. Erasmus iCycle is software die via volledig geautomatiseerde optimalisatie behandelplannen kan maken van een consistent hoge kwaliteit.

We hebben plannen gegenereerd die volledige voorrang gaven aan het sparen van de longen of juist het sparen van het gezonde borstweefsel buiten het doelgebied. Op basis van de resulterende dosisverdelingen werden de risico's op secundaire longtumoren en borstfibrose per behandelplan berekend. Er was gemiddeld een vijfvoudige reductie in het risico op secundaire longtumoren voor het plan dat de longen spaarde vergeleken met het plan dat de borst spaarde. De prijs hiervoor was een verhoging van het risico op borstfibrose van 0.5 procentpunt. Het gebruik van een niet-coplanaire bundelopzet resulteerde in lagere risico's op zowel secundaire longtumoren als borstfibrose. Opvallend was dat het prioriteren van longsparing ook tot een lagere hartdosis leidde voor zowel linkszijdige als rechtszijdige behandelingen, en dus tot een lager risico op cardiovasculaire ziekten. Op basis van deze resultaten raadden wij aan om tijdens het maken van het behandelplan prioriteit te geven aan het sparen van de longen en om een niet-coplanaire bundelopzet te gebruiken. Dit kan mogelijk de overleving op de lange termijn van patiënten met vroeg-stadium borstkanker verhogen.

Het tweede deel van dit proefschrift gaat over de geometrische nauwkeurigheid van geaccelereerde partiële borstbestraling (APBI). Het volume dat behandeld moet worden met bestraling wordt het 'clinical target volume' (CTV) genoemd. Rond dit volume wordt een marge toegepast om te compenseren voor geometrische onnauwkeurigheden tijdens de voorbereiding en uitvoering van de bestraling. De toevoeging van de marge aan het CTV resulteert in het "planning target volume", PTV. De keuze voor een bepaalde PTV marge is een afweging tussen 2 aspecten. Aan de ene kant moet de PTV marge voldoende ruim zijn om de kans op het missen van het doelgebied zo klein mogelijk te houden. Aan de andere kant leidt een grotere PTV marge tot een groter bestraald volume en tot hogere dosissen voor de omliggende gezonde weefsels. De marge moet dus zo klein mogelijk zijn om de kans op bijwerkingen te verlagen. De eerste stap om te komen tot een optimale PTV marge is het bepalen van de grootte van alle geometrische onnauwkeurigheden in het proces van bestralingsvoorbereiding en –uitvoering. Daarna kan de benodigde PTV marge berekend worden aan de hand van erkende methodieken. Een inventarisatie van alle onnauwkeurigheden laat ook zien welke factoren verbeterd kunnen worden om tot een kleinere PTV marge te komen.

In **hoofdstuk 4** worden de resultaten van de analyse van de beweging van het tumor bed tijdens een APBI behandeling besproken. Op basis van de intrafractie beweging tijdens 110 fracties van 22 patiënten concludeerden we dat de PTV marge die nodig is om ademhalingsbeweging te compenseren slechts 0.3 tot 0.6 mm is. Een andere beweging tijdens een fractie is drift, het langzaam veranderen van de houding zoals wegglijden of inzakken. De grootte van de drift nam toe met de duur van de behandeling. 1.0 mm marge was voldoende voor een fractieduur tot 8 minuten na de eerste opnames voor het positioneren van de patiënt. Voor een fractie van 32 minuten of meer was een marge van 2.5 mm

nodig. Technieken die compenseren voor de ademhaling maar niet voor drift, zoals bijvoorbeeld 'breath-hold' en 'gating', kunnen deze marge met 0.1 mm verkleinen. Er was een systematisch trend in de richting van de drift in de dorsale, caudale en mediale richting. Om voor deze trend te compenseren zou een asymmetrische marge gebruikt kunnen worden met een extra expansie van 0.7 mm in deze richtingen. De belangrijkste factoren om de marge voor intrafractie beweging te kunnen verkleinen zijn de duur van de behandeling en de drift.

Naast beweging tijdens een behandelfractie is er ook een verschil in ligging van de patiënt en het doelgebied tussen verschillende fracties. Deze interfractie onnauwkeurigheid dient meegenomen te worden in de PTV marge en wordt besproken in **hoofdstuk 5**. Omdat het tumor bed vaak niet goed zichtbaar is met de afbeeldingstechnieken die gebruikt worden voor het positioneren van de patiënt, wordt er vaak gebruikt gemaakt van fiducials. Dit zijn kleine metalen markeringen in of nabij het te bestralen gebied. Voor een cohort van 70 patiënten hebben we de beweging berekend die optrad tussen de planningsCT en de behandeling voor de fiducials ten opzichte van het tumor bed. Een marge van 1.7 mm is nodig om er voor te zorgen dat bij 90% van de patiënten het CTV voor 100% de voorgeschreven dosis krijgt. Dit geldt als er operatieclips gebruikt worden als fiducials tijdens het positioneren van de patiënt. Met een marge van 2.3 mm stijgt dit tot 95% van de patiënten. De spreiding in de beweging was groot, van 0.1 mm tot 2.9 mm voor het centrum van de operatieclips. Dit pleit voor het gebruik van geïndividualiseerde PTV marges. Onze analysis toonde geen sterke voorspellende factoren aan die ten tijde van de planning bekend zijn. Toch zouden geïndividualiseerde PTV marges ingevoerd kunnen worden door het maken van meerdere plannen met verschillende PTV marges per patiënt. Ten tijde van de behandeling kan de beweging van de fiducials worden gemeten waarop het plan met de juiste PTV marge kan worden geselecteerd voor de behandeling.

De verschillende geometrische onnauwkeurigheden moeten worden gecombineerd tot één gezamenlijke PTV marge voor gebruik in de klinische praktijk. Omdat de verschillende onnauwkeurigheden ongecorreleerd zijn, kunnen de systematische en random fouten kwadratisch opgeteld worden. Hierna kunnen de totale fouten worden gebruikt in een berekening zoals die van van Herk. In de discussie van **hoofdstuk 5** worden voorbeelden getoond van realistische waardes voor de systematische en random fouten tijdens uitwendige APBI. Op basis van deze waardes is de benodigde marge voor VMAT-APBI met een conventionele versneller 4.0 mm voor een behandelschema met 5 fracties. Indien er behandeld wordt op een Cyberknife met fiducial tracking is 2.2 mm marge nodig.

Het laatste aspect dat behandeld wordt in dit proefschrift is de nauwkeurigheid en betrouwbaarheid van de intekening van het tumorbed op de planningsCT scan. Vooral na

het volledig sluiten van het klierweefsel na lumpectomie ("full thickness closure") is de variatie in intekening tussen verschillende personen hoog. Dit kan leiden tot het missen van het werkelijke doelgebied tijdens APBI en tot een verhoogd risico op een lokaal recidief. In **hoofdstuk 6** wordt een studie besproken naar het gebruik van een radiopaque hydrogel om de intekening van het tumorbed te verbeteren. Bij 21 borstkanker patiënten werd 3 tot 9 ml jodium bevattende hydrogel aangebracht in de lumpectomieholte voordat het klierweefsel werd gesloten. 21 andere borstkanker patiënten werden geïncludeerd als vergelijkbare controle patiënten. Het tumor bed werd ingetekend op de planningsCT door 6 ervaren radiotherapeut-oncologen. De mediane conformiteitsindex (Cx) was hoger in de groep met de hydrogel dan in de controle groep (interventie groep Cx 0.70, controle groep Cx 0.54, $p < 0.001$). Ook de score voor de zichtbaarheid van de lumpectomieholte was hoger in de interventiegroep dan in de controle groep (mediaan 3.5 versus 2.5, $p < 0.001$). De haalbaarheid van de interventie was 100% en de kans op wondinfecties was vergelijkbaar met gepubliceerde kansen na lumpectomie. Het gebruik van een radiopaque hydrogel is eenvoudig uit te voeren en kan de nauwkeurigheid van het bepalen van het tumorbed voor adjuvante radiotherapie verbeteren.

In **hoofdstuk 7** worden de resultaten en conclusies van dit proefschrift besproken in een bredere context. De eindconclusie is dat de inductie van secundaire long tumoren de overlevingswinst van adjuvante radiotherapie gedeeltelijk teniet doet. Het prioriteren van het sparen van de longen tijdens het maken van het behandelplan kan het risico op secundaire long tumoren verkleinen en is eenvoudig te implementeren zonder extra kosten. Het gebruik van een niet-coplanaire bundelopzet en het gebruik van methoden die de intrafractie beweging volgen kunnen het risico op secundaire long tumoren verder verlagen.

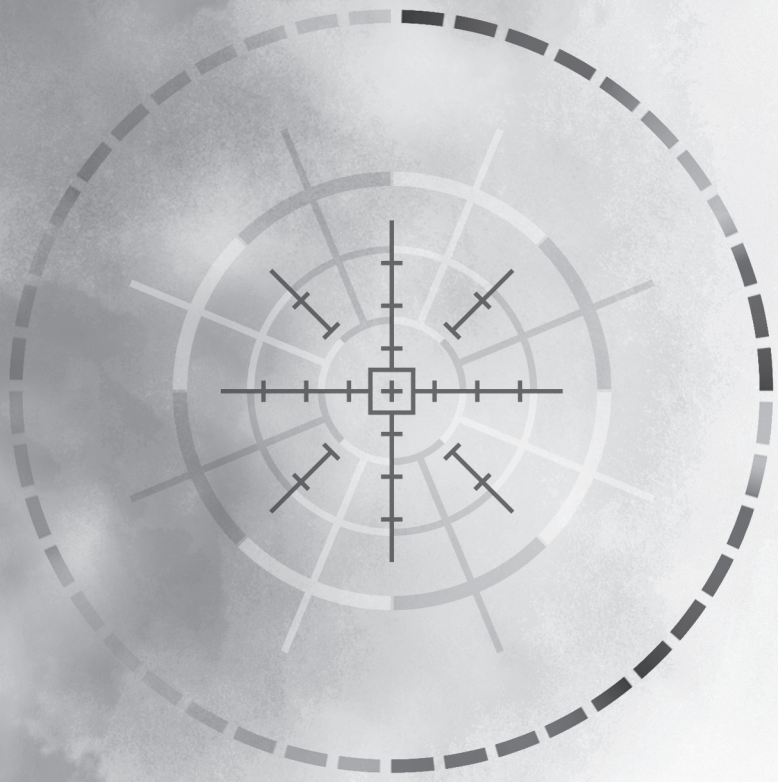

10

Curriculum vitae

Portfolio

List of publications

Dankwoord

Curriculum vitae

Nienke Hoekstra was born on July 17th 1984 in 's-Hertogenbosch, the Netherlands. In 2002, she graduated *cum laude* from the Stedelijk Gymnasium in 's-Hertogenbosch. She started medical school at the Radboud Universiteit Nijmegen and obtained her medical degree in 2008. Next, she worked at the department of surgery of the Slingeland Hospital in Doetinchem and the department of neurology of the Rijnstate Hospital in Arnhem, before finding her passion in radiation oncology. In 2010, she started working as a resident in radiation oncology at the Instituut Verbeeten in Tilburg. Here, she discovered her passion for medical physics. She went to Erasmus MC in Rotterdam in 2011 to start her training as a radiation oncologist. During her residency, she worked on several projects combining medical physics and patient care. This experience lead to the start of a PhD project in 2016 under the supervision of prof. Pignol and prof. Hoogeman. She paused her residency to fully focus on the technical aspects of radiation treatment of early-stage breast cancer. In February 2022, she will finish her residency and defend this thesis. Next, she will start working as a radiation oncologist at the LUMC in Leiden.
Nienke is married to Jasper and together they have three children, Oscar, Marit and Thomas.

Nienke Hoekstra is geboren op 17 juli 1984 in 's-Hertogenbosch. Ze behaalde haar gymnasium diploma *cum laude* aan het Stedelijk Gymnasium te 's-Hertogenbosch in 2002. Vervolgens studeerde ze geneeskunde aan de Radboud Universiteit Nijmegen, waar ze in 2008 haar artsendiploma behaalde. Ze werkte als arts-assistent bij de afdeling chirurgie van het Slingeland ziekenhuis in Doetinchem en bij de afdeling neurologie van het Rijnstate Ziekenhuis in Arnhem, voordat ze haar passie vond bij de radiotherapie. In 2010 begon ze als arts-assistent in het Instituut Verbeeten te Tilburg. Hier ontdekte ze haar voorliefde voor klinische fysica. Ze vertrok naar het Erasmus MC te Rotterdam in 2011 om haar specialisatie tot radiotherapeut-oncoloog te volgen. Gedurende haar opleiding werkte ze aan meerdere projecten die klinische fysica en patiëntenzorg combineerden. Deze ervaringen leidden tot de start van een promotietraject in 2016 onder de supervisie van prof. Pignol en prof. Hoogeman. Ze pauzeerde haar specialisatie om zich volledig te wijden aan de technische aspecten van radiotherapie voor vroeg-stadium borstkanker. In februari 2022 zal zij haar opleiding afronden en dit proefschrift verdedigen. Hierna zal zij gaan werken als radiotherapeut-oncoloog in het LUMC te Leiden.
Nienke is getrouwd met Jasper en samen hebben zij drie kinderen, Oscar, Marit en Thomas.

Erasmus Medical Center Rotterdam

PhD portfolio

Name PhD candidate:	Nienke Hoekstra
Erasmus MC department:	Radiation Oncology
Research School:	Molecular Medicine
PhD period:	2016-2022
Supervisors:	Prof. M.S. Hoogeman, Prof. J.P. Pignol
Co-supervisor:	Dr. S.J.M. Habraken

General courses

EMC - BROK® (Basic course Rules and Organisation for Clinical researchers)	2017
Survival Analysis, Erasmus MC	2017
Basics training OpenClinica, Erasmus MC	2017
CC02A Biostatistical Methods I: Basic Principles Part A	2017
EndNote workshop, Erasmus MC library	2017
Systematic Literature search, Erasmus MC library	2017
Networking basics: what you need to know, Postdoc Network	2017
Photoshop and Illustrator CC, Molmed	2017
Research Integrity, Erasmus MC	2018
Workshop Negatiation, Postdoc Network	2018
Presenting skills for scientists, Molmed	2019
Public Outreach, Postdoc Network	2019
English Biomedical Writing and Communication, Erasmus MC	2020
Data Analysis in Python basic, Molmed	2020
Female Talent class, Erasmus MC	2021

Radiotherapy courses

Physics lectures by prof Pignol	2016
MCNP lectures and hands-on sessions by prof Pignol	2017
European School of Robotic Radiosurgery / Cyberknife school	2017
Cyberknife upgrade course, Accuray Inc. for Erasmus MC	2018
Clinical practice and implementation of image-guided stereotactic body radiotherapy, ESTRO	2018

International conferences

ESTRO 37 Barcelona (poster discussion)	2018
ESTRO 39 online (oral presentation and poster discussion)	2020
ESTRO 40 Madrid (poster discussion)	2021

National conferences

NVKF Scientific project day (oral presentation)	2017, 2020
NVRO research meeting (oral presentation)	2020

Invited speaker

Dalhousie University Research Café	2019
Maastro Research lunch	2020

In-house presentations

Radiation Oncology Research Day (oral presentation)	2017, 2018
R&D meetings, physics section Radiation Oncology	2016-2021
Refereer meetings, department of Radiation Oncology	2016-2021
Journal club, physics section Radiation Oncology	2016-2021
ABC Research meeting (oral presentation)	2019

Other

Peer-reviewer of 8 papers in 5 journals

Clinical trial management for

- CK-APBI trial (NL64643.078.18)
- TARGET trial (NL61639.078.17)
- SAPBI trial (MEC-2020-0415)

Teaching for Technical Medicine bachelor students (KT 3501)

List of publications

Peer-reviewed publications

1. Riberdy V, Ruiz E**, Hoekstra N**, Struik G, Pignol JP, Comparison of Visibility of Iodinated Hydrogel and Gadolinium-Modified Hyaluronic Acid Spacer Gels on Computed Tomography and Onboard Imaging. Submitted.
2. **Hoekstra N**, Habraken S, Swaak-Kragten A, Breedveld S, Pignol JP, Hoogeman M. Fiducial marker motion relative to the tumor bed has a significant impact on PTV margins in partial breast irradiation. Radiother Oncol. 163:1-6, 2021. DOI: 10.1016/j.radonc.2021.07.020.
3. Pignol JP, **Hoekstra N**, Wilke D, Dahn H, Nolan M, Vicini F, Estimation of annual secondary lung cancer deaths using various adjuvant breast radiotherapy techniques for early-stage cancers . Frontiers in Oncology, 2021. DOI: 10.3389/fonc.2021.713328.
4. **Hoekstra N**, Habraken S, Swaak-Kragten A, Hoogeman M, Pignol JP. Intrafraction motion during partial breast irradiation depends on treatment time. Radiother Oncol. 159:176-182, 2021. DOI: 10.1016/j.radonc.2021.03.029.
5. **Hoekstra N**, Habraken S, Swaak-Kragten A, Breedveld S, Pignol JP, Hoogeman M. Reducing the risk of secondary lung cancer in treatment planning of accelerated partial breast irradiation. Frontiers in Oncology, 10:1445, 2020. DOI: 10.3389/fonc.2020.01445
6. Struik GM, **Hoekstra N**, Klem TM, Ghandi A, Verduijn GM, Swaak-Kragten AT, Schoonbeek A, de Vries KC, Sattler MA, Verhoef K, Birnie E, Pignol, JP. Injection of radiopaque hydrogel at time of lumpectomy improves the target definition for adjuvant radiotherapy. Radiother and Oncol. 131: 8-13, 2019 DOI: 10.1016/j.radonc.2018.11.003
7. **Hoekstra N**, Fleury E, Merino Lara TR, van der Baan P, Bahnerth A, Hoogeman MS, Pignol JP. Risks of secondary cancer for whole and partial breast irradiation techniques – proposition for a mean lung dose constraint. Radiother Oncol. 128: 428-433, 2018. DOI: 10.1016/j.radonc.2018.05.032
8. van Linge A, van Os R, **Hoekstra N**, Heijmen B, Stienstra L, Dallenga A, Wolbers J, Mendez Romero A. Progression of hearing loss after LINAC-based stereotactic radiotherapy for vestibular schwannoma is associated with cochlear dose, not with pre-treatment hearing level. Radiation Oncology. 13: 253, 2018. DOI: 10.1186/s13014-018-1202-z
9. Della Gala G, Dirkx MLP, **Hoekstra N**, Fransen D, Lanconelli N, van de Pol M, Heijmen BJM, Petit SF. Fully automated VMAT treatment planning for advanced-stage NSCLC patients. Strahlenther Onkol. 193: 402-409, 2017
10. van Heijst TCF, **Hoekstra N**, Eschbach-Zandbergen D, van Asselen B, Lagendijk JJW, Verkooijen HM, Pijnappel RM, de Waard SN, Witkamp AJ, van Dalen T, van den Bongard HJGD, Philippens MEP. Supine MRI for regional breast radiotherapy: imaging axillary lymph nodes before and after sentinel-node biopsy. Phys Med Biol, 62: 6746-6761, 2017. DOI: 10.1088/1361-6560/aa759f

Correspondence

1. Pignol JP, **Hoekstra N**. Response to Comment on - Long-term risks of secondary cancers for various whole and partial breast irradiation techniques Radiother Oncol. S0167-8140(19)33473-5, 2019. DOI:10.1016/j.radonc.2019.11.007

Book Chapters

1. Pignol JP, **Hoekstra N**, Missohou F, Trombetta T. Accelerated Partial Breast Irradiation. In: Medical Radiology. Springer, Berlin, 2017. DOI: 10.1007/174_2017_96

Dankwoord

Wetenschap is teamwork en dat geldt ook voor dit proefschrift. Hier wil ik graag een aantal mensen in het bijzonder bedanken.

Mijn eerste promotor, prof. Hoogeman. Beste Mischa, bedankt voor je serieuze advies toen ik in 2015 bij je kwam met het verzoek om me te verdiepen in de klinische fysica. In de loop der jaren zijn we elkaar steeds beter gaan begrijpen. Bedankt voor het vertrouwen en de ruimte die je me hebt gegeven, waarbij je er was als het nodig was. Je kritische feedback en realistische kijk op onderzoek neem ik mee in de rest van mijn onderzoekscarrière.

My second promotor, prof. Pignol. Dear JP, I remember our first meeting discussing research as if it was yesterday. Little did I know where this conversation would lead me. You have fundamentally changed my view on research in general and on my own future in particular. Thanks for teaching me a broad range of things, from nuclear physics and research methods to managing intercultural differences. The important thing was not the thesis, but becoming an independent researcher with skills for an excellent academic future. It is not the destination but the road towards it that matters. Thanks for supporting me on that road.

Mijn co-promotor, dr. Habraken. Beste Steven, precies op het juiste moment stapte jij mijn project in. Bedankt voor je optimisme en daadkracht. Ik heb genoten van onze eerlijke en gelijkwaardige discussies. Bedankt dat je altijd tijd voor me vrij wist te maken, ook voor zaken breder dan dit proefschrift.

De leden van de promotiecommissie, prof. dr. Remi Nout, prof. dr. Liesbeth Boersma, prof. dr. Bas Raaymakers, en de leden van de grote commissie, prof. dr. Coen Rasch, prof. dr. Lenny Verkooijen, prof. dr. Marcel van Herk en dr. Linetta Koppert. Hartelijk dank voor het kritisch lezen van mijn proefschrift.

Beste Annemarie Swaak - Kragten, voor mij ben jij mijn tweede co-promotor. Je bent een voorbeeld van hoe patiëntenzorg, commissietaken en het thuisfront te combineren en tegelijkertijd behulpzaam en rustig te blijven. Bedankt voor je steun en vertrouwen toen ik het het hardst nodig had.

Dank aan alle AIOS radiotherapie, van 2011 tot nu, voor de gezelligheid en voor de aanmoedigingen om de uitdaging aan te gaan en vol te houden.

Manouk, bedankt voor je steun aan mijn bijzondere opleidingstraject en je persoonlijke advies voor mijn toekomst daarna. Marjan, lang geleden in het Verbeeten liet je me zien hoe een arts mee kan denken over fysica-aspecten binnen de radiotherapie, heel veel dank!

Dank aan alle radiotherapeuten van de mammagroep en in het bijzonder Raymond en Maugosia voor jullie input in de CK-APBI studie.

All my fellow-researchers at the physics section, thank you for welcoming this medical doctor in your physics group, for the great discussions on research and for the multicultural views on life in general. Lunch is never boring with you! Thanks for the enjoyable times during the ESTRO conferences. Dominique, ondanks onze verschillende achtergrond lijken we erg op elkaar. Bedankt dat je op deze dag als paranimf aan mijn zijde wilt staan. Gerson, bedankt voor je verfrissende kijk op onderzoek, het was een leerzame inter-disciplinaire samenwerking.

Dank aan de afdeling KFM, in het bijzonder aan Peter voor de fantoommetingen (inclusief opgesloten raken in de kelder van de Daniel na een meting) en Ben voor het werk met de TLDs. Ben, je wordt gemist.

Bedankt voor de hulp bij het gebruik van de vele verschillende computersystemen en scripts, in het bijzonder aan Sebastiaan, Andras en Xander.

Alle klinisch fysici, gedurende deze jaren heb ik jullie allemaal wel eens nodig gehad voor advies over zeer uiteenlopende fysica onderwerpen. Dank voor jullie behulpzaamheid.

Jacqueline, bedankt voor je hulp met afspraken plannen, vakantie uren en andere praktische zaken. Ik vond het altijd heel gezellig om wekelijks mijn fruit bij je op te halen!

Zonder de hulp van de CK-laboranten was de klinische studie niet mogelijk geweest, speciale dank aan Michèle, Lisette, Renée en Erik.

Andy, nooit zal ik vergeten hoe ik de mouldroom binnenliep en jij zei; "Ik was net aan het vertellen over jouw neptieten". Bedankt voor de gezelligheid en je praktische oplossingen bij het maken van het fantoom.

Mijn vriendinnen Floor, Marjolein, Marieke en Nathalie, we zijn in verschillende vakgebieden en regio's terecht gekomen na onze studie, maar onze band blijft. Bedankt dat jullie er voor me waren, met leuke dingen en steun. Bedankt voor de herkenbare verhalen over werk en thuis. Nathalie, wat zijn we veranderd sinds die eerste dag in de brugklas! Bedankt dat je mijn paranimf wil zijn.

Lieve papa en mama, bedankt voor de veilige basis. Ik weet dat jullie er altijd voor me zullen zijn.

Oscar, Marit en Thomas, bedankt dat jullie me thuis helemaal in het hier en nu houden. Samen met jullie spelen, knuffelen en lezen is de beste manier om te ontspannen na een drukke werkdag en alle zaken die spelen op het werk helemaal te vergeten.

Jasper, jij bent mijn thuis. Dankzij jouw opofferingen was het praktisch mogelijk om mijn ambities te volgen. Bedankt voor alles. Ik verheug me op onze toekomst samen!